

การศึกษาพารามิเตอร์ของการผลิตไบโอดีเซลในเมทานอลภาวะเหนือวิกฤต
ในเครื่องปฏิกรณ์แบบท่อ



นายเรืองวิทย์ สว่างแก้ว

ศูนย์วิทยพัทยากร
จุฬาลงกรณ์มหาวิทยาลัย

วิทยานิพนธ์นี้เป็นส่วนหนึ่งของการศึกษาตามหลักสูตรปริญญาวิทยาศาสตรดุษฎีบัณฑิต

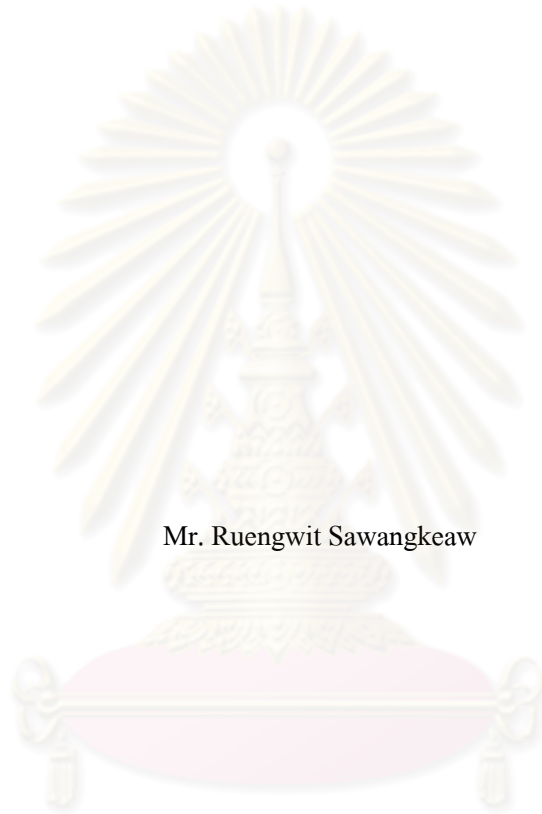
สาขาวิชาเคมีเทคนิค ภาควิชาเคมีเทคนิค

คณะวิทยาศาสตร์ จุฬาลงกรณ์มหาวิทยาลัย

ปีการศึกษา 2553

ลิขสิทธิ์ของจุฬาลงกรณ์มหาวิทยาลัย

PARAMETRIC STUDY OF BIODIESEL PRODUCTION IN SUPERCRITICAL METHANOL
IN A TUBULAR REACTOR



Mr. Ruengwit Sawangkeaw

ศูนย์วิทยทรัพยากร
จุฬาลงกรณ์มหาวิทยาลัย

A Dissertation Submitted in Partial Fulfillment of the Requirements
for the Degree of Doctor of Philosophy Program in Chemical Technology

Department of Chemical Technology

Faculty of Science

Chulalongkorn University

Academic year 2010

Copyright of Chulalongkorn University

เรื่องวิทยุ สว่างแก้ว : การศึกษาพารามิเตอร์ของการผลิตไบโอดีเซลในเมทานอลภาวะเหนือวิกฤตในเครื่องปฏิกรณ์แบบท่อ. (PARAMETRIC STUDY OF BIODIESEL PRODUCTION IN SUPERCRITICAL METHANOL IN A TUBULAR REACTOR)

อ. ที่ปรึกษาวิทยานิพนธ์หลัก : รศ. ดร. สมเกียรติ งามประเสริฐสุทธิ, อ. ที่ปรึกษา

วิทยานิพนธ์ร่วม : รศ. กัญญา บุญเกียรติ, Prof. Jean-Stéphane CONDORET, Doctorat de l'INPT, 3 หน้า.

การผลิตไบโอดีเซลในเมทานอลภาวะเหนือวิกฤตมีข้อได้เปรียบกว่ากระบวนการแบบดั้งเดิมซึ่งใช้ตัวเร่งปฏิกิริยาเอกพันธ์ ได้แก่ มีประสิทธิภาพสูงและใช้วัตถุดิบได้หลากหลายกว่า อย่างไรก็ตามพบว่าร้อยละเมทิลเอสเทอร์สูงสุดในเครื่องปฏิกรณ์แบบต่อเนื่องในเมทานอลภาวะเหนือวิกฤตต่ำกว่าในเครื่องปฏิกรณ์แบบแบตช์เล็กน้อย จุดประสงค์แรกของงานวิจัยนี้คือศึกษาผลของตัวทำละลายร่วมที่ใช้ลดความหนืดในเครื่องปฏิกรณ์แบบต่อเนื่องระดับขยายขนาด โดยศึกษาผลของตัวทำละลายร่วมด้วยการออกแบบการทดลองแบบ 2^3 แฟกทอเรียล พบว่าตัวทำละลายร่วมไม่มีผลอย่างมีนัยสำคัญต่อร้อยละเมทิลเอสเทอร์ จุดประสงค์ที่สองคือการพัฒนาการวิธีประมาณเวลาในการเกิดปฏิกิริยาของการผลิตไบโอดีเซลในเมทานอลภาวะเหนือวิกฤตอย่างต่อเนื่อง โดยใช้แบบจำลองทางเทอร์โมไดนามิกส์ (PR-MHV2-UNIQUAC) ซึ่งมีการปรับพารามิเตอร์อันตรกิริยาร่วมกับจลนพลศาสตร์ของการผลิตไบโอดีเซลในเมทานอลภาวะเหนือวิกฤตจากน้ำมันปาล์มและคุณมวลสารพื้นฐานในเครื่องปฏิกรณ์แบบท่อ พบว่าแบบจำลองที่สร้างขึ้นสามารถทำนายค่าที่ได้จากการทดลองได้ดีที่อุณหภูมิต่ำกว่า 320°C เนื่องจากไม่มีผลของการแตกตัวของความร้อนของกรดไขมันไม่อิ่มตัวและแสดงให้เห็นถึงผลของการเปลี่ยนแปลงแฟกเตอร์สภาพอัดได้ของผสมที่ทำให้อัตราการเกิดปฏิกิริยาช้าลงในเครื่องปฏิกรณ์แบบท่อ นอกจากนี้วิธีประมาณเวลาในการเกิดปฏิกิริยาที่พัฒนาขึ้นโดยสันนิษฐานว่าแฟกเตอร์สภาพอัดได้ไม่คงที่นั้นแสดงให้เห็นว่าร้อยละเมทิลเอสเทอร์ที่ได้จากเครื่องปฏิกรณ์แบบต่อเนื่องมีค่าต่ำลงเล็กน้อยเท่านั้น ซึ่งเกิดจากการแตกตัวของความร้อนที่อุณหภูมิ 350°C และเวลาในการเกิดปฏิกิริยามากกว่า 30 นาที

ภาควิชา เคมีเทคนิคลายมือชื่อนิสิต.....
 สาขาวิชา เคมีเทคนิคลายมือชื่อ อ.ที่ปรึกษาวิทยานิพนธ์หลัก.....
 ปีการศึกษา 2553ลายมือชื่อ อ.ที่ปรึกษาวิทยานิพนธ์ร่วม.....
ลายมือชื่อ อ.ที่ปรึกษาวิทยานิพนธ์ร่วม.....

4873890023 : MAJOR CHEMICAL TECHNOLOGY

KEYWORDS : VEGETABLE OIL / BIODIESEL / TRANSESTERIFICATION /
 SUPERCRITICAL METHANOL / CONTINUOUS PRODUCTION

RUENGWIT SAWANGKEAW : PARAMETRIC STUDY OF BIODIESEL
 PRODUCTION IN SUPERCRITICAL METHANOL IN A TUBULAR REACTOR.

ADVISOR : ASSOC.PROF.SOMKIAT NGAMPRASERTSITH, DOCTORAT DE
 L'INPT., CO-ADVISOR : ASSOC.PROF.KUNCHANA BUNYAKIAT, PROF. JEAN-
 STÉPHANE CONDORET, DOCTORAT DE L'INPT, 3 pp.

Biodiesel production in supercritical methanol (SCM) has several advantages over that employing homogeneous catalysts; i.e. better production efficiency and feedstock flexibility. However, the maximum methyl esters (ME) content, which was found in our continuous SCM reactor, was slightly lower than the batch SCM reactor. The first objective was to investigate effects of co-solvents used for viscosity reduction in scale-up continuous reactor, on ME content. The investigation was successfully done by 2^3 factorial design and found that the amount of co-solvents had no significant effect on ME content. The second objective was to develop residence time estimation method for continuous production of biodiesel in SCM. A compressible flow model, derived from general mole balance in a tubular reactor, transesterification kinetic of palm oil in SCM, and thermodynamic model (PR-MHV2-UNIQUAC) with adjusted binary interaction parameters was employed. The model was adequate to predict final conversion at below 320 °C, when thermal degradation reaction of unsaturated fatty acids (UFA) did not interfere. It was illustrated that development of compressibility factor slowed down the rate of transesterification reaction in SCM in a tubular reactor. Finally, the residence time estimation method based on compressibility changes was successfully attempted and demonstrated that ME content in continuous tubular reactor was only slightly reduced by thermal degradation of UFA at 350 °C and residence time longer than 30 min

Department : Chemical Technology Student's Signature *Ruengwit Sawangkeaw*
 Field of Study : Chemical Technology Advisor's Signature *Somkiat Ngamprasertsith*
 Academic Year : 2010 Co-Advisor's Signature *Kunchana Bunyakiat*
 Co-Advisor's Signature *[Signature]*

ACKNOWLEDGEMENTS

I would like to express my deepest gratitude my supervisors, Associate Professor Somkiat Ngamprasertsith, Ph.D., Associate Professor Kunchana Bunyakiat and Professor Jean-Stéphane CONDORET, Ph.D. who reviewed this thesis during its preparation and offered many helpful suggestions, supervision and much encouragement throughout pass five years of my research. I also would like to acknowledge Associate Professor Tharapong Vitidsant, Ph.D., Assistant Professor Chawalit Ngamcharussrivichai, Ph.D. Mr. Kunakorn Poochinda, Ph.D. and Miss Suchada Butnark, Ph.D. for their participation on the dissertation chairman and members of thesis committee, respectively.

I wish to express my thankfulness to all people in the associated institution and companies for their kind assistance and collaboration: Madam Séverine CAMY, Ph.D. and Monsieur Pablo E. HEGEL, Ph.D. for encouragements and helpful suggestion during this research at Institut National Polytechnique de Toulouse, Laboratoire de Génie Chimique in France.

Sincerest appreciation also extends to Chulalongkorn University Dutsadi Phiphat Scholarship, the Center of Excellence for Petroleum, Petrochemicals and Advanced Materials for financial support of this research and Chumporn Palm Oil Industry Co. Ltd. for supplying the palm kernel oil samples.

Many thanks are due to technicians, researchers, colleagues, fellow students and friends at the Department of Chemical Technology for their helps, supports, encouragement and friendships.

Finally, I wish to acknowledge the support, encouragement and love of my friends and family throughout my Ph.D. program.

CONTENTS

| | Page |
|--|------|
| ABSTRACT (IN THAI) | iv |
| ABSTRACT (IN ENGLISH)..... | v |
| ACKNOWLEDGEMENTS | vi |
| CONTENTS..... | vii |
| LIST OF TABLES | x |
| LIST OF FIGURES | xii |
| CHAPTER I: INTRODUCTION..... | 1 |
| 1.1. Background..... | 1 |
| 1.2. Objectives | 2 |
| 1.3. Scope of dissertation..... | 3 |
| CHAPTER II: THEORY AND LITERATURE REVIEWS | 4 |
| 2.1. Biodiesel | 4 |
| 2.2. Biodiesel production with conventional method | 4 |
| 2.3. Biodiesel production with heterogeneous catalysts and lipase | 7 |
| 2.4. Biodiesel production with supercritical methanol (SCM) | 8 |
| 2.4.1. Chronological development of biodiesel production with SCM..... | 10 |
| 2.4.2. Effect of operating parameters on biodiesel production with SCM..... | 11 |
| 2.4.2.1. Temperature..... | 11 |
| 2.4.2.2. Pressure..... | 15 |
| 2.4.2.3. Methanol to oil molar ratio..... | 15 |
| 2.4.2.4. Reaction time..... | 16 |
| 2.4.2.4.1. Batch reactor..... | 17 |
| 2.4.2.4.2. Continuous reactor (residence time)..... | 17 |
| 2.4.2.5. Mixing intensity and dispersion in tubular reactor..... | 19 |
| 2.4.3. Chemical kinetics of biodiesel production with SCM | 22 |
| 2.4.4. Phase behavior and binary vapor-liquid equilibrium (VLE) of biodiesel production with SCM..... | 25 |

| | |
|--|----|
| 2.4.5. Innovative technologies for milder operating parameters in biodiesel production with SCM..... | 29 |
| 2.4.5.1. Addition of co-solvents | 29 |
| 2.4.5.2. The addition of catalysts to the SCM reaction | 33 |
| 2.4.5.3. Modification of the SCM reaction..... | 34 |
| 2.5. Literature reviews | 36 |
| CHAPTER III: EQUIPMENTS AND EXPERIMENTAL PROCEDURES..... | 47 |
| 3.1. Effect of co-solvents | 47 |
| 3.1.1. Equipments | 47 |
| 3.1.2. Materials | 47 |
| 3.1.3. Experimental procedure..... | 47 |
| 3.1.3.1. The 250-mL reactor..... | 47 |
| 3.1.3.2. The 5.5-mL reactor..... | 48 |
| 3.1.4. Analysis of methyl esters..... | 48 |
| 3.2. Effect of additional parameters and scale-up reactor optimization | 49 |
| 3.2.1. Equipments | 49 |
| 3.2.1.1. The scale-up reactor | 49 |
| 3.2.1.2. The 250-mL and 5.5-mL reactors..... | 50 |
| 3.2.2. Materials | 50 |
| 3.2.3. Experimental procedure..... | 50 |
| 3.2.3.1. The scale-up reactor | 50 |
| 3.2.3.2. The 250-mL and 5.5-mL reactor | 50 |
| 3.2.3.3. The 5.5-mL reactor to investigate the effect of delay quenching time..... | 50 |
| 3.2.4. Analysis of methyl esters..... | 51 |
| 3.3. Residence time estimation method | 51 |
| 3.3.1. Equipments | 51 |
| 3.3.2. Materials | 52 |
| 3.3.3. Experimental procedure..... | 52 |
| 3.3.4. Analysis of methyl esters..... | 52 |

| | |
|--|-----|
| CHAPTER IV: EFFECT OF CO-SOLVENTS | 53 |
| 4.1. Reaction among vegetable oil, methanol and co-solvents | 53 |
| 4.2. Effect of co-solvents on ME content in a 250-mL reactor..... | 55 |
| CHAPTER V: EFFECT OF ADDITIONAL PARAMETERS AND SCALE-UP REACTOR OPTIMIZATION | 58 |
| 5.1. Effect of reaction time on ME content in 250-mL batch reactor | 58 |
| 5.2. Effect of temperature gradient between reactor wall and bulk fluid | 58 |
| 5.3. Effect of contaminants in crude palm kernel oil..... | 60 |
| 5.4. Effect of co-solvents on ME content in biodiesel production in a 5.5-mL reactor..... | 61 |
| 5.5. Effect of delayed quenching time | 64 |
| 5.5.1. Effect of delayed quenching time in a 5.5-mL batch reactor | 64 |
| 5.5.2. Effect of delay quenching time in scale-up reactor | 64 |
| 5.6. Effect of pressure and process optimization | 66 |
| CHAPTER VI: RESIDENCE TIME ESTIMATION METHOD..... | 70 |
| 6.1. Description of the compressible flow model as a tool to estimate the residence time | 70 |
| 6.1.1. Thermodynamic model..... | 70 |
| 6.1.2. Compressible flow model..... | 71 |
| 6.2. Fitting of the thermodynamic model and binary interaction parameters | 73 |
| 6.3. ME content prediction by the compressible flow model | 77 |
| 6.4. Residence time estimation procedure | 83 |
| CHAPTER VII: CONCLUSIONS AND RECOMMENDATION..... | 84 |
| 7.1. Conclusions..... | 84 |
| 7.2. Recommendation | 85 |
| REFERENCES | 87 |
| APPENDICES | 96 |
| APPENDIX A THE STATISTICAL ANALYSIS OF THE REGRESSION MODEL FOR SCALE-UP REACTOR..... | 97 |
| APPENDIX B THE EXAMPLES OF PROGRAMING CODE FOR MATLAB ® SOFTWARE WITH SIMULIS TOOLBOX | 101 |
| BIOGRAPHY | 105 |

LIST OF TABLES

| | Page |
|---|------|
| Table 2.1 Advantages and disadvantages of heterogeneous and lipase catalysts. | 7 |
| Table 2.2 Operating parameters for a high conversion efficiency of lipid to biodiesel with SCM. | 13 |
| Table 2.3 Molar ratio and mole fraction at the inlet and outlet of the tubular reactor, calculated by assuming 100% conversion at the outlet. | 18 |
| Table 2.4 Optimal condition, reactor design, Reynolds and axial Péclet number of the continuous biodiesel production with SCM in a tubular reactor. | 21 |
| Table 2.5 Reactions rate constant (k) as linear function of temperature, pre-exponential factor (k_0) and activation energy (E_a). | 24 |
| Table 2.6 Studies on the VLE of biodiesel production with SCM summary. | 27 |
| Table 2.7 Binary interaction parameters of the VdW mixing rule which correspond with the thermodynamic model in Table 2.6. | 28 |
| Table 2.8 Demonstrated techniques for reducing the operating parameters of biodiesel production with SCM. | 30 |
| Table 2.9 New operating parameters of biodiesel production with SCM by the techniques outlined in Table 2.8. | 31 |
| Table 4.1 Experimental data from employed THF process in 250-mL reactor for 10 min with crude PKO as reactant | 55 |
| Table 4.2 Experimental data from employed hexane process in 250-mL reactor for 10 min with crude PKO as reactant | 56 |
| Table 4.3 Analysis of variance from employed THF process in 250-mL reactor for 10 min with crude PKO as reactant | 56 |
| Table 4.4 Analysis of variance from employed hexane process in 250-mL reactor for 10 min with crude PKO as reactant | 57 |
| Table 5.1 Experimental data from 5.5-mL reactor for 10 min with crude PKO as reactant, temperature controlled by fluidized sand bath. | 60 |
| Table 5.2 Experimental data from employed THF process in 5.5-mL reactor for 10 min with refined PKO as reactant | 61 |

| | |
|---|----|
| Table 5.3 Experimental data from employed hexane process in a 5.5-mL reactor for 10 min with refined PKO as reactant | 62 |
| Table 5.4 Analysis of variance from employed THF process in a 5.5-mL reactor for 10 min with refined PKO as reactant | 62 |
| Table 5.5 Analysis of variance from employed hexane process in 5.5-mL reactor for 10 min with refined PKO as reactant | 63 |
| Table 5.6 The ME content in products from scale-up reactor with different cooling systems | 65 |
| Table 5.7 The experimental conditions and results from CCD to reinvestigate the effect of pressure, temperature and methanol to oil molar ratio in scale-up reactor | 66 |
| Table 5.8 Analysis of variance of results in Table 5.7 | 67 |
| Table 6.1 Calculated binary interaction coefficients for UNIQUAC model. | 73 |
| Table 6.2 Methanol mole fraction in liquid (x) and vapor (y) phase of triolein + methanol VLE. | 74 |
| Table 6.3 The methanol mole fraction in liquid (x) and vapor (y) phase of methyl oleate + methanol VLE. | 75 |
| Table 6.4 The methanol mole fraction in liquid (x) and vapor (y) phase of glycerol + methanol VLE. | 76 |
| Table 6.5 The observed and calculated ME content from various reacting conditions. | 78 |
| Table A1. The statistical values of the regression model for scale-up reactor from Design Expert ® 6.0 software..... | 97 |
| Table A2. The estimated coefficients and its standard error in the regression model for scale-up reactor at $\pm 95\%$ confident interval from Design Expert ® 6.0 software | 98 |
| Table A3. The residual analysis of actual and predicted value for the regression model for scale-up reactor | 99 |

LIST OF FIGURES

| | Page |
|---|------|
| Figure 2.1. Common reactions for biodiesel production processes | 5 |
| Figure 2.2. Conventional biodiesel production scheme from waste cooking oils with acid pretreatment followed by alkaline catalytic process or two-step acidic-basic transesterification. | 6 |
| Figure 2.3. Biodiesel production with SCM scheme. | 8 |
| Figure 3.1 Schematic diagram of scale-up tubular reactor for biodiesel production with SCM | 49 |
| Figure 3.2 Schematic diagram of lab-scale tubular reactor | 51 |
| Figure 4.1 GC-MS chromatogram of mixed methyl esters standard. | 53 |
| Figure 4.2 GC-MS chromatogram of biodiesel from employed THF process in 250-mL reactor for 10 min with crude PKO as reactant. | 53 |
| Figure 4.3 GC-MS chromatogram of THF phase in 250-mL reactor for 10 min with crude PKO as reactant. | 54 |
| Figure 4.4 GC-MS chromatogram of hexane phase in 250-mL reactor for 10 min with crude PKO as reactant. | 54 |
| Figure 5.1 Changes in ME content with time of co-solvent free process from transesterification of crude PKO in 250-mL reactor at 350 °C and the methanol to oil molar ratio of 42:1. | 58 |
| Figure 5.2 Comparison of GC chromatogram of biodiesel product from crude PKO at various temperatures, indicating some noises observed as in c) and d). | 59 |
| Figure 5.3 The ME content versus the delayed quenching time in 5.5-mL tube reactor. | 64 |
| Figure 5.4 The scale-up reactor after replaced cooling bath with heat exchanger. | 65 |
| Figure 5.5 The plot of experimented and calculated value by Equation 5.3. | 68 |
| Figure 5.6 The response surface of ME content versus temperature and pressure at methanol to oil of 35:1 | 68 |
| Figure 6.1 Experimental (Exp) and calculated (Cal) P-x-y diagram of triolein + methanol VLE. | 75 |
| Figure 6.2 Experimental (Exp) and calculated (Cal) P-x-y diagram of methyl oleate + methanol VLE | 76 |

| | |
|--|-----|
| Figure 6.3 Experimental (Exp) and calculated (Cal) P-x-y diagram of glycerol + methanol VLE..... | 77 |
| Figure 6.5 The plot of experimented and calculated ME content by Eq. 6.6 (◆) or Eq.6.7 (○) | 78 |
| Figure 6.6 The relationship between %relative error of calculated value from Eq. 6.6 and reaction temperature | 79 |
| Figure 6.7 The relationship between %relative error of calculated value from Eq. 6.6 and methanol to oil molar ratio | 79 |
| Figure 6.8 The relationship between %relative error of calculated value from Eq. 6.6 and pressure..... | 80 |
| Figure 6.9 The changes in the compressibility of the reaction mixture along the length of the tubular reactor in run no. 1 (◇), 2 (+), 3 (□), 4 (×), 5 (○), 17 (●) and 22 (▲)..... | 81 |
| Figure 6.10 The changes in the molar volume of the reaction mixture along the length of the tubular reactor in run no. 1 (◇), 2 (+), 3 (□), 4 (×), 5 (○), 17 (●) and 22 (▲).. | 82 |
| Figure A1. The normal plot of the residuals | 100 |
| Figure A2. The relationship between residuals and run number | 100 |
| Figure A3. The relationship between residuals and predicted values..... | 100 |

CHAPTER I

INTRODUCTION

1.1. Background

The demand for biodiesel, the fatty acid-alcohol esters derived from, typically, triglyceride in vegetable or animal oils/fats and methanol or ethanol, as an alternative and potentially sustainably renewable fuel for diesel engines, is increasing steadily due to economic and environmental issues. These include increases in the crude oil price, as well as the dwindling but limited supplies of the non-renewable conventional diesel. Before the 1990s, the relatively high price of biodiesel that was mainly produced from virgin or refined vegetable oils, was the most serious obstacle to its development and its use could not economically compete against conventional diesel [1]. However, due to the relatively high price of conventional diesel at present, biodiesel produced from both refined and used vegetable or animal oils/fats became competitive [2]. On the other hand, the global warming issue makes biodiesel attractive as it has a closed carbon cycle and can effectively reduce the CO₂ emission burden from transportation and industry. For instance, biodiesel decreases the net CO₂ emission by 78% compared with conventional [3, 4]. Furthermore, biodiesel emits a lower level of CO, SO_x and unburned hydrocarbons after combustion than that from conventional diesel [5]. Finally, biodiesel has the potential to be a sustainable renewable resource. Therefore, research on biodiesel production technologies has received continuous attention globally.

Conventional biodiesel production process using either strong acidic or basic catalyst is performed at 30 - 60 °C and atmospheric pressure. This process has some disadvantages such as; long reaction time (over 30 min), wastewater treatment needed, soap and low quality crude glycerol by-products, and some non-recoverable chemicals needed [6]. The novel biodiesel production in supercritical methanol has advantages such as short reaction time (lower than 30 min) and less wastewater produced. Moreover, the supercritical methanol process does not require any additional chemicals, and the by-product is high purity glycerol. The more detailed advantages of the biodiesel production in supercritical methanol were discovered recently. For example, it was found that free fatty acids, that posed some problems in conventional method, did

not affect the supercritical methanol process. Also, the supercritical methanol is easier to improve than conventional process because the overall configuration is not complex [6, 7].

The improvement of biodiesel production in supercritical methanol has been reported continuously. Firstly, the use of carbon dioxide and propane was introduced by Chinese researchers in order to reduce temperature, pressure and methanol to vegetable oil molar ratio at the optimal condition [8]. Secondly, the continuous production of biodiesel via transesterification in supercritical methanol in a lab-scale reactor was successfully attempted in Thailand [9], Japan [10] and China [11]. Thirdly, many useful data were reported, such as an axial dispersion number in tubular reactor for biodiesel production in supercritical methanol [12], heat recovery process for biodiesel production in supercritical methanol [13], and vapor-liquid phase equilibria of the major components such as vegetable oil, methyl esters and glycerol with supercritical methanol [14-19]. The details of reports are summarized in the literature review section.

Data from lab-scale reactor successfully attempted in our laboratory were used for constructing a scale-up reactor. As we tested the reactor, it was found that the high viscosity of vegetable oil posed a problem on the pumping system. This problem was solved by an addition of some co-solvents such as THF and hexane [20]. However, the methyl ester content in biodiesel obtained from this scale-up reactor was lower than that from the lab-scale reactor.

1.2. Objectives

- 1.2.1. To investigate effects of co-solvents on methyl ester content in biodiesel produced from transesterification of vegetable oil in supercritical methanol.
- 1.2.2. To develop residence time estimation method for continuous production of biodiesel in supercritical methanol by the Equation of state.
- 1.2.3. To develop a biodiesel process using supercritical alcohol that produces biodiesel that conforms to the standard biodiesel specification of Thailand at approximately 10 liters per day.

1.3. Scope of dissertation

- 1.3.1. Effect of co-solvents (THF and hexane) employed to reduce viscosity is investigated in 250-mL and 5.5-mL batch reactors by 2^k factorial design.
- 1.3.2. Residence time estimation procedure based on the inconstant fluid properties is developed.
- 1.3.3. Additional effects such as interference of co-solvents, thermal degradation of unsaturated fatty acids, contaminants in crude vegetable oil, pressure, delayed quenching time and development of compressibility of mixture on ME content are studied and used to improve the biodiesel production with supercritical alcohol process.



CHAPTER II

THEORY AND LITERATURE REVIEWS

2.1. Biodiesel

Before 2000, biodiesel was widely referred to an alternative diesel fuel which was made from renewable biological sources such as vegetable or animal oils/fats [21]. In actuality, the use of vegetable or animal oils/fats as alternative fuels can be achieved in several ways; a heat fuel, a blending with diesel fuel, and as micro-emulsion mixture. However, vegetable or animal oils/fats have the major composition as triglyceride which may cause some combustion problems, e.g. coking and carbon deposits on the injectors and increasing the lubricant viscosity due to its high molecular weight and high viscosity. Thus, chemical modification processes such as thermal cracking, soap pyrolysis and transesterification were introduced to reduce the molecular weight of vegetable or animal oils/fats before using them as alternative fuel [22]. Among the chemical modification processes, the transesterification of triglyceride is the most promising process to produce alternative fuels from vegetable or animal oils/fats. For instance, the process produces the oxygenate fuels that burn cleaner than conventional diesel and do not generate the aromatic compounds. The term “biodiesel” is now specifically referred to the mixture alkyl esters of long chain fatty acids practically derived from the transesterification reaction between glycerides feedstock and low molecular weight alcohols such as methanol or ethanol, for use in compression ignition engine [22-25].

2.2. Biodiesel production with conventional method

Typical reactions that take place during biodiesel production are shown in Figure 2.1. Transesterification reaction, which is a major path to produce biodiesel, occurs between triglyceride vegetable or animal oils/fats with alcohols to form esters (biodiesel) and glycerol. The overall transesterification is simplified in Figure 2.1(a). In the presence of water, triglyceride can be partially hydrolyzed to fatty acids and diglyceride under suitable conditions (catalyzed or supercritical condition), as shown in Figure 2.1(b). Those fatty acids, including the free fatty acids (FFA) present in the feedstock, also convert to the desired product (biodiesel) through esterification reaction in present of acid catalysts or supercritical condition, as shown in Figure 2.1(c), or undesired product (fatty acid salt or soap), as shown in Figure 2.1(d).

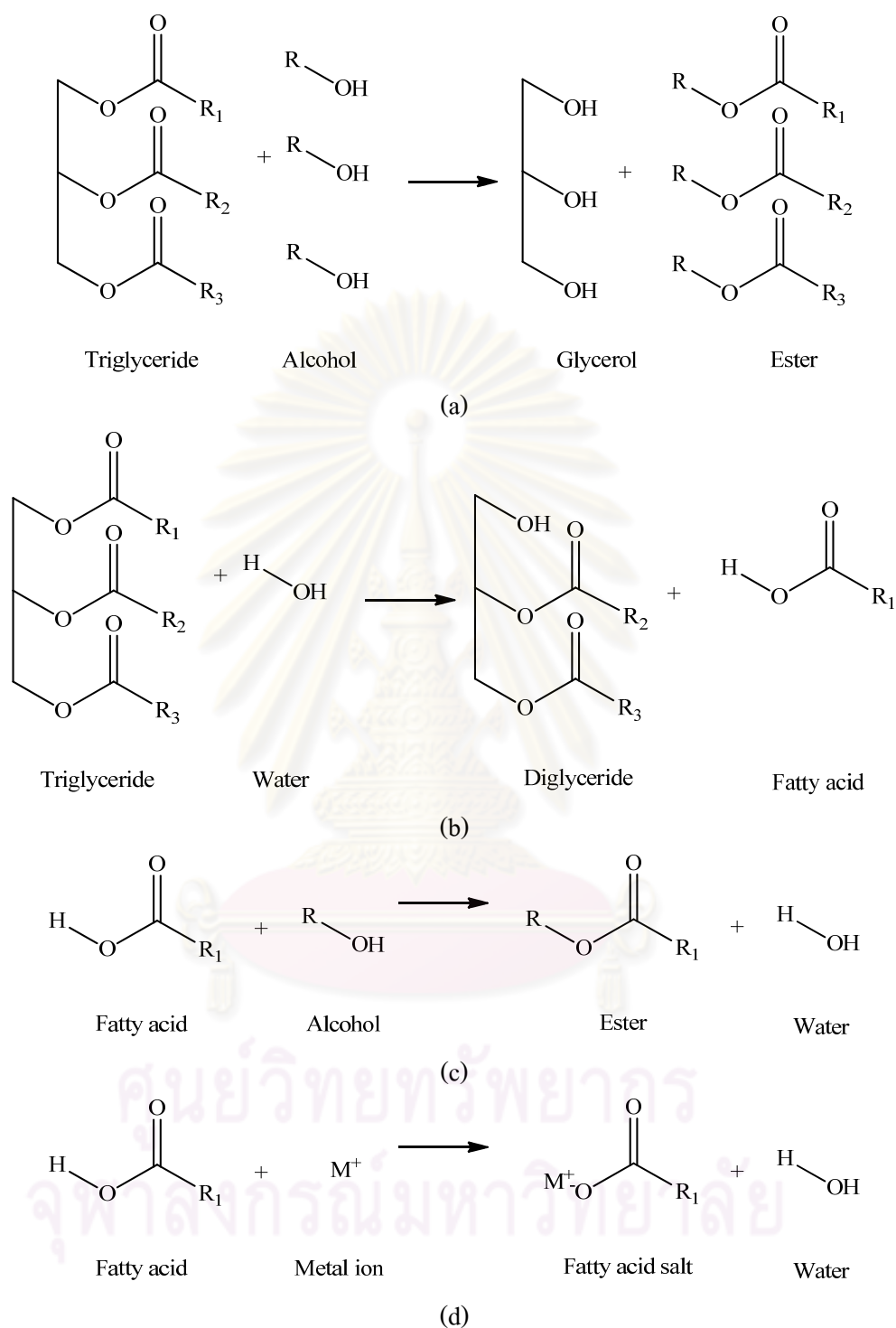


Figure 2.1. Common reactions for biodiesel production processes: (a) transesterification, (b) hydrolysis, (c) esterification and (d) saponification.

Conventional biodiesel production uses inexpensive feedstocks such as waste cooking oils, and employs homogeneous catalysts, such as NaOH and H₂SO₄ (Figure 2.2). Note that the

first set of reactor, separator and methanol recovery units is not needed when pretreated or refined triglyceride is used as feedstock.

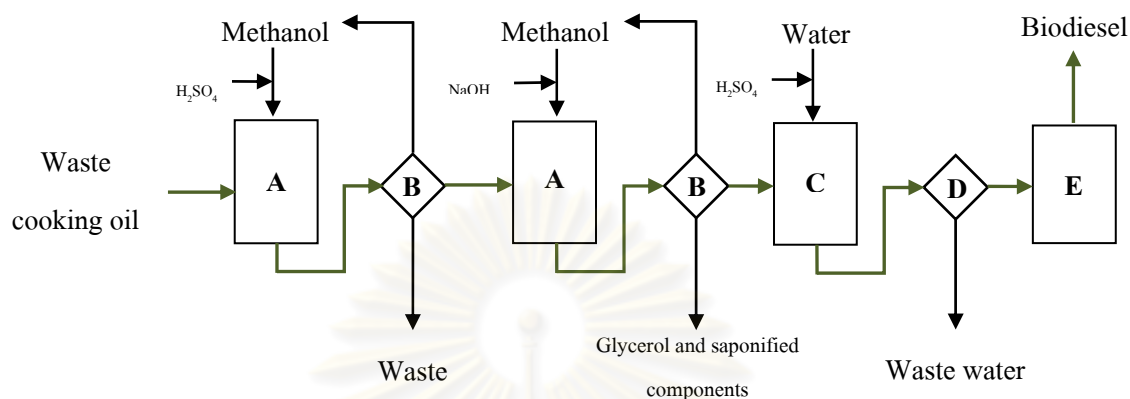


Figure 2.2. Conventional biodiesel production scheme from waste cooking oils with acid pretreatment followed by alkaline catalytic process or two-step acidic-basic transesterification: (A) Reactor (60 – 65 °C, 0.1 MPa and 6:1 – 9:1 methanol to oil molar ratio) , (B) Product separation and methanol recovery unit, (C) Water washing unit, (D) Separation unit and (E) Biodiesel drying unit.

The conventional process has some disadvantages, especially from environmental, production efficiency and feedstock flexibility points of view [21-23]. Firstly, the conventional process produces large volume of waste water and some saponified components that need to be treated before discharging to the environment or recycling to the process. Chemicals that are used as a catalyst and neutralizers are difficult to recover. Secondly, as the conventional production process for pretreated or refined triglyceride consists of four separate steps, namely, reacting, separating, washing and drying, the overall production time takes over four hours. The washing step that removes the saponified components in the crude biodiesel is the longest of these steps, since the saponified components interfere with and retard phase separation. Thirdly, the conventional process requires refined and expensive vegetable oils as feedstocks, i.e. lower than 0.06% (v/v) moisture and 0.50% (w/w) free fatty acids [21]. As a consequence, this increases the price of the biodiesel and reduces its sustainability, since the requirement of such virgin oils, rather than waste cooking oils, is indirect conflict with human or animal food grade feedstocks.

A two-step acidic-basic transesterification process is an alternative for inexpensive feedstocks, including spent waste and crude vegetable oils, it is more complicated, more time consuming and generates more waste that requires subsequent treatment than the single step transesterification [26, 27]. For instance, the acidic pretreatment step does not only generate additional wastes, but also requires more basic catalyst to neutralize the pretreated product.

2.3. Biodiesel production with heterogeneous catalysts and lipase

Novel catalytic processes, such as heterogeneous and lipase catalysts, have been developed to disentangle the drawbacks of homogeneous catalysts, but they still have some hurdles themselves. [28-38]. The advantages and disadvantages of heterogeneous and lipase catalysts are summarized in Table 2.1.

Table 2.1 Advantages and disadvantages of heterogeneous and lipase catalysts.

| Catalysts | Advantage | Disadvantage |
|-------------------------------|---|---|
| Heterogeneous acid catalysts | <ul style="list-style-type: none"> - Less sensitive to FFA and water in feedstocks - Catalyze esterification and transesterification reaction simultaneously | <ul style="list-style-type: none"> - Complicated catalyst synthesis procedures may lead to higher cost - Reaction normally take place at high temperature and high methanol to oil molar ratio - Leaching of catalyst active sites may result in catalyst deactivate and product contamination |
| Heterogeneous basic catalysts | <ul style="list-style-type: none"> - Relatively faster rate of reaction than acid catalysts - Reaction can occur at mild conditions - High possibility to reuse and regenerate | <ul style="list-style-type: none"> - Poisoning of catalyst when exposed to air and moisture - Soap will form at the FFA content > 2%wt - Leaching of catalyst active sites may result in catalyst deactivation and product contamination |

Table 2.1 (Cont'd) Advantages and disadvantages of heterogeneous and lipase catalysts.

| Catalysts | Advantage | Disadvantage |
|-----------|--|---|
| Enzyme | <ul style="list-style-type: none"> - Insensitive to FFA and water in feedstocks - Transesterification can take place at temperature lower than conventional catalysts, e.g. NaOH or KOH - Product purification is very simple | <ul style="list-style-type: none"> - Very slow rate of reaction - Relatively higher cost than other catalysts - Sensitive to alcohol, typically methanol that can denature and deactivate enzyme |

2.4. Biodiesel production with supercritical methanol (SCM)

Biodiesel production with SCM has been introduced to overcome catalytic problems. A simple schematic for biodiesel production with SCM is shown in Figure 2.3.

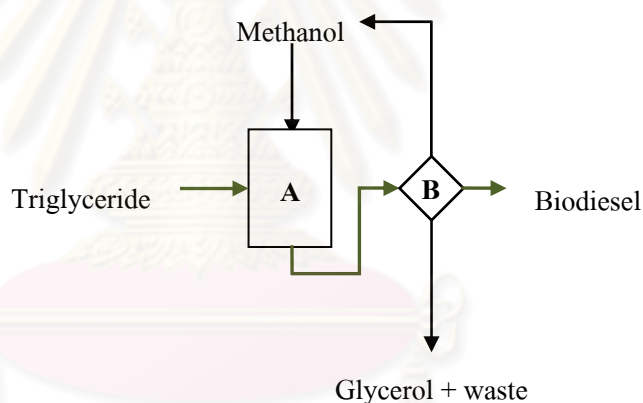


Figure 2.3. Biodiesel production with SCM scheme: (A) Reactor (300 – 350 °C, 19 – 45 MPa and 40:1 – 42:1 methanol to oil molar ratio) and (B) Product separation and methanol recovery unit.

With regard to environmentally friendly aspects, transesterification, for the case of transfer of the fatty acid components from glycerol to methanol to form fatty acid methyl esters (FAME), biodiesel in SCM does not require any catalysts or auxiliary chemicals and does not generate significant wastes [6, 7, 39, 40]. With regard to the FAME production efficiency, biodiesel production by SCM requires a minimum number of processing steps because the feedstock pretreatment to remove moisture and free fatty acids, as well as some of the product post treatment steps, such as neutralization, washing and drying, are not necessary. As a consequence, biodiesel production with SCM has a low overall production time. In addition, the rate of reaction at supercritical conditions is fast, so that the biodiesel production with SCM

requires a small reactor size for a given production output. With regard to feedstock flexibility, as the moisture and FFA contents in the feedstock do not significantly affect biodiesel production by SCM [41, 42] it is suitable for use with waste cooking oils or other low-grade feedstocks.

Biodiesel production with SCM offers an optimistic alternative to the catalytic method since it does not have inherent disadvantages such as saponified products or catalyst deactivation. Biodiesel production process with SCM has advantages over other processes in its low use of auxiliary chemicals, and chemicals associated with waste water treatment and feedstock pre-treatment. Even though the energy requirement could be a major operating cost, this is much easier to deal with than chemicals. The overall process is simple since many discrete operations such as catalyst preparation, product neutralization and purification are not required. Although biodiesel price depends greatly on feedstock price [2], feedstock flexibility becomes a remarkably strong advantage of the biodiesel production with SCM.

Biodiesel production with SCM still has several challenges in its research and development. The key operating parameters are pressure, temperature and methanol to oil molar ratio. To achieve the highest oil and methanol to FAME conversion rates and yields, high pressures (19 to 45 MPa), high temperatures (320 to 350 °C) and high methanol to oil ratios (40:1 to 42:1) have been reported in early studies [6, 7, 39]. In fact, the high pressure and temperature reaction conditions require not only an expensive reactor but also a sophisticated energy and safety management policy. Furthermore, the high methanol to oil ratio needs a significant energy input to recover the excess methanol for recycle. Using the parameters mentioned earlier on a commercial scale results in the capital costs being somewhat higher than the conventional process.

Therefore, current research is focused upon reducing the high operating pressure, temperature and methanol to oil molar ratio required for biodiesel production with SCM. To date the operating pressure, temperature and methanol to oil molar ratio that employ in early studies have been reduced successfully by several techniques, such as the addition of co-solvents or catalysts and by using a modified supercritical process (see section 2.4.5.) On the one hand, the goal to reduce operating pressure, temperature and methanol to oil molar ratio altogether is certainly the most challenging aspect of biodiesel production with SCM, while on the other hand, parameters, such as pressure, methanol to oil molar ratio and residence time, can be simultaneously reduced by increasing the operating temperature.

2.4.1. Chronological development of biodiesel production with SCM

In 1998, non-catalytic transesterification of soybean oil at near-critical point of methanol (230 °C, 6.2 MPa and 27:1 methanol to oil molar ratio) was invented to provide an alternative biodiesel production method, but this method obtained only 85 % by weight of methyl esters in product at over 10 hours [43]. Until 2001, Japanese pioneers promoted the transesterification of rapeseed oil with SCM at 350 °C, 45 MPa and 42:1 methanol to oil molar ratio, this process was given a high degree of attention due to the methyl esters (ME) content (98%) was observed at only 4 min [6, 39]. Then, the biodiesel production with SCM has been evolved continuously since 2001.

In 2002, the transesterification of cottonseed, hazelnut kernel, poppy seed, safflower and sunflower oil in SCM was investigated and nearly complete reaction was reported [7]. At the same time, continuous production of biodiesel from palm kernel and coconut oil with SCM in lab-scale tubular reactor was developed in our laboratory [44] and then the scale-up reactor was constructed in 2005 [20]. Meanwhile, the effect of water and free fatty acids in vegetable oils feedstock [41] and the catalytic effect of metal reactor in biodiesel production with SCM [45] and the reactivity of triglyceride with supercritical alcohols were also reported [46]. However, during the year of 2001 – 2005, the maximum ME content was generally observed at the same condition as reported earlier by the Japanese pioneers [6, 39].

In 2005, carbon dioxide and propane were introduced as co-solvents to obtain milder operating parameters of biodiesel production with SCM [8, 47]. Then, the two-step supercritical process [10] was also demonstrated to reduce those operating parameters. In the following years, various catalysts were employed to assist the SCM process to achieve the maximum ME content at milder operating conditions [48-52]. Furthermore, the first article on continuous production of biodiesel with SCM was published by our research group [9], then by the Japanese [10] and Chinese [11] researchers, respectively. Therefore, the research focus on reduction of the elevated operating conditions and continuous process has been ongoing since 2005.

In 2007, the gradual heating technique was introduced to prevent thermal degradation that cause low ME content [11]. At the same time, the effect of co-solvents employed to reduce viscosity of vegetable oils was investigated successfully in our laboratory [53]. From 2007 to 2009, numerous additional studies such as vapor-liquid equilibria of binary systems [16-19, 54, 55], phase behavior of reaction mixture [15, 56, 57], thermal stability of unsaturated fatty acids in

SCM [58] and process and economic analysis [12, 13, 59, 60] were reported to the better understanding of biodiesel production with SCM.

2.4.2. Effect of operating parameters on biodiesel production with SCM

Operating parameters, as employed by previous researchers, to obtain high yield of FAME production with SCM are summarized in Table 2.2. The extent of reaction is reported either as methyl esters (ME) content or as triglyceride conversion. It should be noted that the ME content refers to methyl esters of common FFA in vegetable or animal oils/fats that can be identified by different analytical techniques, while the triglyceride conversion implies the remaining triglyceride reactant. The discussion for each parameter is presented accordingly.

2.4.2.1. Temperature

All the reported studies to date have shown that the reaction temperature is the most critical parameter for determining the extent of reaction, especially across the critical temperature of methanol (239.6 °C). The ME content level rises two- to three-fold as the temperature increases from 200 to 350 °C at a constant pressure and methanol to oil molar ratio. The temperature has a strong influence on the conversion rate. For instance, the rate constant increases approximately seven-fold as the temperature is increased from 210 to 280 °C at a pressure of 28.0 MPa and a methanol to oil molar ratio of 42:1. Likewise, the apparent activation energy increases from 11.2 kJ/mol at 210 to 230 °C (subcritical region) to 56.0 kJ/mol at 240 to 280 °C (supercritical region) at 28.0 MPa and 42:1 methanol to oil molar ratio [61].

Although, high temperature clearly enhances the rate of reaction, an excessively high temperature can lead to a negative effect on the ME content. Thermal degradation of unsaturated fatty acids (UFA) was reported in some studies within the temperature range of 320 to 350 °C. For example, Sawangkeaw et al. [53] found thermal degradation of UFA in a 250-mL batch reactor due to the temperature gradient between the reactor wall and the bulk fluid. However, the ME content was only slightly reduced because the feedstock used (palm kernel oil) was low in UFA. In contrast, when using soybean oil, which contains over 80% UFA as a feedstock, thermal degradation of the UFA significantly reduces the ME content obtained [11].

Thermal degradation of UFA is a prominent concern in the selection of the triglyceride source against those sources with a high level of UFA. Appropriate temperature for biodiesel production with SCM in an isothermal system is lower than 300 °C, and is preferably less than 270 °C so that the maximum ME content in the biodiesel can be obtained [58]

Gradual heating of the reaction mixture has been shown to be effective in avoiding UFA thermal degradation [11]. By gradual heating (100 to 320 °C) the reaction mixture, the ME content obtained improved to 96%, compared to 77% obtained from uniform heating at 310 °C.

Some studies have reported that the thermal degradation of UFA at 350 °C significantly decreases the ME content but slightly increases the cloud point [58] and decreases the viscosity [62] of the obtained biodiesel. For instance, the FAMES obtained from rapeseed and linseed oil decompose by approximately 20 and 50 % by weight, respectively, at 350 °C after 40 min of contact time, while the cloud point increases by only 1 or 2 °C.

The thermal degradation of UFA esters, triglyceride and glycerol at 400 to 450 °C in SCM has been reported to generate several low-molecular weight compounds that could improve the cold flow properties as well as the viscosity of the biodiesel produced [63-65]. However, biodiesel production with SCM at temperature higher than 350 °C is considered as a modification of supercritical process to lower other operating parameters and additional details are described in Section 2.4.5.

Table 2.2 Operating parameters for a high conversion efficiency of lipid to biodiesel with SCM.

| Researchers | T (°C) | P (MPa) | MeOH to Oil molar ratio | Reaction time (min) | Oil type | Reactor type | Heating and cooling rate (°C/sec) | ME content/ Conversion (%) |
|-------------------------|--------|---------|-------------------------|---------------------|--------------------------------|--------------|-----------------------------------|----------------------------|
| Saka and Kusdiana [6] | 350 | 45 | 42:1 | 4 | Rapeseed | 5-mL BRsh | 30 and -100 | >95% ME content |
| Demirbas [7] | 350 | N/R | 41:1 | 5 | Hazelnut kernel and Cottonseed | 100-mL BR | 0.33 and N/R | 95% ME content |
| Madras et al. [66] | 400 | 20 | 40:1 | 30 | Sunflower | 8-mL BR | N/R | 97% Conversion |
| Rathore and Madras [67] | 400 | 20 | 50:1 | 30 | Palm and Groundnut | 11-mL BR | N/R | 95% Conversion |
| Yin et al. [68] | 350 | 20 | 42:1 | 30 | Soybean | 250-mL BRs | 0.33 and N/R | 95% ME content |
| He et al. [61] | 280 | 25 | 42:1 | 30 | Soybean | 200-mL BRs | N/R | 90% ME content |
| Sawangkeaw et al. [53] | 350 | 20 | 42:1 | 30 | Palm kernel | 250-mL BRs | N/R | 95% ME content |
| Cao et al. [47] | 320 | N/R | 33:1 | 10 | Soybean | 250-mL BRs | 0.33 and N/R | 95% ME content |
| Bunyakiat et al. [9] | 350 | 19 | 42:1 | 7 to 15 | Coconut and Palm kernel | 251-mL TR | N/R | 95% ME content |

N/R: Not Reported; BR: Batch Reactor; BRsh: Batch Reactor with shaking, BRs: Batch Reactor with stirrer, TR: Tubular Reactor, MFR: Mixed Flow Reactor

Table 2.2 (cont'd) Operating parameters for a high conversion efficiency of lipid to biodiesel with SCM.

| Researchers | T (°C) | P (MPa) | MeOH to Oil molar ratio | Reaction time (min) | Oil type | Reactor type | Heating and cooling rate (°C/sec) | ME content/ Conversion (%) |
|-----------------------|------------|--------------|-------------------------|---------------------|-------------|----------------------------|-----------------------------------|---|
| He et al. [11] | 310 to 320 | 32 | 40:1 | 25 | Soybean | MFR and 75-mL TR in series | N/R | 77% ME content (Uniform heating) 96% ME content (Gradual heating) |
| Minami and Saka [10] | 350 | 20 | 42:1 | 30 | Rapeseed | 200-mL TR | N/R | 87% ME content |
| Anitescu et al. [54] | 350 to 400 | 10.0 to 25.0 | 3:1 to 6:1 | 1 to 2.5 | Soybean | 7-mL TR | N/R | ~98% Conversion |
| Marulanda et al. [63] | 400 | 30 | 9:1 | 6 | Chicken fat | 2-mL TR | N/R | 80% ME content 99% Conversion |

N/R: Not Reported; BR: Batch Reactor; BRsh: Batch Reactor with shaking, BRs: Batch Reactor with stirrer, TR: Tubular Reactor, MFR: Mixed Flow Reactor

2.4.2.2. Pressure

Data on the effect of pressure on biodiesel production with SCM are limited since these reactions have principally been conducted in batch reactors. The pressure in a batch reactor cannot be controlled independently from density since it varies with the presence of both the reactants and products. In practice, the reaction pressure can be adjusted by altering the initial amounts of oil and methanol, calculated by the use of appropriate Equations of State and mixing rules for triglyceride and methanol [14], but the final pressure will deviate from its calculated value due to composition change during the reaction.

The effect of pressure on the extent of reaction can, however, be investigated with a tubular flow reactor in which the system pressure is controlled by a backpressure regulator. A wide range of operating pressures from 10 to 35 MPa has been investigated with respect to the maximum conversion efficiency to FAME. Below 20 MPa, the reaction pressure affects the ME content significantly within the temperature range of 270 to 350 °C, but the effect decreases above this pressure [11, 61] For example, at a temperature of 280 °C, a residence time of 30 min and a methanol to oil molar ratio of 42:1, the MEs content increases significantly from 55 % to 85 % as the pressure increases from 7.5 to 20 MPa, yet only slightly increases to 91 % at 35 MPa. The reaction pressure does not significantly affect the conversion efficiency at 400 °C, but rather slightly changes the composition of product [63]. At an operating pressure between 10 and 30 MPa at 400 °C, a methanol to oil molar ratio of 3:1 to 9:1 and a residence time of 3 to 10 min, complete conversion (>99 %) while approximately 80 % ME content was found [54, 63].

2.4.2.3. Methanol to oil molar ratio

The transesterification reaction requires a stoichiometric methanol to oil molar ratio of 3:1, while the operating ratio varies from 3:1 to 42:1. From Table 2.2, a ME content of the FAME produced at 270 to 350 °C was up to 95 % for a batch reactor and up to 85 % for a continuous flow reactor when a methanol to oil molar ratio of over 40:1 was employed. A high molar ratio of methanol increases the contact area and reduces the transition temperature (see Section 2.4.3.) [6].

Nevertheless, further increasing the methanol ratio above 50:1 yields no further benefits [11]. When a methanol to oil molar ratio of 6:1 to 9:1 at 400 to 450 °C is used, complete conversion can be achieved. Excess methanol is also consumed for other thermal reactions such as etherification of glycerol [63].

The relatively high methanol to oil molar ratio requires an enormous energy expense for recycling the excess methanol, as well as requiring a large volume of methanol within the recycle loop. In fact, energy plays an important role in the operating cost as well as the environmental load of biodiesel production with SCM. An LCA study revealed that biodiesel production by a single stage SCM transesterification consumes more energy in recycling the excess methanol than for feedstock pumping and reactor heating and also generates a significant environmental load [69]. Techniques to reduce the consumed energy for methanol recycle are urgently needed to develop practical green biodiesel production processes.

Diaz et al. introduced a medium pressure flash drum and heat pump to recover the excess methanol in biodiesel production by SCM at the methanol to oil molar ratio of 24:1 or 40:1 in their model-based cost minimization studies. The use of a heat pump significantly reduces the energy consumption and operating cost, rendering the operating costs at the methanol to oil molar ratio of 24:1 and a 40:1 to be only slightly different [59].

2.4.2.4. Reaction time

In general, the effect of the reaction time in a batch reactor can be studied and obtained simply by first heating the reactor to initiate the reaction, holding at this temperature for various times to allow the reaction to go to completion and then quenching the reactor to terminate the reaction. In contrast, the reaction time in a continuous reactor is estimated by the reactor volume over the volumetric flow rate and is influenced by a non-ideal flow behavior. The residence time is treated not as a single-value variable but rather is treated as an average value as shown in Table 2.2. The effect of reaction time will be discussed separately in the following section.

2.4.2.4.1. Batch reactor

The effect of reaction time on conversion efficiency in biodiesel production with SCM follows the general rate law. For instance, the ME content increases gradually with reaction time and then levels off when the maximum ME content or optimal point is achieved. The optimal reaction time varied between 4 to 30 min

The reactor heating and cooling rates need to be maximized for the best precision of reaction time measurement in batch reactor studies. For example, the accurate optimal reaction time obtained by Saka and Kusdiana [39], was by using the fastest heating rate (30 °C/s) and cooling rate (100 °C/s). For slow heating rate (0.33 °C/s), the optimal reaction time is lower than the actual value as the reaction can occur before the temperature set point is reached. On the other hand, during cooling, the reaction continues until the ambient temperature is reached. Saka and Kusdiana [6] used a molten tin bath as the heating medium whereas in other works, electrical heating was used. The difference in the heating source may affect the results.

The optimal reaction time, as assigned by the rate law, is a function of the temperature and concentration. Therefore, the optimal reaction time cannot significantly increase with the reactor volume in an isochoric system. However, the optimal reaction time in a larger batch reactor was observed to be higher than that of Saka and Kusdiana [6], probably because of some unconsidered effects, such as the degree of mixing intensity, as discussed in Section 2.4.2.5.

2.4.2.4.2. Continuous reactor (residence time)

Studies on the residence time in tubular reactors [40, 41] have employed the Equation (2.1):

$$\tau = \frac{V}{F_M \frac{\rho_M}{\rho'_M} + F_O \frac{\rho_O}{\rho'_O}} \quad (2.1)$$

Where τ is the residence time, V is the reactor volume, F is the volumetric flow rate at ambient conditions and $\frac{\rho}{\rho'}$ is the density ratio between the ambient and supercritical condition. The subscripts M and O refer to

methanol and vegetable oil, respectively. The density of SCM can be found from the literature [70], while the density of vegetable oil is assumed to be constant from ambient to system conditions.

The volumetric flow rate of a compressible fluid mixture depends on the mixture density, which is a function of pressure, temperature and composition. Therefore, changing the mole fraction as the reaction progresses and decreasing the pressure probably influences the volumetric flow rate in the isothermal system. It is clear that the mole fraction at the inlet and the outlet deviate largely with a declining methanol to oil molar ratio, as show in Table 2.3.

Table 2.3 Molar ratio and mole fraction at the inlet and outlet of the tubular reactor, calculated by assuming 100% conversion at the outlet.

| | | Molar ratio at inlet | | | | Molar ratio at outlet | | | |
|----------|----------|----------------------|-------|----------|----------|-----------------------|-------|----------|--|
| MeOH:Oil | Methanol | Oil | FAMEs | Glycerol | Methanol | Oil | FAMEs | Glycerol | |
| High | 42 | 1 | 0 | 0 | 39 | 0 | 3 | 1 | |
| Medium* | 24 | 1 | 0 | 0 | 21 | 0 | 3 | 1 | |
| Low* | 6 | 1 | 0 | 0 | 3 | 0 | 3 | 1 | |

| | | Mole fraction at inlet | | | | Mole fraction at outlet | | | |
|----------|----------|------------------------|-------|----------|----------|-------------------------|-------|----------|--|
| MeOH:Oil | Methanol | Oil | FAMEs | Glycerol | Methanol | Oil | FAMEs | Glycerol | |
| High | 0.98 | 0.02 | 0.00 | 0.00 | 0.91 | 0.00 | 0.07 | 0.02 | |
| Medium* | 0.96 | 0.04 | 0.00 | 0.00 | 0.84 | 0.00 | 0.12 | 0.04 | |
| Low* | 0.86 | 0.14 | 0.00 | 0.00 | 0.43 | 0.00 | 0.43 | 0.14 | |

* A small amount (0.1 mole per mole of methanol) of CO_2 was added as co-solvent but the CO_2 mole fraction is ignored for simplicity.

The global fluid density, as represented by the summation of the methanol and oil densities, is not appropriate at supercritical conditions. However, Equation (2.1) could be an acceptable approximation for a methanol to oil molar ratio of 42:1 to avoid the otherwise complicated calculation, because the fluid properties deviate slightly from those of pure methanol. The residence time estimation method has to be modified for varying volumetric flow rates

because it becomes important as the methanol to oil molar ratio is reduced as discussed in Section 2.4.4.

Equation (2.1) has been found to be adequate to estimate the residence time at high methanol to oil molar ratios (40:1 to 42:1) [9, 10]. The residence time significantly effects the conversion to FAMES at temperatures higher than 280 °C as the rate constant increases sharply beyond this temperature. For tubular reactor studies, Bunyakiat et al. [9] showed that the residence time impacts the conversion efficiency largely at temperatures higher than 300 °C, a finding which agrees with the work of Minami and Saka [10] who studied conditions at ~20 MPa and a 42:1 methanol to oil molar ratio. As for mixed flow and tubular reactors in series, He et al. [11] reported that the conversion increased strongly with a residence time above 280 °C, at 32 MPa and a 40:1 methanol to oil molar ratio. However, they did not present the detailed calculation of the residence time. The effect of residence time is related directly to the chemical kinetics of transesterification as illustrated in Section 2.4.2.

2.4.2.5. Mixing intensity and dispersion in tubular reactor

The effect of the mixing intensity has not been investigated directly according to the information summarized in Table 2.2. A high mixing intensity will enhance the rate of heat and mass transfer in the reactor and this will reflect upon the reaction time required for the maximum conversion.

With respect to batch reactors, the highest conversions can be achieved in a short time by shaking the reactor as the reaction progresses. For instance, the highest ME content of >95 % at ~ 4 min was found with shaking [6], while in similar studies but using a slightly different feedstock and elevated temperatures revealed high ME content but at ~30 min [66, 67], while in stirred batch reactors (250 mL) with a somewhat poor mixing behavior, the highest ME content was found after 30 min reaction time [53, 68]. In contrast, using a large reactor without shaking, Demirbas reported a high conversion to FAME of 95 % in ~ 5 to 11 min [7]. This seemingly conflicting result should be investigated further by varying the mixing intensity in a batch reactor equipped with a stirring mechanism.

For a tubular flow reactor, the reaction mixture is largely mixed by the fluid shear force that depends on flow patterns, which can be identified by the Reynolds number. At a high methanol to oil molar ratio, the Reynolds number calculation might be simplified by using the properties of SCM only, and is estimated by Equation (2.2).

$$\text{Re} = \frac{D(v\rho)}{\mu} \quad (2.2)$$

where D , $(v\rho)$ and μ are the tube inside diameter, total mass flux and dynamic viscosity, respectively.

Busto et al. [12] introduced an axial Péclet number, calculated by Equation (2.3), to describe the performance of the tubular reactor for biodiesel production with the SCM:

$$\text{Pe} = \frac{vL}{D_M} \quad (2.3)$$

where v , L and D_M are the fluid velocity, reactor length and molecular diffusivity, respectively. For estimation of the fluid velocity, the density of fluid was assumed to be pure methanol. They assumed that the molecular diffusivity of SCM was $5 \times 10^{-7} \text{ m}^2/\text{s}$. The Reynolds and Péclet number are calculated, base on the obtained from literatures, and are summarized in Table 2.4.

Some assumptions were made in calculating the results shown in Table 2.4. The mass flow rate was evaluated by the residence time and the methanol to oil molar ratio used was that at optimal conditions, except for the work of Bunyakiat et al. [9], where the data was available in our research group. The density of methanol, rapeseed and soybean oil at ambient conditions were assumed to be 792, 920 and 905 kg/m^3 respectively. Finally, He et al. [11] employed a gradual heating technique and, therefore, the density and dynamic viscosity of methanol were estimated from the average temperature between the inlet and outlet of the reactor.

Table 2.4 Optimal condition, reactor design, Reynolds and axial Péclet number of the continuous biodiesel production with SCM in a tubular reactor.

| Parameters | Bunyakiat et al. [9] | Minami and Saka [10] | He et al. [11] |
|--|-------------------------|-------------------------|-----------------------|
| Temperature (°C) | 350 | 350 | 340 |
| Pressure (MPa) | 19 | 20 | 32 |
| Methanol to oil molar ratio | 42:1 | 42:1 | 40:1 |
| Reactor inside diameter (m) | 7.75×10^{-3} | $1.20 \times 10^{-3**}$ | 4.00×10^{-3} |
| Reactor length (m) | 5.50 | 80.00** | 6.00 |
| Mass flow rate (kg/s) | 7.97×10^{-5} | 1.43×10^{-5} | 2.42×10^{-5} |
| Cross sectional area (m ²) * | 4.71×10^{-5} | 1.13×10^{-6} | 1.26×10^{-5} |
| Total mass flux (kg/m ² s) * | 1.69 | 12.69 | 1.93 |
| Fluid dynamic viscosity (kg/m s) * | 3.09×10^{-5} | 3.22×10^{-5} | 2.48×10^{-5} |
| Fluid density (kg/m ³) * | 188.80 | 197.53 | 541.19 |
| Fluid average velocity (m/s) * | 8.96×10^{-3} | 6.42×10^{-2} | 3.56×10^{-3} |
| Reynolds number * | 424 | 473 | 310 |
| Péclet number * | 9.85×10^4 | 1.03×10^7 | 4.27×10^4 |

* As calculated by the authors ** Values from personal communication

The performance of the FAME production with SCM in the tubular reactors can be interpreted via the Reynolds and Péclet numbers (Table 2.4), where the calculation of all reactors shows similar results. The Reynolds number indicates the effect of the mixing intensity, and the Péclet number indicates the effect of dispersion. All reactors are in a laminar regime at optimal conditions, so that, the maximum conversion is found at higher residence time than the reaction time in a batch reactor due to somewhat poor mixing intensity. All reactors have a Péclet number of over 1,000 and so their behavior are somewhat close to that of an ideal plug flow reactor and the effect of dispersion or back-mixing is diminished [12].

The performance of tubular reactors can be improved by increasing the mixing intensity; however, enhancing either the mass flux or the reactor diameter to maximize the Reynolds number is not an attractive idea. Both terms cannot be

increased simultaneously for the synergistic effect because the mass flux is inversely related to internal diameter at a fixed mass flow rate.

A better mixing intensity in the tubular reactor for biodiesel production with SCM can be achieved by other operations. The reduction of the fluid viscosity by adding some co-solvents, such as CO₂ or propane, can increase the Reynolds number. On the other hand, the addition of inert packing materials or static mixers into the tubular reactor can also enhance the mixing intensity. However, for tubular reactors with a small diameter, a static mixer is more interesting than packing material to avoid reactor channeling and plugging. In conclusion, further study into the effect of mixing intensity will be required to improve the efficiency of the supercritical process.

2.4.3. Chemical kinetics of biodiesel production with SCM

Transesterification rate equations were first proposed by Diasakou et al. [43] in 1998 and simplified by Kusdiana and Saka [39] in 2001. Since excess methanol is used, the methanol concentration is assumed to be constant during the reaction. Therefore, the simplified equation is pseudo-first order with respect to triglyceride concentration alone. The reaction rate constants for rapeseed oil transesterification at temperatures from 200 °C to 487 °C increase sharply at 280 °C [39]. Hegel et al. [56] found similar result using soybean oil and explained that the sharp increase was due to a phase transition from two-phase to single-phase. The evaluation of soybean oil transesterification over the temperature range of 210 °C to 280 °C shows that the rate constants increase sharply at the critical temperature of methanol (239 °C) [61]. On the other hand, rate constants of several vegetable oils fall onto one straight line from subcritical to critical and supercritical temperatures of methanol (200 to 400 °C) [66, 67, 71]. To extract more information, an overlay of Arrhenius' plot of various vegetable oils is shown in Figure 2.4 and the rate constants (k), pre-exponential factor (k_0) and activation energy (E_a) are summarized in Table 2.5.

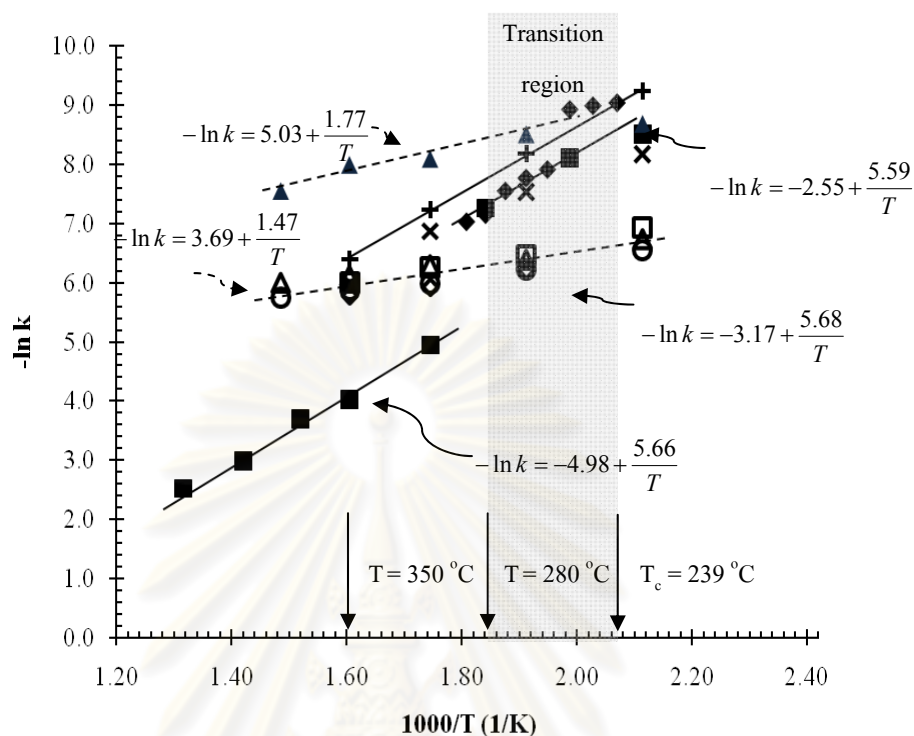


Figure 2.4. Overlay Arrhenius plot of (■) Rapeseed [39], (◆) Soybean oil [61], (▲) Sunflower [66], (□) Palm, (Δ) Groundnut, (○) *P. pinnata* and (◇) *J. curcas* [67] and (×) Castor and (+) Linseed oil [71] transesterification in the SCM reaction.

According to Figure 2.4, the slopes of the lines for each vegetable oil with SCM have different temperature sensitivities. For example, the rate constants of rapeseed, soybean, castor and linseed oils depend more strongly on the temperature than that for sunflower, palm, groundnut, *P. pinnata* and *J. curcas* oils.

He et al. [61] studies the effect of pressure on the conversion in the transition region (239 to 280 °C) and modifies the Arrhenius Equation by including the pressure term as shown in Equation (2.4):

$$k = k_0 \exp\left(-\frac{E^\ddagger + P\Delta V^\ddagger}{RT}\right) \quad (2.4)$$

where k , k_0 , E^\ddagger , ΔV^\ddagger , P , R and T are the rate constant, pre-exponential factor, activation energy, reaction activation volume, pressure, universal gas constant and temperature, respectively. The numerator in the parentheses ($E^\ddagger + P\Delta V^\ddagger$) implies the apparent activation energy of the reaction. From their experimental results [61], the product of activation volume and pressure ($P\Delta V^\ddagger$) contributes to approximately 10% of

the apparent activation energy at pressures above 20 MPa. The modified Arrhenius Equation provides a better estimate of the transesterification rate constant with SCM.

Table 2.5 Reactions rate constant (k) as linear function of temperature, pre-exponential factor (k_0) and activation energy (E_a)

| Researchers | Oil type | Investigated conditions | | | $\ln k = \ln k_0 - \frac{E_a}{RT}$ | | E_a (kJ/mol) |
|---------------------------|-------------------|--------------------------|----------------------|-------------------------------|------------------------------------|------------------------|-------------------|
| | | T (°C) | P (MPa) | MeOH to oil molar ratio | k_0 (s ⁻¹) | $\frac{E_a}{R}$ (K) | |
| Kusdiana and Saka [39] | Rapeseed | 200 to 270 300 to 487 | 7 to 12 19 to 105 | 42:1 | 0.30 6.87E-3 | 4.63 5.66 | 38.48 47.09 |
| He et al. [61] | Soybean | 210 to 230 240 to 280 | 28 | 42:1 | 514.96 5.85E-3 | 1.35 6.72 | 11.22 55.91 |
| Mardas et al. [66] | Sunflower | 200 to 400 | 20 | 40:1 | 0.39 | 1.77 | 14.74 |
| Rathone et al. [67] | Palm | 200 to 400 | 20 | 40:1 – | 2.60 | 1.80 | 14.94 |
| | Groundnut | | | 50:1 | 1.30 | 1.27 | 10.54 |
| | <i>P. Pinnata</i> | | | | 0.82 | 1.14 | 9.45 |
| | <i>J. Curcas</i> | | | | 1.68 | 1.37 | 11.37 |
| Verma et al. [71] | Castor | 200 to 350 | 20 | 40:1 | 0.54 | 4.21 | 35.00 |
| | Linseed | | | | 7.80E-2 | 5.59 | 46.50 |

Song et al. [72] studied the chemical kinetics of transesterification of refined, bleached and deodorized (RBD) palm oil with SCM. The rate constant was found by an integral method or numerical fitting of the experimental data to the kinetic model. However, they found that the second order rate Equation, with respect to both the concentration of oil and methanol, fit the data almost as well as the first order rate Equation. The rate constants that were predicted from the subcritical to the supercritical region were somewhat different from earlier works [39, 61]. However, the apparent activation energy of the transesterification reaction was nearly the same as that of Diasakou et al. [43] and also obeyed the second order model. Their kinetic model had a coefficient of determination of $R^2 = 0.9578$ and was able to predict the observed

conversion well. This model seems to be more suitable than the pseudo-first order model at a low methanol to oil molar ratio because the concentration of methanol is included in the model.

2.4.4. Phase behavior and binary vapor-liquid equilibrium (VLE) of biodiesel production with SCM

The phase behavior in biodiesel production with SCM has gained much interest due to the unusual behavior of the rate constant that increases with increasing pressure and the fact that the required optimal operating parameters can become milder with the addition of co-solvents.

Early works on the transesterification with SCM were based on the supercritical conditions of methanol, under which a single-phase mixture was assumed. However, more recent works on phase behavior, performed in a high-pressure view cell reveal that complete reaction can be obtained in either a single-phase supercritical or a two-phase VL region [56, 57]. For instance, the reaction between soybean oil and methanol at 300 °C and 9.6 MPa is observed as a two-phase VL, resulting in biodiesel with a ME content of 99% [56], while a single-phase supercritical mixture is observed beyond 350 °C and 10.0 MPa, with 99% triglyceride conversion [54].

Transition temperature of VLL to VL equilibria decrease with increasing methanol to oil molar ratios [54, 56]. For example, Anitescu et al. reported [54] that reaction mixtures are partially miscible up to temperature close to 350 °C at a methanol to oil molar ratio of 24:1, while Hegel et al. [48] observed that the two liquid phases become completely miscible at 180 °C and 157 °C with a methanol to oil molar ratio of 40:1 and 65:1, respectively.

Transition from a two-phase VL system to a one-phase supercritical system is found to occur near the critical temperature (T_c) of the mixture, as calculated from the methanol to oil molar ratio and co-solvents [54]. For instance, the critical temperature of the mixture predicted by Group Contribution with Association (GCA) EOS was 377 °C at a methanol to oil molar ratio of 24:1 [56] where the transition temperature observed is higher than 350 °C [54]. Marulanda et al. [65] also reported that a critical point of

triglyceride + methanol mixture has T_c of 300 and 400 °C at molar ratio of 42:1 and 6:1, respectively which corresponds with the optimal conditions for high conversion.

The addition of propane reduces the transition temperature of the two-phase VL to a one-phase supercritical. For example, the transition temperature at a methanol to oil molar ratio of 65:1 can be reduced from 315 °C (predicted T_c of 327 °C) to 243 °C (predicted T_c of 247 °C) when 24% by weight of propane is added to the reaction [56].

In actuality, the vapor-liquid equilibrium (VLE) of biodiesel production with SCM is complicated because the system is not only a multi-component one, but also is under supercritical conditions [73]. A biodiesel system can consist of 5 to 8 types of FAMES, reaction intermediates such as mono- and diglycerides, and a combination of FFAs in the triglyceride feedstock.

Binary systems have been investigated in some fundamental studies on the phase behavior in SCM, of major components and methanol and correlated with particular thermodynamic models summarized in Table 2.6, with the binary interaction parameters for the van der Waals (VdW) mixing rule being given in Table 2.7.

The binary VLE of triolein + methanol [19] and sunflower oil + methanol [14] were investigated at temperatures below the critical point of methanol so as to avoid the effects of interference due to composition changes as the transesterification reaction progressed. Since the exact molecular structure of sunflower oil is unknown, the critical properties of triolein are assumed, as estimated by Gani et al. [74, 75]. The Peng–Robinson (PR EOS) and the VdW mixing rule models have been tested on the sunflower oil + methanol system and give approximately 1 to 2 % relative deviation at temperatures below 220 °C. Therefore, it can be deduced that the PR EOS and VdW mixing rules can be used to predict the triolein + methanol system within the temperature range of 60 to 220 °C, due to the agreement between these two reports [14, 19].

Table 2.6 Studies on the VLE of biodiesel production with SCM summary.

| Researchers | Binary system | Measurement range | | Proposed thermodynamic model |
|-----------------------|--|-------------------|--------------|--|
| | | T (°C) | P (MPa) | |
| Tang et al. [19] | Triolein + MeOH | 60 – 190 | 6.00 – 10.00 | PR EOS and VdW mixing rule |
| Glišić et al. [14] | Sunflower oil + MeOH | 200 – 230 | 2.90 – 5.60 | RK-ASPEN EOS and VdW mixing rule |
| Shimoyama et al. [18] | Methyl myristate + MeOH Methyl laurate + MeOH | 220 – 270 | 2.16 – 8.49 | PRASOG model |
| Fang et al. [55] | FAMES C18 mixture + MeOH | 250 – 300 | 2.45 – 11.45 | PR EOS and VdW mixing rule |
| Shimoyama et al. [16] | Methyl myristate + MeOH Methyl laurate + MeOH | 220 – 270 | 2.16 – 8.49 | SRK, WS mixing rule and COSMO-SAC theory |
| Shimoyama et al. [17] | Glycerol + MeOH | 220 – 300 | 2.27 – 8.78 | PR-SV EOS and VdW mixing rule |
| Hegel et al. [56, 57] | Methyl oleate + Glycerol + MeOH + Propane | 270 – 315 | 7.00 – 21.1 | GCA EOS model |
| Glišić et al. [15] | Sunflower oil + MeOH | 150 – 210 | 1.1 – 4.5 | RK-ASPEN EOS and VdW mixing rule |

Flash calculations, using the Redlich-Kwong-ASPEN (RK-ASPEN) EOS and VdW mixing rules with optimized binary interactions [14], of the triolein + methanol system have been used for methanol to oil molar ratios of 42:1 to clarify the role of phase behavior on the rate constants. From the calculations, one can infer that a high rate of reaction takes place only in the vapor phase at low density, whereas in the liquid phase a low reaction rate mainly occurs. Thus, it can be concluded that biodiesel production with SCM at a methanol to oil molar ratio of 42:1 is a low-density vapor phase reaction.

Table 2.7 Binary interaction parameters of the VdW mixing rule which correspond with the thermodynamic model in Table 2.6.

| Researchers | EOS | Binary system | Binary interaction parameter | |
|-----------------------|-------|----------------------------------|-------------------------------------|------------------------------------|
| | | | k_{ij} | l_{ij} |
| Tang et al. [19] | PR | Triolein + MeOH | 0.0289 | -0.0109 |
| Glišić et al. [14] | RK- | Sunflower oil + | $\frac{-2.0000T(K)}{1000} + 0.6799$ | $\frac{1.7589T(K)}{1000} - 1.2175$ |
| | ASPEN | MeOH | | |
| Fang et al. [55] | PR | Methyl C18 esters mixture + MeOH | $\frac{-261.7100}{T(K)} + 0.6069$ | 0.1450 |
| Shimoyama et al. [18] | PR-SV | Glycerol + MeOH | $\frac{176.7000}{T(K)} - 0.3977$ | -0.0990 |

The binary VLE of methyl laurate (C₁₂) + methanol and methyl myristate (C₁₄) + methanol is found to correlate with the mole fraction of each phase using the Peng–Robinson Stryjek–Vera (PR-SV) EOS and ASOG mixing rule (PRASOG model) [18]. The FAMES C18 mixture + methanol [55] system have also been studied in a similar apparatus with the classical PR EOS and VdW mixing rules to model the system. The C18-methyl ester mixture + methanol system obeys the PR EOS and VdW mixing rule as equally well as did the triolein + methanol system, although the temperature range between the two systems was different.

The phase behavior of soybean oil + methanol + propane has been investigated and modeled by Group Contribution with Association (GCA) EOS [56, 57]. Unlike the previous works, which were aimed to fit the model to the composition of each phase, this work calculated the phase envelope of the final reaction mixture (methyl oleate + methanol + glycerol + propane) to study the role of phase behavior on conversion. The results show that the reaction mixture possibly becomes a single phase at lower temperatures by adding propane as co-solvent.

Studies on the VLE of biodiesel production with SCM shows that the initial (triglyceride + methanol) and final (FAMES + glycerol + methanol) reacting systems follow different thermodynamic models, and this is probably because of the changing polarity of the mixing fluids and that the polarity of the mixed fluids affects the

predictive ability of the model. For instance, the COSMO-SAC model is more predictive than the UNIFAC model for the FAMES + methanol system [16]. Therefore, it should be noted that no single thermodynamic model is available that can correlate the VLE of both the initial and the final states of the reaction system.

The VLE of sunflower oil + methanol was observed in high-pressure view cell and simulated composition profile during the reaction took place by ASPEN PLUS® software ® at 210 °C, 4.5 MPa and 42:1 methanol to oil molar ratio [15]. The mixture at the beginning of reaction is the equilibria of two liquids (methanol rich phase and oil phase) and one vapor phase (pure methanol). After 10 hours the reaction was complete and obtained single phase mixture of 52.3, 42.4 and 5.3 % by weight of methanol, FAMES and glycerol, respectively. The composition profile in each phase during the reaction took place was predicted well by thermodynamic model which proposed in their previous work [14].

2.4.5. Innovative technologies for milder operating parameters in biodiesel production with SCM

Elevated operating temperature, pressure and methanol to oil molar ratio are the primary obstacles for commercial scale biodiesel production with SCM, as mentioned in the introduction. The demonstrated techniques for lowering those operating parameters and the new parameters are summarized in Tables 2.8 and 2.9, respectively. The demonstrated techniques can be divided into three groups: (i) the addition of co-solvents, (ii) the addition of catalysts and (iii) the modification of the SCM reaction.

2.4.5.1. Addition of co-solvents

The addition of co-solvents can decrease the optimal operating parameters i.e. temperature, pressure and methanol to oil molar ratio because the co-solvents assist the VLL methanol-oil mixture transition to VL and become a single phase. Carbon dioxide is a good solvent for small and moderate sized organic molecules, while propane is an excellent solvent for vegetable oils. Small amounts of co-solvents, for example, 0.10 mole of CO₂ or 0.05 mole of propane per mole of methanol are typically used [8, 47] resulting in high conversion at relatively low

operating parameters because the co-solvents increase the homogeneity of the system and do not affect the reaction mechanism.

Table 2.8 Demonstrated techniques for reducing the operating parameters of biodiesel production with SCM.

| Researchers | Demonstrated technique | Lowered operating parameter |
|---------------------------|---|-----------------------------|
| Cao et al. [47] | Using propane as a co-solvent | T, P, M and t |
| Han et al. [8] | Using CO ₂ as a co-solvent | T, P, M and t |
| Anitescu et al. [54] | Using CO ₂ as a co-solvent | P, M and t |
| Wang et al. [48] | Using 0.5% (w/v) NaOH as a catalyst | T, P, M and t |
| Yin et al. [51] | Using 0.1% (w/v) KOH as a catalyst | T, P, MeOH and t |
| Wang et al. [50] | Using 0.2% (w/v) H ₃ PO ₄ as a catalyst | T, P and t |
| Demirbas [49] | Using 3% (w/v) CaO as a catalyst | T, P and t |
| Wang and Yang [52] | Using 3% (w/v) Nano-MgO as a catalyst | T, P, M and t |
| Minami and Saka [10] | Using two-step technology | T, P, MeOH and t |
| D'Ippolito et al. [13] | Using separated two tubular reactors | T, P and M |
| Marulanda et al. [64, 65] | Using high operating temperature | P, M and t |

T: temperature; P: pressure; M: methanol to oil molar ratio; t: reaction time

Anitescu et al. [54] suggested that biodiesel production with SCM should be carried out within the temperature range of 350 to 400 °C, a pressure range of 10.0 to 30.0 MPa and a residence time of 2 to 3 min with CO₂ as co-solvent. Under these conditions, they report that the decomposition (or dehydration) of glycerol takes place and the transesterification reaction is shifted forward. The authors claim that the inert co-solvent (e.g., CO₂) used to enhance the oil-alcohol miscibility may also act as diluents to slow down the FAME thermal decomposition. Since the addition of CO₂ increases the oil-methanol miscibility, the methanol to oil molar ratio can be reduced to 6:1 while maintaining nearly complete conversion. Additionally, they state that an enormous excess of methanol is not necessary within the temperature

range of 350 – 400 °C as the reaction occurs instantly at the inlet and then forms a homogeneous phase and reacts to completion shortly afterwards.

Table 2.9 New operating parameters of biodiesel production with SCM by the techniques outlined in Table 2.8.

| Researchers | T (°C) | P (MPa) | MeOH to Oil molar ratio | Reaction time (min) | Oil type | Reactor type | ME content/ Conversion (%) |
|---------------------------|--------|---------|-------------------------|---------------------|-----------|---------------|----------------------------|
| Cao et al. [47] | 280 | 12.8 | 24:1 | 10 | Soybean | 250-mL BRs | 98% ME content |
| Han et al. [8] | 280 | 14.3 | 24:1 | 10 | Soybean | 250-mL BRs | 98% ME content |
| Anitescu et al. [54] | 400 | 20.0 | 6:1 | 1.6 | Soybean | 7-mL TR | ~98% Conversion |
| Wang et al. [48] | 250 | 6.0 | 24:1 | 10 | Rapeseed | 200-mL BRs | 97% ME content |
| Yin et al. [51] | 160 | 10.0 | 24:1 | 10 | Soybean | 250-mL BRs | 98% ME content |
| Wang et al. [50] | 310 | 13.0 | 40:1 | 12 | Soybean | TR | 96% ME content |
| Demirbas [49] | 252 | N/R | 41:1 | 6 | Sunflower | 100-mL BR | 98% ME content |
| Wang and Yang [52] | 250 | 24.0 | 36:1 | 10 | Soybean | 200-mL BRs | 96% ME content |
| Minami and Saka [10] | 280 | 20.0 | 24:1 | 30 | Rapeseed | 200-mL TR | 95% ME content |
| D'Ippolito et al. [13] | 290 | 14.0 | 10:1 | N/R | N/R | TR | ~99% Conversion |
| Marulanda et al. [64, 65] | 400 | 10.0 | 6:1 to 9:1 | 4 | Soybean | TR | ~99% Conversion |

N/R: Not Reported; BR: Batch Reactor; BRsh: Batch Reactor with shaking, BRs: Batch Reactor with stirrer, TR: Tubular Reactor, MFR: Mixed Flow Reactor

Imahara et al. [76] hypothesized that the addition of CO₂ improves the conversion in a batch reactor because the system pressure is enhanced, since the pressure of the CO₂ containing system is higher than the base system, which consisted of methanol and vegetable oil in the isothermal reactor. The hypothesis was tested under mild conditions of 270 °C and 10.8 MPa for a slow reaction to clarify the effect of adding CO₂ on the conversion. However, it was found that the addition of CO₂ did not increase the ME content significantly in either batch or continuous reactors in a quasi-constant pressure. Moreover, an excess amount of CO₂ reduces the ME content due to the dilution and obstruction of the reactants.

Other co-solvents, such as N₂, hexane and THF, are presently being investigated for their effect on biodiesel production with SCM, but to date, the co-solvents evaluated do not significantly increase the conversion, specifically at high methanol to oil molar ratios where, for example, Imahara et al. [76] reported no benefit for a methanol to oil molar ratio of 42:1, but could not draw a conclusion for lower methanol to oil molar ratios. However, Anitescu et al. [54] observed a two-phase mixture of methanol and soybean oil at 400 °C and 20.0 MPa with a 6:1 methanol to oil molar ratio, which merged into a single phase with almost 100% conversion by the addition of 4% mole of CO₂ in methanol. In conclusion, additional studies on the effect of co-solvents at low methanol to oil molar ratios are necessary to clarify the role of co-solvents in biodiesel production with SCM.

In terms of product purification and co-solvent recycling, gaseous co-solvents, such as CO₂ and propane, are more attractive than liquid co-solvents. Only a small amount of gaseous co-solvents (0.1 mole per mole of methanol) are required for milder operating parameters, and these can be easily separated from the final product by expansion. While liquid co-solvents and methanol can be simultaneously recovered by distillation, as their boiling points are close to that of methanol (65 °C, 66 °C and 69 °C for methanol, THF and *n*-hexane respectively), this requires an additional energy input. On the one hand, hexane is immiscible in methanol, thus phase separation is necessary for hexane recycling. On the other hand, THF is completely miscible in methanol and improves the solubility of methanol in vegetable oils and forms a single phase mixture of vegetable oil/methanol/THF at

ambient temperature and pressure [77, 78]. Such phase behavior is beneficial as the methanol/THF mixture can be recycled directly, with only a small amount of methanol addition being required to replace that lost in each cycle. In conclusion, the addition of liquid co-solvents requires additional separation steps, while the addition of gaseous co-solvents requires only a few additional separation steps that offset its strong point in biodiesel production with SCM.

2.4.5.2. The addition of catalysts to the SCM reaction

By adding the appropriate catalysts, it has been shown that both the optimal temperature and reaction time become lower, but the methanol to oil molar ratio could not be reduced. For example, the addition of nano-MgO increases the rate constant some 11.2 fold from $4.20 \times 10^{-4} \text{ s}^{-1}$ to $4.72 \times 10^{-3} \text{ s}^{-1}$ at a temperature of 250 °C, and transesterification with nano-MgO catalysts reach the point of maximum conversion faster than that in the absence of the catalyst at low temperatures [52].

Wang et al. [48] studied the reaction of crude rapeseed oil in the SCM reaction with NaOH as a catalyst and reported that soap formation does not take place at supercritical conditions and that the rate of reaction is faster than that in the catalyst free condition. The crude rapeseed oil employed in their work had a 1% (w/w) moisture content and an unknown FFA content. In fact, the reaction between NaOH and the FFA occurs rapidly due to the strong opposite charges of both species. Thus, it can be deduced that the reaction between the SCM and the FFAs is possibly faster than that between the strong base and weak acid reaction, and as a result, the soap formation did not occur in the SCM reaction. When 0.1% (w/v) KOH was added [51], the reaction of refined soybean oil went to completion under milder conditions, as expected. On the other hand, in the investigation into the reaction of acidic and refined soybean oil with SCM, with and without the addition of H_3PO_4 as the catalyst, the acidic soybean oil provides a higher ME content than the refined oil, as the FFAs probably act as catalyst [50]. The addition of H_3PO_4 accelerates the reaction markedly because it is a stronger acid than the FFAs. Therefore, the presence of a weak acid in the feedstock, or the addition of H_3PO_4 , improves the ME content in the SCM reaction under these conditions.

In general, the addition of homogeneous catalysts to the SCM reaction is not an attractive idea, despite the faster resultant rate of reaction than the catalyst free process, because of the problems of subsequent product purification and waste management that are seen in the conventional process.

Heterogeneous catalysts, such as nano-MgO and CaO, have been applied for biodiesel production with SCM [49, 52], where maximum conversion is achieved at relatively low temperatures and pressures compared with catalyst-free conditions. The addition of heterogeneous catalysts to the SCM reaction is an attractive idea to lower the operating parameters, since the subsequent catalyst separation is easier and can be recycled, unlike the homogeneous catalysts. In conclusion, further studies on heterogeneous catalysts in the SCM reaction, such as the effect of water and FFAs, and the durability and reusability of catalysts, would be very interesting.

2.4.5.3. Modification of the SCM reaction

The first modification of the SCM reaction, namely the two-step or the Saka-Dadan process was presented by Minami and Saka. [10] In the first step, vegetable oils are hydrolyzed in subcritical water at 280 °C and 20.0 MPa to obtain fatty acid products. Then, glycerol and water are removed from the fatty acid products in a high-pressure phase separator. In the second step, the fatty acids are esterified in SCM at 280 °C and 20.0 MPa to biodiesel.

The two-step process reduces the harsh optimal operating parameters successfully due to several points. First, the hydrolysis reaction does not need to go to completion because all the glycerides (mono-, di- and tri-glycerides) are converted to FAMES in the next step. Second, mono- and di-glycerides have a higher reactivity than the triglyceride and so, these undergo almost complete reaction. Third, the esterification and transesterification reactions in the SCM reaction are driven forward as a result of the removal of the by-products (both water and glycerol). Fourth, the fatty acids have a somewhat better solubility in the SCM because they are relatively smaller molecules with a higher polarity than the triglyceride. Finally, Minami and Saka reported that the rate of the esterification reaction is enhanced since fatty acids act as acidic catalysts [10].

However, against the above is that the two-step process is more complicated than the single-step process, especially from the point of view of the process design, where it requires both more design and operating skills. The process has high-pressure reactors that connect in series with a high-pressure water-glycerol-FFA phase separator. Furthermore, the sweet water (aqueous solution of glycerol) stream, which is contaminated by trace amounts of FFAs, requires more separation units to manage. For instance, the distillation tower is the simplest separation unit for handling the sweet water, but consumes a large amount of energy to operate, being somewhat the same as in the case of methanol recycling.

The second modification of the SCM reaction, the dual-reactor process, was introduced by D'Ippolito et al. [13], who suggested the technique of employing two reactors with intermediate glycerol removal to lower the operating parameters. This technique has been studied in biodiesel production by homogeneous, heterogeneous and enzyme catalytic systems [79-81]. Computer simulation shows that by using this technique, the methanol to oil molar ratio and pressure can be reduced from 42:1 to 10:1 and from 14.0 to 10.0 MPa, respectively, but the temperature cannot be significantly reduced without loss of transesterification efficiency. These authors suggest that approximately 75% of the conversion can be achieved in the first reactor and that the reaction proceeds to completion in the next reactor. Although the dual-reactor process can significantly improve the economical feasibility of biodiesel production with SCM in computer simulations, it should be noted that the optimal operating parameters from simulation results were low and, this means that some experimental verification is still required.

The third modification of the SCM reaction was the increasing of operating temperature to 400 to 450 °C by Marulanda et al [64, 65]. The operating pressure, methanol to oil molar ratio and reaction time for complete conversion were reduced to values of 10.0 MPa, 6:1 and 4 min, respectively. Since the critical point of mixture depend on the methanol to oil molar ratio as mention in Section 2.4.4, the reaction mixture at 6:1 methanol to oil molar ratio can perform in single phase at 400 °C effectively.

According to the reactions of vegetable oil with SCM above 400 °C, the UFA is partially consumed by thermal degradation then the oxidation resistance or storage stability of the biodiesel is enhanced. Marulanda et al. [64, 65] reported that thermal degradation at 400 °C simultaneously converts UFA esters, triglyceride and glycerol to oxygenated liquid fuel with triglyceride conversion up to 99.5 % and without gaseous product loss. In addition, glycerol dehydration not only increases the fuel yield by up to 10 %, but also reduces the amount of glycerol by-products [82]. Given that the price of glycerol decreased in price by 1/10th of its value from 2004 to 2006 [83], the reduction in glycerol yield will have no detrimental consequence. Rather, the simultaneous conversion of glycerol to liquid fuel is an alternative option will increase the profitability of biodiesel production with SCM. Furthermore, the transesterification with SCM at 400 to 450 °C reduces the required reaction time by significantly enhancing the chemical kinetics of the transesterification and other side-reactions. The reactions of vegetable oil with SCM at 400 to 450 °C illustrate several advantages for biodiesel production with SCM, such as improvement of fuel properties, conversion of glycerol to liquid fuel and acceleration of the reaction kinetics.

Triglycerides conversion to biodiesel with SCM at 400 to 450 °C might ultimately lead to a biodiesel product that fails to meet the designated International standard (EN14214) as its ME content is less than 96.5 %. However, such a biodiesel product might be considered as an alternative biofuel that would require further studies on engine testing and fuel properties itself [63].

2.5. Literature reviews

Diasakou and coworkers studied on the thermal non-catalytic transesterification of soybean oil with methanol [43]. Experiments were carried out at temperature of 220 and 235°C, initial pressure of 5.5 and 6.2 MPa and methanol to oil molar ratio of 6:1 to 27:1 in a Parr reactor model 4560. After the reaction was finished, the samples withdrawn from the reactor were rapidly cooled and stored about 24 hours, a spontaneous phase separation occurred. The lower, heavy glycerol phase was glass clear, and the top, ester phase, were obtained. The ester phase was washed four times with water at 30 °C to

remove the possible traces of alcohol and glycerol and then analyzed. The samples were analyzed by thin layer chromatograph fitted with a flame ionization detector (TLC/FID). A reaction mechanism was proposed as a first order irreversible reaction and a corresponding kinetic model had fitted with the experimental data. The rate constants of the kinetic model were determined. It is observed that ME content has surpassed 85 wt% after 10 h reaction time at 235°C and 67 wt% after 8 h at 220°C.

Saka and Kusdiana investigated transesterification reaction of rapeseed oil with SCM [6]. The experiment was carried out in a 5-mL batch reactor made of Inconel-625 at temperature of 350 and 400 °C, pressure of 45 to 65 MPa, and with methanol to oil molar ratio of 42:1. The reactor was charged with a given amount of rapeseed oil (2.00 g) and methanol (3.36 g). Then, the reactor was shaken and quickly immersed into the molten tin bath at 350 or 400 °C, and kept for a set time (10 to 240 seconds). When the set time was achieved, the reactor was quenched in a water bath to stop the reaction. The content in the reactor was then allowed to settle for phase separation. The upper and lower portions were analyzed by HPLC. The lower portion was glycerol by comparing with standard glycerol chromatogram, and the upper portion was methyl ester. From the result, the optimal conditions found were temperature of 350 °C, pressure of 19.0 MPa and 240 seconds, with 98 % ME content in product.

Kusdiana and Saka studied the kinetic of transesterification reaction of rapeseed oil in subcritical and supercritical methanol within temperature range of 200 to 500 °C, pressure range of 10.0 to 65.0 MPa and methanol to oil molar ratio range of 3.5:1 to 42:1 [39]. The equipments and experimental procedure were employed from their previous work [6]. The results indicated that the rate of reaction increased dramatically in the supercritical region. It was evident that at subcritical temperature below 239 °C, the reaction rates were slow but much higher at supercritical state, with the rate constant increased by a factor of about 85 at the temperature of 350 °C. The reaction temperature of 350 °C was considered as the best condition, with the methanol to oil molar ratio being 42:1 and pressure of 45.0 MPa.

Demirbas investigated the transesterification of six vegetable oils (cottonseed, hazelnut kernel, poppy seed, rapeseed, safflower seed and sunflower seed) with SCM [7]. The study was carried out in a 100-mL reactor made of 316-stainless steel at reaction temperature in range of 177 to 350 °C and methanol to oil molar ratio in range of 1:1 to 41:1. In typical run, the reactor was charged with given amount of vegetable oil (20 to 30 g) and methanol (30 to 50 g). After each run, the gas was vented, and the content was poured into a collecting vessel, then the ME content was analyzed by GC. The optimal conditions were temperature of 350 °C, mole of methanol in vegetable oil of 41:1 and 200 seconds of reaction time, with product of over 95 % ME content.

Kusdiana and Saka investigated the effect of water and free fatty acid on the yield of methyl esters in transesterification of triglycerides and esterification of fatty acids as treated by SCM comparing with homogeneous catalytic process [41]. The reactor and experimental employed procedure the same as in their previous study [6]. For transesterification reaction, the presence of water (less than 5 %wt) and free fatty acid (less than 30 %wt) did not have a significant effect on the ME content, as complete conversions were achieved regardless of the content of water or free fatty acid. For acidic and basic catalyzed reaction, the ME content dramatically decreases with increasing water and free fatty acid content. For esterification reaction, the amount of water had a negative effect on the ME content which was catalyzed by both acidic and basic catalyst.

Warabi and coworkers investigated the reactivity of esterification and transesterification reaction with various alcohols (C_1 to C_8) with fatty acids (C_{16} to C_{18}) and rapeseed oil, respectively [46]. The reactor and experimental procedure employed were the same as in their previous study [6]. The reaction temperature was set at 300 °C in all experiments while the pressure varied due to vapor pressure each alcohol was unequal. The results showed that transesterification of rapeseed oil were slower than esterification of fatty acids for any type of alcohols. According to types of alcohol and reactivity, methanol was the most reactive, while 1-octanol was the less reactive, that was in correspondence with their critical point. Furthermore, saturated fatty acids such as palmitic and stearic acids had slightly lower reactivity than that of the unsaturated fatty acids such as oleic, linoleic and linolenic acid.

Madras and coworkers studied the transesterification of rapeseed oil and cottonseed oil in SCM and supercritical ethanol (SCE) [66]. The effects of temperature (200 to 400 °C) and methanol to oil molar ratio (40:1 to 42:1) were studied in a 8-mL batch reactor. The amount of methanol and vegetable oil were adjusted by trial and error to maintain the pressure of 20.0 MPa at desired temperature. This study indicated that the conversion in SCM was slightly lower than that in SCE, which was contrasting with Warabi and coworkers finding [46]. An explanation for higher conversions in SCE may be attributed to the solubility of the oil in the SCE system. The optimal conditions were 400 °C, 20 MPa and alcohol to oil molar ratio of 40:1 at 30 min for both alcohols. Moreover, this study investigated the enzyme-catalyzed biodiesel production in supercritical carbon dioxide (SCO₂), but only 30% conversions were obtained at optimal conditions.

Cao and coworkers prepared biodiesel from soybean oil with SCM and propane as co-solvent [47]. A 250-mL cylindrical reactor made of stainless steel, equipped with a magnetic stirrer and internal cooling was used. The reaction vessel was charged with a given amount of soybean oil (50 to 70 g) and methanol (60 to 80 g) with different molar ratios, and a known amount of propane was then added to the reactor as co-solvent. The addition of propane at the propane to methanol molar ratio of 0.02:1 to 0.1:1 in the reaction system significantly decreased the severity of the conditions required for the supercritical reaction. The optimal conditions found from this study were the temperature of 280 °C, the pressure of 13 MPa, methanol to vegetable oil molar ratio of 24:1 and propane to methanol molar ratio of 0.04:1.

Han and coworker investigated effect of carbon dioxide as co-solvent in biodiesel production from soybean oil in SCM [8]. The study was conducted in a 250-mL stainless steel reactor. The given amount of soybean oil, methanol and carbon dioxide were charged altogether in the reactor. The addition of carbon dioxide significantly reduced the optimal conditions of production biodiesel with SCM. The optimal amount of carbon dioxide was 0.1 per mole of methanol. At the temperature of 280 °C, the pressure of 13 MPa and methanol to vegetable oil molar ratio of 24:1, nearly complete conversions were obtained. The results from this work were similar with the addition of

propane as co-solvent [47]; carbon dioxide is non-flammable, it is more appropriate than propane.

Bunyakiat and coworkers invented the continuous production of biodiesel by the transesterification reaction of coconut oil (CCO) and palm kernel oil (PKO) in supercritical methanol without using any catalyst [9, 44]. The oil and methanol were pumped in two different lines by HPLC pumps, preheated separately while flowing in the coil preheaters. After preheating, the two lines were mixed at the reactor inlet. Both the preheat lines and the reactor were immersed in an electrically heated salt bath. Experiments were studied at 270, 300 and 350 °C at a pressure of 10.0 and 19.0 MPa with various methanol to oil molar ratios from 6:1 to 42:1. It was found that the best condition to produce biodiesel from CCO and PKO was; reaction temperature 350 °C; methanol to vegetable oil molar ratio 24 and residence time 400 seconds. The ME content was 90 % and 85 % for CCO and PKO, respectively. The produced methyl ester fuel properties met the specification of the ASTM biodiesel standards.

He and coworkers developed the continuous system for transesterification of vegetable oil with SCM in a tubular reactor [11]. Increasing the methanol to vegetable oil molar ratio, reaction pressure and reaction temperature enhanced the ME content in the product effectively. However, thermal degradation of unsaturated fatty acid (UFAs) methyl esters occurred when the reaction temperature was over 300 °C, leading to loss of material. The optimal reaction condition under isothermal process was 310 °C, 35 MPa, 40:1 methanol to vegetable oil molar ratio at 25 min of residence time; whereas, the maximum ME content was only 77%. Consequently, they proposed a gradual heating to solve the thermal degradation of UFAs, then ME content could be increased to 96 %.

Minami and Saka studied kinetics of triglyceride hydrolysis in subcritical water and fatty acid methyl esterification in SCM for biodiesel production in a two-step process in a continuous tubular reactor [10]. The objectives of this paper were two folds; to obtain the high-quality biodiesel fuel and to reduce the temperature and pressure at optimal condition. In the two-step method, backward reaction of glycerol with methyl esters can be suppressed because glycerol is removed prior to methyl esterification. The high-quality biodiesel fuel can be produced, which has low total glycerol content comparing with the one-step method [6]. The hydrolysis of triglyceride in subcritical

water and methyl esterification in supercritical methanol can allow more moderate reaction conditions (270 °C, 7 to 20 MPa and 1:1 v/v water to oil or methanol to oil ratio). Furthermore, initial fatty acid in vegetable oil was found to act as acid catalyst, and simple mathematical models were proposed in which regression curves could fit well with experimental results. The optimal condition of this process was 270 °C and 24:1 methanol to vegetable oil molar ratio, that was milder than the one-step process [6].

He and coworkers investigated transesterification kinetic of soybean oil with supercritical methanol at temperature range of 200 to 280 °C and pressure range of 8.7 to 36 MPa in 200-mL batch reactor [61]. The apparent activation energies were found different with the subcritical and supercritical temperature of methanol, which were 11.2 and 56.0 kJ/mole, respectively. The reaction pressure considerably influenced the ME content in the pressure range from ambient pressure up to 25.0 MPa (280 °C, 42:1). At pressure below 15.5 MPa, the pressure had a considerable impact on the ME content, for instance, the ME content increased from 56.1 % at 8.7 MPa to 81.7 % at 15.5 MPa. However, the influence of pressure on ME content was small within the at pressure range of 15.5 to 25.0 MPa and it was negligible above 25.0 MPa. The effect of pressure on the rate of reaction could be interpreted with the transition-state theory that was described by the reaction activation volume (ΔV^\ddagger) in Equation (2.4). At pressure of 28 MPa, the product between the reaction activation volume and pressure accounts for 10.3% of the apparent activation energy.

Varma and Madras investigated the kinetics of biodiesel production with SCM and SCE from 200 to 350 °C at 200 bar [71]. The kinetics of the reaction was assumed to be the first order, and the activation energies were determined. The rate constants for the transesterification in SCM were influenced by the composition of the vegetable oils. For example, the rate constants decreased with amount of saturated and mono-unsaturated fatty acid in vegetable oils. This clearly shows that the transesterification reaction rate in SCM was the highest for the triglycerides of saturated fatty acid followed by triglycerides of unsaturated acids. The activation energies determined from the slope of the regressed line of Arrhenius plot are 35, 55, 46.5, and 70 kJ/mole for castor oil methyl ester, castor oil ethyl ester, linseed oil methyl ester, and linseed oil ethyl ester, respectively.

Kasteren and coworkers described a process model to estimate the cost of industrial scale biodiesel production from waste cooking oil with SCM [60]. A continuous production of biodiesel from waste cooking oil model has been studied for three plant capacities (125,000, 80,000 and 8,000 tones biodiesel/year) by ASPEN Plus® simulation software ®. It was found that biodiesel with SCM can be scaled up yielding high purity of methyl esters (99.8%) product and almost pure glycerol (96.4%) attained as by-product. The economic assessment of the biodiesel plant shows that biodiesel can be sold at US\$ 0.17/L for the largest capacity, US\$ 0.24/L for the medium capacity and US\$ 0.52/L for the smallest capacity. The sensitive key factors for the economic feasibility of the plant were ranked as raw material price, plant capacity, glycerol price and capital cost. Overall conclusion was that the process can technically and economically compete with existing alkali and acid catalyzed processes, especially for using waste cooking oil as feedstock.

Busto and coworkers studied the influence of the axial dispersion on the performance of tubular reactors during the transesterification vegetable oil in supercritical methanol [13]. The miscibility of the FAME + MeOH + TG system was measured at various methanol to oil molar ratios, 40 °C and 0.1 MPa. Furthermore, the Pressure-Temperature curve was determined in a 32-mL autoclave vessel at various methanol molar to ratios at temperature range of 40 to 300 °C and pressure range of 0.1 to 20 MPa. The miscibility of the FAME + MeOH +TG system, Pressure-Temperature diagram and kinetic data from the other literatures [39] were used to predict the conversion by computer simulation. The axial dispersion was described by Péclet Number, $Pe = Lu/D_M$; L is length of the reactor; u is the space velocity; and D_M is molecular diffusivity. The lower Pe number decreased global conversion by performs the back-mixing phenomena, while it increased with temperature and methanol to oil molar ratio. In conclusion, the Pe number should be in the range of 100 to 1000 to diminish the effects of back-mixing phenomena in tubular reactors and residence time should also be equal or lower than an hour, while axial lengths cannot be lower than 2 meters.

Imahara and coworkers investigated thermal stability of biodiesel as prepared by SCM process [58]. Due to conditions in high temperature and high pressure, biodiesel prepared may possibly be thermally degraded. Thermal stability of pure FAME and actual biodiesels from various feedstocks was studied, and discussed the effect of thermal degradation on fuel properties, mainly cold flow properties. It was found that polyunsaturated methyl esters such as methyl linoleate and methyl linolenate were partly decomposed and isomerized from *cis*-type to *trans*-type at the temperature higher than 300 °C. These behaviors were also observed for actual biodiesel fuels prepared from linseed and safflower oils, which consist of high polyunsaturated fatty acids. However, their temperatures of cloud point and pour point are not significantly changed above 300°C after exposure to SCM.

Demirbas investigated biodiesel production in supercritical methanol with calcium oxide [49]. The experiments were performed in a 100-mL reaction vessel equipped with a magnetic stirrer. The calcium oxide (60 to 120 mesh) was soaked in methanol with vigorous stirring in another small reactor before adding into reaction vessel. The catalytic transesterification ability of CaO was quite weak under ambient temperature. For instance, the ME content was observed only to be 5 % in 3 hours at temperature of 62 °C, while the addition of CaO at higher temperature evidently increased the rate of reaction. The transesterification reaction was essentially completed (over 99%) at 253 °C within 6 min with 3 wt% CaO and 41:1 methanol to oil molar ratio that approximately 2.5-fold faster than non-catalytic process.

D'Ippolito and coworkers proposed a process design in order to minimize the heat consumption and pumping power in biodiesel production with SCM. The two reactors with intermediate glycerol removal are used coupling with a heat recovery by heat exchangers and adiabatic flash drums were proposed. A computer simulation was built with experimental and literatures data. The operation mode and the process conditions were determined on the basis of the minimization of the energy consumption (heat duty, cooling services, pumping power) and the fulfillment of product quality constraints (maximum amount of bound glycerin and methanol in biodiesel). The results indicate that carrying out the transesterification reaction in two reactors enables the use of a low methanol to oil molar ratio of 10:1 – 15:1. The preferred operation mode

designed first reaction stage in the perfectly mixed state and the second reaction stage in plug flow mode. The process design under these conditions not only can reduce the total pressure of the system but also recover the sensible heat of the product outlet stream which can be used to completely vaporize the unreacted methanol in final product.

Glišić and coworkers discovered vapor-liquid equilibria (VLE) of triglycerides + methanol mixtures at different temperatures between 200 and 230 °C, and a range of pressures between 1.0 and 5.6 MPa in a 2000-mL batch reactor [14]. The vapor and liquid phase samples were taken from the bottom and top of the reactor, respectively, then methanol was evaporated and subsequently the triglycerides content present in both the liquid and vapor phase was determined gravimetrically using a high precision analytical balance. The experimental data were correlated using the Peng-Robinson, Soave-RK and RK-ASPEN equations of state and different mixing rules. The best results were obtained with the RK-ASPEN EOS and the VdW mixing rule, which was then used to calculate the distribution of the phases at designed pressures and temperatures use for biodiesel production with SCM.

Shimoyama and coworkers introduced activity coefficient models since they are usually predictive without needing to optimize the entire binary interaction parameters to available VLE data [16]. The authors reported that the COSMO-Segment Activity Coefficient (COSMO-SAC) model was suitable for use with a high-pressure system, including both polar and non-polar components. The COSMO-SAC model was compared with the Universal Functional Activity Coefficient (UNIFAC) model using SRK EOS and Wong-Sandler (WS) mixing rules [84]. The COSMO-SAC model gave a better estimation for the methyl myristate + methanol and methyl laurate + methanol systems than PRASOG model [18]. Unfortunately, the authors did not predict the C18-methyl ester mixture + methanol VLE using COSMO-SAC model [16].

Shimoyama and coworkers also studied the VLE of the glycerol + methanol system using the PRASOG model to correlate the data, comparing with the PR-SV EOS and VdW mixing rules [17]. Interestingly, the PRASOG model without interaction parameters predicted the vapor phase composition more precisely than the VdW mixing rules with adjusted binary interaction parameters. However, the calculated results derived from the PR-SV EOS and VdW mixing rules with two adjustable parameters have a

lower average relative deviation in both the liquid and vapor phases than those derived from the PRASOG model.

Glišić and Skala analyzed the energy consumption in biodiesel production with SCM by ASPEN Plus® simulation software [85]. This study analyzed the existing and recently published data related to design of larger scale plant for biodiesel production with SCM and illustrated the problem of insufficiency of the previously in the literature published. The continuous process flow sheets for biodiesel production (10,000 ton/year) with SCM and homogenous catalytic conventional was constructed by using the thermodynamic model which proposed in their previous work [14]. This study indicated that sensitivity of energy balance calculation depended strongly on thermodynamic models for representing a real complex mixture. Although the biodiesel production with SCM consumes large energy in reaction step, but a small amount of energy could be used for biodiesel and glycerol purification. In conclusion, the total energy consumption was 2326kW for conventional process and 2407kW for SCM process.

Kiwjaroun and coworkers employed the Life Cycle Assessment (LCA) as a tool to study the environmental impact of biodiesel production by homogeneous catalytic and SCM process from refined and crude palm oil [69]. The energy consumption for 10,000 ton/year capacity plant of each process was calculated in HYSIS ® process simulator with the NRTL and UNIQUAC as thermodynamic model. It was found that the supercritical process always generated a higher impact on the environment for both crude palm oil and refined palm oil due to it required large amounts of methanol during the reaction and consequently the energy consumption in methanol recirculation in the recycle loop. For instance, the SCM process at 42:1 methanol to oil molar ratio had 18,140 kg/h of methanol in recycle loop, compared to only 1,400 kg/h in the conventional process. Therefore, the energy consumption for methanol recycling has to be reduced by additional technique such as replacing the dilation column with medium pressure flash drum [59] or innovative technologies as mention in Section 2.4.5. to make the SCM process feasible from the environmental point of view.

Wang and Yang employed nano-MgO as a catalyst for biodiesel production by soybean oil with SCM [52]. The experiments were carried out in a 200-mL batch reactor (diameter 50 mm, height 128 mm) with a magnetic stirrer. It was observed that the transesterification reaction was essentially completed at 230 °C within 10 min with 3 wt% nano-MgO and the methanol to oil molar ratio of 36:1. Such high reaction rate with nano-MgO was mainly owing to the lower activation energy of 75.94 kJ/mol. However, the activity of nano-MgO was slightly lower than the 60 to 120 mesh CaO as reported by Demirbar [49].

Demirbas used waste cooking oil as a feedstock to produce biodiesel with SCM comparing with homogeneous catalytic process [42]. The presence of free fatty acids (FFA) and water always produced negative effects in homogeneous catalytic process, whereas FFA react with methanol to perform biodiesel in SCM process. The effect of temperature and methanol to oil molar ratio were investigated in a batch reactor as described in his previous work [7]. In conclusion, the 98 % ME content was obtained from waste cooking oil at 300 °C and 40:1 methanol to oil molar ratio within 20 min of reaction time while approximately 85% ME content was observed at 60 °C with 6%wt of KOH and 24:1 methanol to oil molar ratio and 2 h reaction time.

CHAPTER III

EQUIPMENTS AND EXPERIMENTAL PROCEDURES

3.1. Effect of co-solvents

3.1.1. Equipments

First, the effect of co-solvents was studied in a 250-mL batch reactor (Parr Instrument Company, model 4576), equipped with a mechanical stirrer and internal cooling. The reactor was heated with an external electrical heater. The maximum pressure and temperature values of the equipment were 50 MPa and 500°C, respectively. The temperature of the reactor was measured with a j-type thermocouple and controlled at $\pm 5^\circ\text{C}$ for a set time. The pressure of the reactor was measured with a pressure gauge and transducer.

As the highest ME content obtained from the 250-mL reactor was slightly lower than expected, the effect of co-solvent was studied in a smaller batch tube reactor, whose dimension was 9.525 mm O.D., 0.213 mm thickness and 200 mm length. The total volume was 5.5 mL. The reactor was heated by immersion in a fluidized sand bath and the temperature was measured by a k-type thermocouple.

3.1.2. Materials

Crude palm kernel oil (PKO) was supplied by Chumporn Palm Oil Industry, PCL. The sample was warmed and filtered prior to use. Commercial grade methanol, hexane (mixture of C6 isomers containing more than 65% n-hexane) and tetrahydrofuran (THF) were used with no further purification. All standard methyl esters for gas chromatograph calibration and methyl undecanoate (internal standard) were supplied by Fluka. Analytical grade carbon disulfide (CS_2), which was used as a dilution solvent for the gas chromatograph, was supplied by Merck.

3.1.3. Experimental procedure

3.1.3.1. The 250-mL reactor

The reaction vessel was charged with a given amount of vegetable oil, methanol and co-solvent and was then heated to the desired temperature. The reaction time and stirring speed were fixed at 10 min and 500 rpm, respectively, for every experiment. At the end of the reaction, the reactor was quenched in an ice-water bath to about room temperature and pressure. The content in the reaction vessel was weighed and put in a

rotary evaporator to remove the solvent phase (co-solvent and methanol). The oil phase was left to settle for at least 8 hours in a separatory funnel to ensure complete separation. Two liquid phases were obtained; ester (top layer) and crude glycerol (bottom layer). The ester layer was then analyzed for ME content.

3.1.3.2. The 5.5-mL reactor

The reaction vessel was charged with a given amount of PKO, methanol and co-solvent and was immersed in a fluidized sand bath at the designed temperature and was shaken manually from time to time to ensure uniform mixing. The reaction time was held constant at 10 min. At the end of the reaction, the reactor was then quenched in an ice-water bath to stop the reaction. The solvent phase was then evaporated by warming in a water bath at 80°C for 2 hours. Glycerol was separated by centrifuging at 4000 rpm for 10 min. The ester (top layer) phase was then analyzed for %ME content.

3.1.4. Analysis of methyl esters

For the ME content measurement, a gas chromatograph (Varian Model CP-3800), equipped with a capillary column coated with polydimethylsiloxane (30 m x 0.25 mm x 0.25 µm, DB-1, J&W Scientific) and an FID detector, was used with helium as carrier gas. The ester product and the known amount of internal standard was diluted with CS₂ before injection and standardized by the internal standard method. The temperature of the injection port and detector were 250°C and 280°C, respectively. The column oven was held at 110°C for 2 min and then raised to 260°C at 15°C/minute. The final temperature was held constant for 10 min.

The ME content was calculated from their content in the biodiesel product as analyzed by GC. The content (or purity) was defined as a ratio of the weight of methyl esters, as obtained from GC, to the total weight of the biodiesel product.

For the GC-MS analysis, a Shimadzu Model GCMS-QP2010 gas chromatograph coupled with a mass spectrometer and equipped with a capillary column coated with polydimethylsiloxane (30 m x 0.25 mm x 0.25 µm, DB-1ms, J&W Scientific) was used with helium as carrier gas. The biodiesel sample was diluted in CS₂ before injection. The injection port, ion source and interface temperature were 250, 200 and 230°C, respectively. The molecular weight scan range was 50-800 m/z and 3 min of solvent cut time. The column was held at 90°C for 5 min and then raised to 260°C at 20°C/minute. The final temperature was held constant for 10 min.

3.2. Effect of additional parameters and scale-up reactor optimization

3.2.1. Equipments

3.2.1.1. The scale-up reactor

A coiled tubular reactor made from stainless steel (SUS316 tubing of 9.525 mm O.D., 0.138 mm-thickness) was employed. The reactor received oil/hexane mixture and methanol, preheated separately in a coiled preheater made from stainless steel (SUS316 tubing of 3.175 mm O.D., 0.094 mm thickness). Both reactor and preheater were immersed in a molten salt bath. The molten bath was electrically heated and controlled by a temperature controller (Sigma Model SF48). Temperature sensors were equipped at reactor inlet, molten salt bath and heater. The inlet was connected with a high pressure pump (Thar technology Model P-50 and P-200), while the outlet was connected to a cooling coiled tube immersed in a cooling bath. The outlet was equipped with a Tee type filter (140 μm), a pressure sensor (Kyowa Electronic Instruments Model PGM-500KE) and a back pressure regulator (Go-regulator Model BP-66). The inlet pressure was monitored by high pressure pump software and outlet pressure was monitored by Hengstler Process Indicator Model 0735A60000. Complete experimental setup is shown in Figure 3.1.

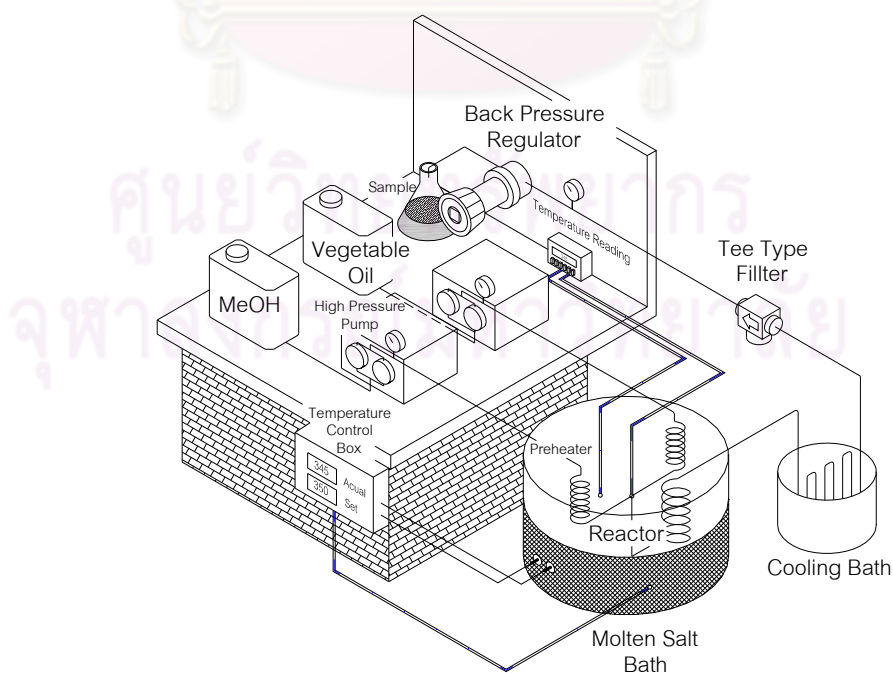


Figure 3.1 Schematic diagram of scale-up tubular reactor for biodiesel production with SCM.

3.2.1.2. The 250-mL and 5.5-mL reactors

The 250-mL and 5.5-mL batch reactors are described in section 3.1.1.

3.2.2. Materials

Palm kernel oil (PKO) sample was warmed and filtered prior to use. Commercial grade methanol and hexane (mixture of hexane isomers contain more than 65% of n-hexane) were used with no further purification. Standard mixture methyl esters that has composition refer to Lauric oil were supplied by Restek. A mixed molten salt consisted of NaNO_3 , NaNO_2 and KNO_3 (1:5:6 weight ratio) was used as a heating medium for both the preheaters and the reactor.

3.2.3. Experimental procedure

3.2.3.1. The scale-up reactor

The methanol and vegetable oil mass flow rate was measured by weighting method at the outlet high-pressure pumps before feeding the reactants into the reactor. The molten salt bath was first heated to designed temperature before feeding the reactants, after inlet and outlet flow rate were approximately equal; the back pressure regulator was then closed to increase the system pressure. When the system reached steady state, as noticed from a constant ME content over 90 min, the product was collected. The liquid product was weighed and put in a rotary evaporator to remove solvent phase. Oil phase was left to settle for several hours in a separatory funnel, preferably overnight, to ensure complete separation. Two liquid phases were obtained, ester (top layer) and crude glycerin (bottom layer). The ester layer was measured for %ME content.

3.2.3.2. The 250-mL and 5.5-mL reactor

The experimental procedure described in Section 3.1.3.1 and 3.1.3.2 were used to study the effect of reaction time on ME content, temperature gradient between reactor wall and bulk fluid and effect of contaminants in crude PKO.

3.2.3.3. The 5.5-mL reactor to investigate the effect of delay quenching time

The reaction vessel was charged with a given amount of methanol and palm kernel oil at molar ratio of 42:1 was immersed in a fluidized sand bath at 350°C and was shaken manually from time to time. The reaction time was held constant at 10 min The

reactor was then allowed to stand at ambient temperature for varying time then quenched in an ice-water bath. The samples were treated before analyzed employing the same method as described in section 3.1.3.2.

3.2.4. Analysis of methyl esters

The ME content in biodiesel samples were measured by employing the same method described in section 3.1.4.

3.3. Residence time estimation method

3.3.1. Equipments

A coiled tubular reactor (SUS316 tubing of 1/8 in.-o.d., 0.028 in.-thickness and 80 m-length) and two coiled preheaters (SUS316 tubing of 1/8 in.-o.d., 0.028 in.-thickness and 6 m-length) were employed. Both reactor and preheater were immersed in a molten salt bath. The k-type thermocouples were equipped at reactor inlet, outlet and molten salt bath. The inlet was connected with a high pressure pump, while the outlet was connected to cooling bath, an inline filter (0.50 μm), a pressure gauge (Swagelok PG5000) and a back pressure regulator (Go-regulator Model BP-66). The schematic diagram of the reactor is shown in Figure 3.2.

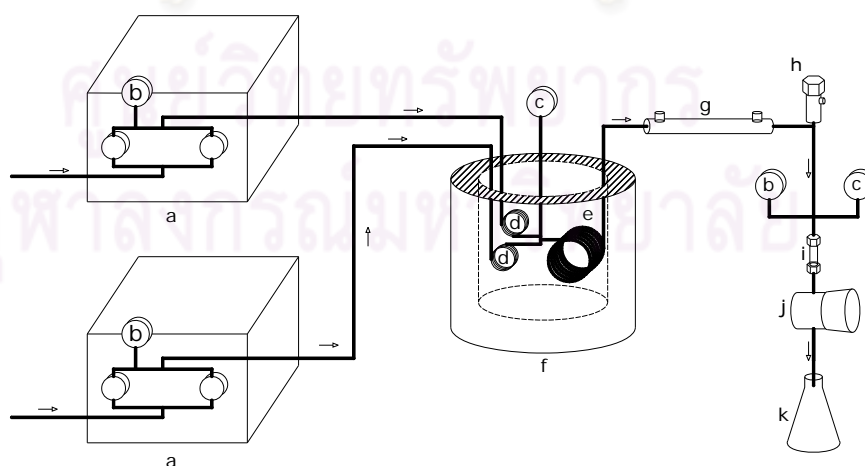


Figure 3.2 Schematic diagram of lab-scale tubular reactor (a) high pressure pump (b) pressure gauge (c) thermocouple (d) preheater (e) reactor (f) molten salt bath (g) double pipe heat exchanger (h) relief valve (i) back-pressure regulator (j) inline filter and (k) sampling flask.

3.3.2. Materials

Commercial grade methanol from I.C.P. Chemicals Co.,Ltd and palm olein oil (major fatty acids composition are palmitic acid 37 %, oleic acid 46 % and linoleic acid 11 %) from Morakot Industries Co., Ltd were used with no further purification. The analytical grade methyl heptadecanoate (99.5 %) and n-heptane (99.5 %) for measurement of ME content in biodiesel were supplied by Fluka and Fisher, respectively.

3.3.3. Experimental procedure

A molten salt bath heated to the reacting temperature was used for temperature control and methanol and vegetable oil mass flow rate was measured by weighting method at the outlet high-pressure pumps before feeding the reactants into the reactor. After temperature stabilization of the bath, palm olein oil and methanol, separately preheated in tubular preheaters made from stainless steel (SUS316 tubing of 1/8-in.-o.d., 0.028-in. thickness and 6 m-length), were pumped into the reactor. Both reactor and preheaters were immersed in a molten salt bath. The K-type thermocouples were set at reactor inlet, outlet and molten salt bath. After the outlet flow was steady, the back pressure regulator was closed to increase the pressure of the system. After system pressure was constant, approximately 3 hours generally required for the system to reach a steady state, three biodiesel products were then sampled at 15 min intervals and analyzed for ME content following the EN14103 standard method.

3.3.4. Analysis of methyl esters

The ME content was measured by EN14214 standard method using Shimadzu Model GC-14B SPL gas chromatograph equipped with auto injector model AOC-17 and DB-WAX capillary column (30 m length, 0.25 mm i.d. and 0.25 μm thickness) from J&W Scientific. The temperature of the injection port and detector were 250 °C and 300 °C, respectively. The column oven was held at 120 °C for 2 min and then raised to 260 °C at 10 °C/minute. The final temperature was held constant for 5 min.

CHAPTER IV

EFFECT OF CO-SOLVENTS

4.1. Reaction among vegetable oil, methanol and co-solvents

To ensure that the reaction between co-solvent and other reactants did not occur, the GC-MS chromatograms of mixed methyl esters standard and biodiesel products, obtained from employed THF at 350 °C and the methanol to oil molar ratio of 42:1 and THF of 5 mol in vegetable oil at reaction time of 10 min, were obtained as illustrated in Figures 4.1 and 4.2.

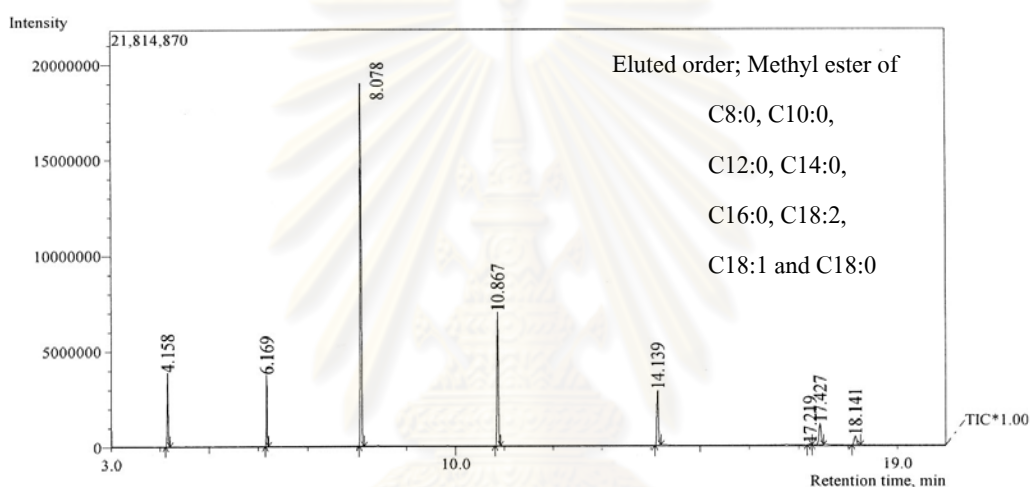


Figure 4.1 GC-MS chromatogram of mixed methyl esters standard.

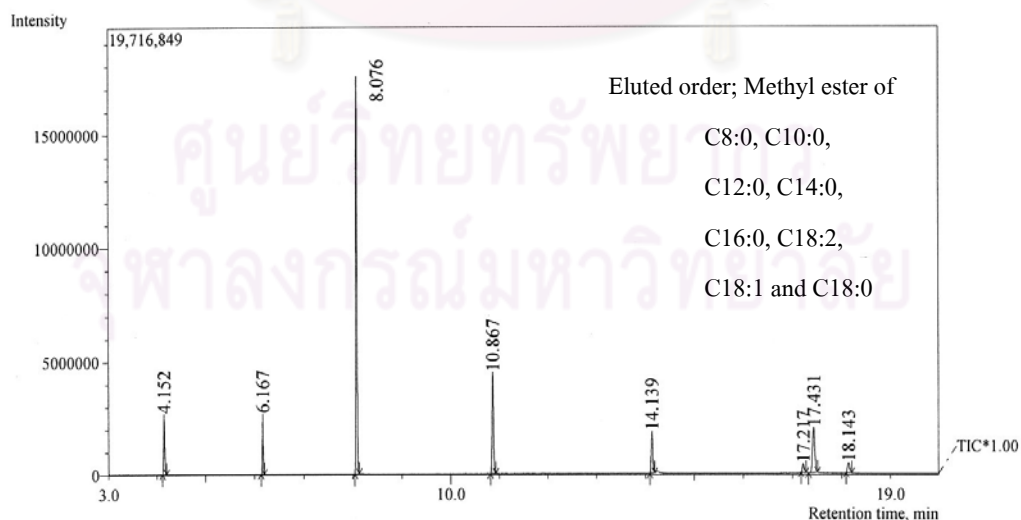


Figure 4.2 GC-MS chromatogram of biodiesel from employed THF process in 250-mL reactor for 10 min with crude PKO as reactant.

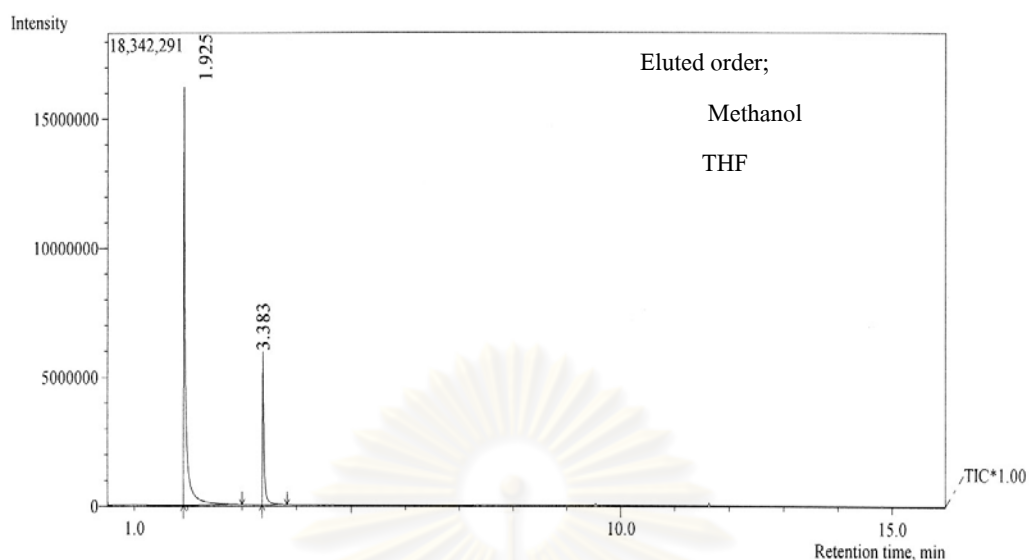


Figure 4.3 GC-MS chromatogram of THF phase in 250-mL reactor for 10 min with crude PKO as reactant.

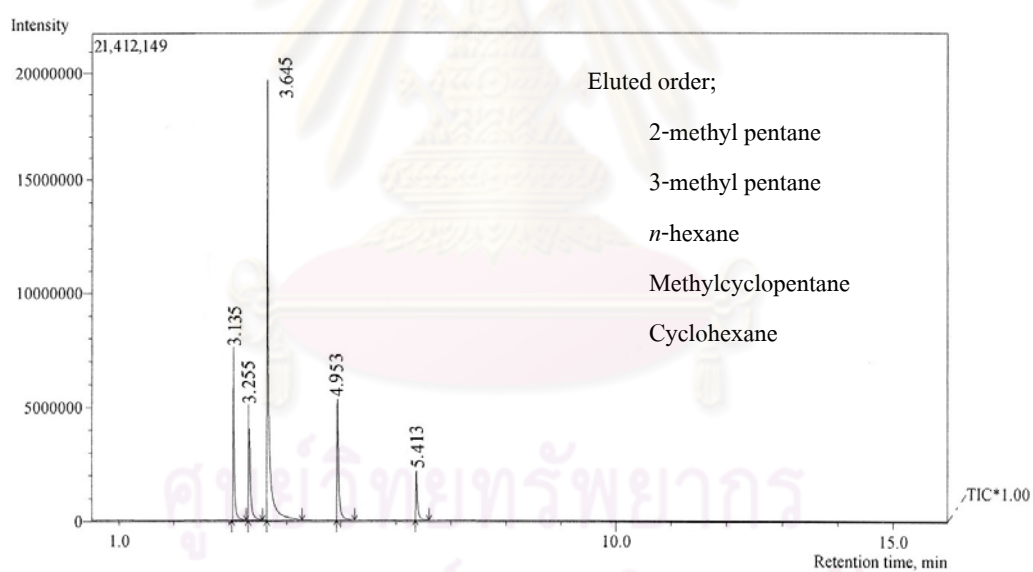


Figure 4.4 GC-MS chromatogram of hexane phase in 250-mL reactor for 10 min with crude PKO as reactant.

Comparing Figure 4.1 with Figure 4.2, it can be seen that the biodiesel composition from the employed THF process was basically the same as the mixed fatty acid methyl esters standard. On the other hand, from the THF and hexane chromatograms in Figures 4.3 and 4.4, one can deduce that THF and hexane peaks did not show up in Figure 4.2. Therefore, it is concluded that there was no co-solvent interference in the transesterification reaction.

4.2. Effect of co-solvents on ME content in a 250-mL reactor

The experimental order (Table 4.1 and run order 1 to 12 in Table 4.2) was done randomly. For run order 13 to 20 in Table 4.2, i.e. the co-solvent free process, the experimental data were obtained from Table 4.1.

To eliminate the effect of pressure, the amount of reactants and co-solvent was adjusted to a specified pressure (19.0 MPa) by using the Redlich-Kwong Equation of State and the Lorentz-Berthelot-type mixing rule [86]. Unfortunately, the calculated pressure was not exactly equal to the observed pressure. In some experiments, where there was a large difference between the calculated and observed pressure, the amounts of reactant and co-solvent were readjusted by trial and error. The observed pressures for each experiment are shown in Tables 4.1 and 4.2.

All experimental data were analyzed by the factorial design procedure [87] to obtain the analysis of variance tables (ANOVA), which are shown in Tables 4.3 and 4.4.

Table 4.1 Experimental data from employed THF process in 250-mL reactor for 10 min with crude PKO as reactant

| Run order | Temperature (°C) | Pressure (MPa) | THF to oil molar ratio | MeOH to oil molar ratio | ME content (%wt) |
|-----------|------------------|----------------|------------------------|-------------------------|------------------|
| 1 | 350 | 17.9 | 0.0 | 12.1 | 79.7 |
| 2 | 290 | 17.5 | 5.6 | 41.3 | 72.6 |
| 3 | 350 | 19.3 | 4.8 | 39.9 | 86.5 |
| 4 | 290 | 17.4 | 5.0 | 41.9 | 73.2 |
| 5 | 350 | 19.0 | 0.0 | 41.3 | 84.9 |
| 6 | 290 | 16.6 | 0.0 | 42.2 | 63.7 |
| 7 | 320 | 19.0 | 2.4 | 24.0 | 79.6 |
| 8 | 350 | 19.8 | 5.0 | 12.2 | 79.6 |
| 9 | 320 | 17.8 | 2.5 | 23.9 | 80.4 |
| 10 | 350 | 19.4 | 4.9 | 41.9 | 79.3 |
| 11 | 350 | 19.8 | 0.0 | 12.1 | 80.9 |
| 12 | 320 | 19.1 | 2.6 | 24.1 | 79.7 |
| 13 | 350 | 19.6 | 0.0 | 42.1 | 85.1 |
| 14 | 290 | 16.3 | 5.1 | 11.9 | 45.0 |
| 15 | 350 | 21.6 | 5.1 | 12.1 | 82.5 |
| 16 | 290 | 15.6 | 0.0 | 12.1 | 43.7 |
| 17 | 290 | 16.2 | 0.0 | 11.2 | 47.6 |
| 18 | 290 | 15.9 | 5.1 | 12.3 | 47.3 |
| 19 | 320 | 18.0 | 2.5 | 24.1 | 78.6 |
| 20 | 290 | 16.9 | 0.0 | 42.1 | 62.3 |

Table 4.2 Experimental data from employed hexane process in 250-mL reactor for 10 min with crude PKO as reactant

| Run order | Temperature (°C) | Pressure (MPa) | Hexane to oil molar ratio | MeOH to oil molar ratio | ME content (%wt) |
|-----------|------------------|----------------|---------------------------|-------------------------|------------------|
| 1 | 290 | 19.6 | 4.7 | 41.3 | 62.4 |
| 2 | 350 | 18.7 | 4.6 | 40.9 | 87.6 |
| 3 | 290 | 19.2 | 5.1 | 12.4 | 46.2 |
| 4 | 290 | 20.0 | 4.8 | 42.6 | 65.2 |
| 5 | 350 | 18.6 | 5.0 | 12.4 | 79.8 |
| 6 | 320 | 19.2 | 2.5 | 24.2 | 77.8 |
| 7 | 290 | 20.0 | 4.9 | 12.2 | 48.5 |
| 8 | 320 | 18.6 | 2.6 | 24.3 | 78.2 |
| 9 | 350 | 17.7 | 5.0 | 43.4 | 88.1 |
| 10 | 320 | 18.2 | 2.5 | 24.2 | 76.5 |
| 11 | 320 | 19.6 | 2.4 | 24.1 | 76.6 |
| 12 | 350 | 19.0 | 5.2 | 12.4 | 85.9 |
| 13 | 290 | 15.6 | 0.0 | 12.1 | 43.7 |
| 14 | 290 | 16.2 | 0.0 | 11.1 | 47.6 |
| 15 | 350 | 19.8 | 0.0 | 12.1 | 80.9 |
| 16 | 350 | 17.9 | 0.0 | 12.1 | 79.7 |
| 17 | 290 | 16.6 | 0.0 | 42.2 | 63.7 |
| 18 | 290 | 16.9 | 0.0 | 42.1 | 62.3 |
| 19 | 350 | 19.6 | 0.0 | 42.1 | 85.1 |
| 20 | 350 | 19.0 | 0.0 | 41.3 | 84.9 |

Table 4.3 Analysis of variance from employed THF process in 250-mL reactor for 10 min with crude PKO as reactant

| Source | Sum of Squares | Degree of Freedom | Mean Square | F Value | Prob. > F |
|-----------------|----------------|-------------------|-------------|---------|-----------|
| A (Temperature) | 2583.77 | 1 | 2583.77 | 69.47 | < 0.0001 |
| B (THF to oil) | 18.28 | 1 | 18.28 | 0.49 | 0.4966 |
| C (MeOH to oil) | 538.21 | 1 | 538.21 | 14.47 | 0.0025 |
| AB | 31.45 | 1 | 31.45 | 0.85 | 0.3759 |
| AC | 338.75 | 1 | 338.75 | 9.11 | 0.0107 |
| BC | 10.41 | 1 | 10.41 | 0.28 | 0.6065 |
| ABC | 39.51 | 1 | 39.51 | 1.06 | 0.323 |
| Residual | 446.29 | 12 | 37.19 | | |
| Total | 4043.78 | 19 | | | |

Table 4.4 Analysis of variance from employed hexane process in 250-mL reactor for 10 min with crude PKO as reactant

| Source | Sum of Squares | Degree of Freedom | Mean Square | F Value | Prob. > F |
|-------------------|----------------|-------------------|-------------|---------|-----------|
| A (Temperature) | 3374.01 | 1 | 3374.01 | 142.32 | < 0.0001 |
| B (Hexane to oil) | 15.18 | 1 | 15.18 | 0.64 | 0.4391 |
| C (MeOH to oil) | 421.18 | 1 | 421.18 | 17.77 | 0.0012 |
| AB | 2.16 | 1 | 2.16 | 0.091 | 0.7679 |
| AC | 141.41 | 1 | 141.41 | 5.96 | 0.0310 |
| BC | 4.314E-03 | 1 | 4.32E-03 | 1.8E-04 | 0.9895 |
| ABC | 0.082 | 1 | 0.082 | 3.4E-03 | 0.9539 |
| Residual | 284.49 | 12 | 23.71 | | |
| Total | 4249.48 | 19 | | | |

From Tables 4.3 and 4.4, the molar ratio of co-solvent to oil (factor B) and its interaction (factors AB, BC and ABC) had no significant effect on ME content, as noticed from the probability of F value less than 0.05, at the confidence level of 95%. Thus, it was concluded that the addition of a co-solvent in this process did not show either negative or positive effect on ME content.

The regression models in terms of coded units of employed THF and hexane process can be then correlated as shown in Equations 4.1 and 4.2, respectively.

$$\%ME = 71.88 + 12.67A + 5.90C - 4.67AC \quad (4.1)$$

$$\%ME = 71.21 + 14.53A + 5.12C - 2.99AC \quad (4.2)$$

where %ME is ME content in biodiesel product (%wt)

A is temperature in terms of coded unit, derived by the Equation (4.3)

$$A = \frac{\text{Temperature } (^{\circ}\text{C}) - 320}{30} \quad (4.3)$$

C is the methanol to oil molar ratio in terms of coded unit, derived by the Equation (4.4)

$$C = \frac{\text{Mole of MeOH (mole)} - 27}{15} \quad (4.4)$$

Temperature (A) and the methanol to vegetable oil molar ratio (C) has positive effects on ME content, and the temperature effect has a higher magnitude than the methanol to oil molar ratio effect by approximately two folds. It should be noticed that temperature and methanol to oil molar ratio had an interaction due to the amount of methanol affect the transition temperature as mentioned in section 2.4.3. The interaction term (AC) indicated the complete regression model might be of second order; which is consistent with our previous finding [20].

CHAPTER V

EFFECT OF ADDITIONAL PARAMETERS AND SCALE-UP REACTOR OPTIMIZATION

5.1. Effect of reaction time on ME content in 250-mL batch reactor

Refer to Tables 4.1 and 4.2, the highest ME content obtained was found to be not over 88 % in 250-mL batch reactor at 10 min reaction time, which is lower than that reported in the literature employing co-solvents [8, 47]. According to the relevant literature, the conditions were: reaction temperature 350 to 400 °C; methanol to oil molar ratio of 40:1 to 42:1; reaction time of 2.4 to 40 min; and, reactor volume of 5 to 250-mL [6, 8, 39, 47]. To confirm that the reaction reached equilibrium under the present conditions, we ran another set of experiments for 5 to 60 min and the result is illustrated in Figure 5.1.

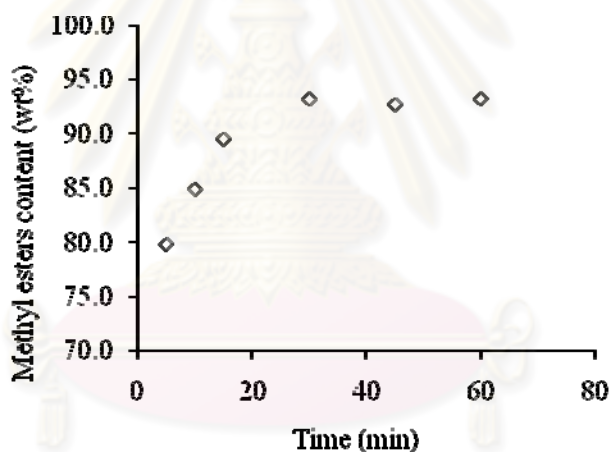


Figure 5.1 Changes in ME content with time of co-solvent free process from transesterification of crude PKO in 250-mL reactor at 350 °C and the methanol to oil molar ratio of 42:1.

From Figure 5.1, maximum ME content was reached after reaction time of 30 min and a ME content of $92.0 \pm 1\%$ was observed. Due to slightly lower ME content, we further established two possible hypotheses and verified them as follows:

5.2. Effect of temperature gradient between reactor wall and bulk fluid

In the 250-mL reactor, the reaction vessel employed was heated externally and the contents in the vessel were mixed by a stirrer. As the temperature near the wall of the vessel is somewhat higher than in the center, it may cause an in situ thermal cracking reaction, resulting in slightly lower ME content. To verify this hypothesis, the experiments were performed at high

temperature, i.e. 350 and 400 °C, in both 5.5 and 250-mL reactors at 30 min of reaction time, and the biodiesel samples were analyzed. The chromatograms obtained were then compared with that obtained from the conventional method at 60 °C, 30 min reaction time, 1% NaOH, and methanol to oil molar ratio of 6:1.

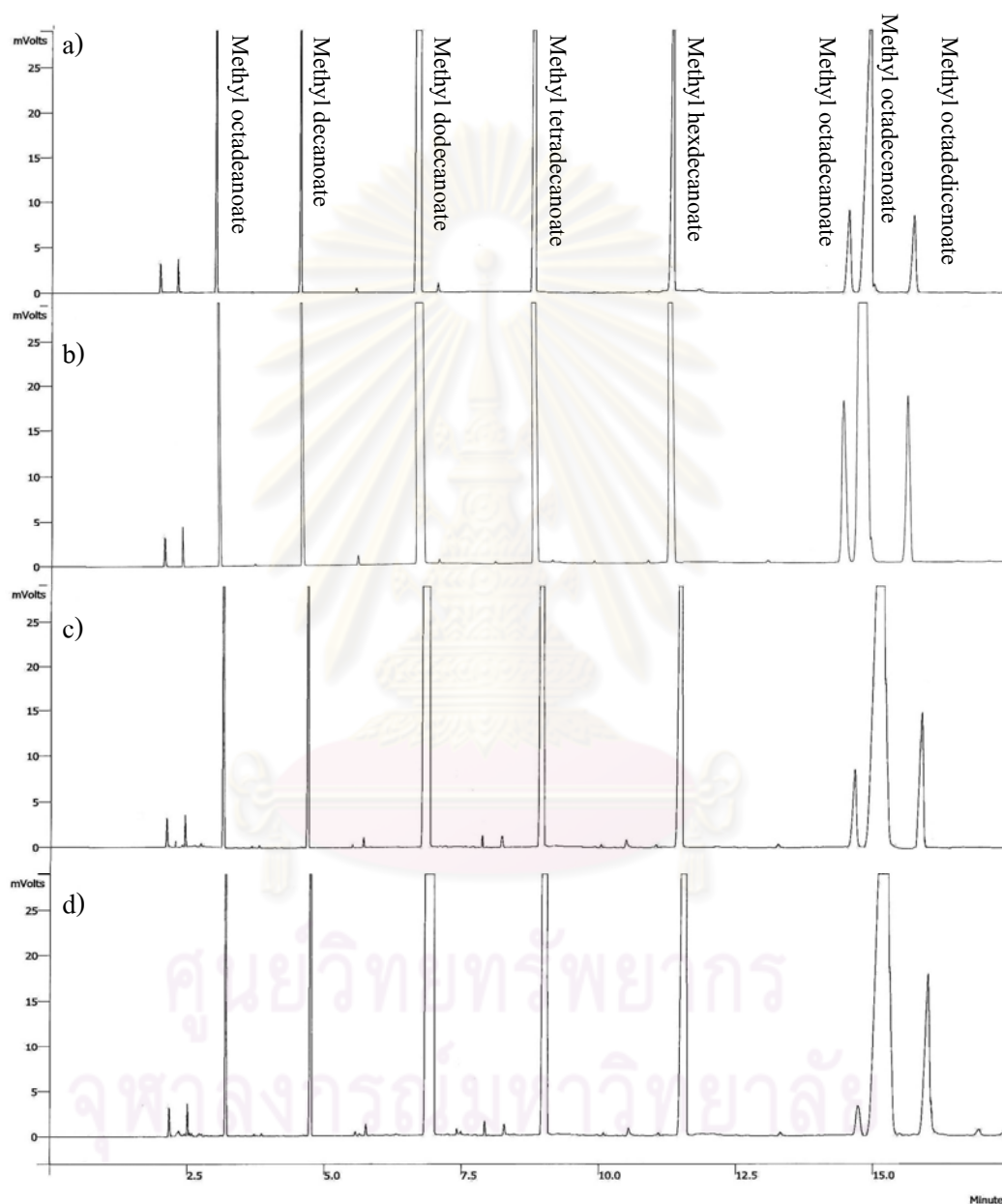


Figure 5.2 Comparison of GC chromatogram of biodiesel product from crude PKO at various temperatures, indicating some small peaks observed as in c) and d).

- | | |
|--------------------------------|-----------------------------|
| a) conventional method (60 °C) | b) 350 °C in 5.5-mL reactor |
| c) 400 °C in 5.5-mL reactor | d) 350 °C in 250-mL reactor |

From Figure 5.2, sample (a), no thermal cracking occurred. In the chromatogram of this sample, no noise was detected, same as in sample (b). Therefore, it was concluded that thermal cracking did not take place in the 5.5-mL reactor at 350°C. Comparing samples (c) and (d) with the sample (a) and (b), it was found that the chromatograms of both samples (c) and (d) had higher small peaks, and their retention times were nearly the same. These small peaks, for instance, at retention time of 6 and 8 min, were probably from the same compounds derived from the thermal cracking reaction at temperature over 350°C.

According to the ME content obtained from the 5.5-mL reactor, it was assumed that there was no temperature gradient between reactor wall and bulk fluid, at 350 °C, methanol to oil molar ratio of 42:1, co-solvent to oil molar ratio of 0 to 5 and reaction time of 10 min. The experimental data are illustrated in Table 5.1. The ME content of the biodiesel products was slightly higher than those obtained from the 250-mL reactor at the same conditions (see Tables 4.1 and 4.2). Therefore, the hypothesis that thermal cracking occurred in the 250-mL reactor could be valid. However, the ME content was still slightly lower than the literature value, especially for the employed co-solvent process. Therefore, we established a second hypothesis, which is discussed in next section.

Table 5.1 Experimental data from 5.5-mL reactor for 10 min with crude PKO as reactant, temperature controlled by fluidized sand bath

| Process | Temperature (°C) | Co-solvent to oil molar ratio | Methanol to oil molar ratio | ME content (%wt) |
|-----------------------|------------------|-------------------------------|-----------------------------|------------------|
| Unemployed co-solvent | 350 | 0.0 | 42.0 | 95.5 |
| | 350 | 0.0 | 42.1 | 96.3 |
| THF | 350 | 5.1 | 41.1 | 94.7 |
| | 350 | 6.8 | 45.1 | 93.8 |
| Hexane | 350 | 5.2 | 40.3 | 93.9 |
| | 350 | 5.8 | 42.3 | 94.5 |

5.3. Effect of contaminants in crude palm kernel oil

The crude PKO contained 95 to 98% of triglycerides and 2 to 5% complex minor compounds such as wax ester, hydrocarbons, pigments and alcoholic compounds [88]. Thus, the slightly lower ME content obtained from crude PKO than that from refined PKO was probably due to the percentage of triglycerides. This hypothesis was verified in the 5.5-mL reactor, to ensure that thermal cracking did not take place, by using refined PKO as the reactant. The effect

of co-solvent by using the experimental design as mentioned earlier was also reinvestigated and the results were illustrated in next section.

5.4. Effect of co-solvents on ME content in biodiesel production in a 5.5-mL reactor

The experimental data, as shown in Tables 5.2 and 5.3, were treated by the factorial design procedure and the ANOVA tables, as shown in Tables 5.4 and 5.5, respectively.

Table 5.2 Experimental data from employed THF process in 5.5-mL reactor for 10 min with refined PKO as reactant

| Run order | Temperature (°C) | THF to oil molar ratio | MeOH to oil molar ratio | ME content (%wt) |
|-----------|------------------|------------------------|-------------------------|------------------|
| 1 | 350 | 0.0 | 44.5 | 99.3 |
| 2 | 320 | 3.7 | 24.3 | 83.2 |
| 3 | 350 | 5.2 | 12.0 | 83.3 |
| 4 | 320 | 2.1 | 20.2 | 81.3 |
| 5 | 290 | 0.0 | 12.0 | 53.6 |
| 6 | 350 | 5.0 | 43.0 | 97.5 |
| 7 | 350 | 0.0 | 12.0 | 81.1 |
| 8 | 350 | 0.0 | 40.8 | 99.4 |
| 9 | 290 | 8.3 | 20.1 | 56.5 |
| 10 | 290 | 4.8 | 40.7 | 78.3 |
| 11 | 290 | 5.0 | 12.0 | 54.2 |
| 12 | 320 | 2.3 | 21.7 | 82.5 |
| 13 | 350 | 5.1 | 41.9 | 98.7 |
| 14 | 350 | 5.3 | 12.2 | 84.6 |
| 15 | 290 | 0.0 | 41.9 | 78.2 |
| 16 | 320 | 2.5 | 22.9 | 84.6 |
| 17 | 350 | 0.0 | 12.0 | 82.6 |
| 18 | 290 | 0.0 | 41.8 | 76.8 |
| 19 | 290 | 5.2 | 42.4 | 77.5 |
| 20 | 290 | 0.0 | 12.0 | 57.0 |

From Table 5.2 and 5.3, the maximum ME content obtained from both THF and hexane co-solvents was 99.4 % compared to 94.7 and 94.5 % obtained from crude PKO (Table 5.1). It was clear that the maximum ME content from refined PKO was higher than that from crude PKO, which was 96.3 % (Table 5.1). Therefore, the slightly lower ME content obtained from crude PKO than that from refined PKO was due to the lower percentage of triglyceride in crude PKO.

Table 5.3 Experimental data from employed hexane process in a 5.5-mL reactor for 10 min with refined PKO as reactant

| Run order | Temperature (°C) | Hexane to oil molar ratio | MeOH to oil molar ratio | ME content (%wt) |
|-----------|------------------|---------------------------|-------------------------|------------------|
| 1 | 320 | 2.6 | 23.9 | 80.5 |
| 2 | 290 | 5.4 | 42.0 | 79.5 |
| 3 | 320 | 2.5 | 23.9 | 81.2 |
| 4 | 290 | 5.4 | 12.0 | 52.2 |
| 5 | 350 | 5.1 | 11.9 | 76.0 |
| 6 | 290 | 5.0 | 11.9 | 54.4 |
| 7 | 350 | 6.8 | 43.5 | 97.1 |
| 8 | 320 | 2.6 | 23.7 | 80.2 |
| 9 | 290 | 5.0 | 41.1 | 80.1 |
| 10 | 320 | 2.5 | 23.0 | 80.2 |
| 11 | 350 | 4.9 | 37.9 | 86.7 |
| 12 | 350 | 5.0 | 12.2 | 78.1 |
| 13 | 290 | 0.0 | 12.0 | 57.0 |
| 14 | 290 | 0.0 | 12.0 | 53.6 |
| 15 | 290 | 0.0 | 41.8 | 76.8 |
| 16 | 290 | 0.0 | 41.9 | 78.2 |
| 17 | 350 | 0.0 | 12.0 | 81.1 |
| 18 | 350 | 0.0 | 12.0 | 82.6 |
| 19 | 350 | 0.0 | 44.5 | 99.4 |
| 20 | 350 | 0.0 | 40.8 | 99.3 |

Table 5.4 Analysis of variance from employed THF process in a 5.5-mL reactor for 10 min with refined PKO as reactant

| Source | Sum of Squares | Degree of Freedom | Mean Square | F Value | Prob. > F |
|-----------------|----------------|-------------------|-------------|---------|-----------|
| A (Temperature) | 2400.84 | 1 | 2400.84 | 138.81 | < 0.0001 |
| B (THF to oil) | 2.00 | 1 | 2.00 | 0.12 | 0.7399 |
| C (MeOH to oil) | 1340.93 | 1 | 1340.93 | 77.53 | < 0.0001 |
| AB | 6.11 | 1 | 6.11 | 0.35 | 0.5634 |
| AC | 58.91 | 1 | 58.91 | 3.41 | 0.0898 |
| BC | 0.02 | 1 | 0.02 | 0.00 | 0.9756 |
| ABC | 8.39 | 1 | 8.39 | 0.49 | 0.4994 |
| Residual | 207.55 | 12 | 17.30 | | |
| Total | 3950.57 | 19 | | | |

Table 5.5 Analysis of variance from employed hexane process in 5.5-mL reactor for 10 min with refined PKO as reactant

| Source | Sum of Squares | Degree of Freedom | Mean Square | F Value | Prob. > F |
|-------------------|----------------|-------------------|-------------|---------|-----------|
| A (Temperature) | 1783.85 | 1 | 1783.85 | 136.94 | < 0.0001 |
| B (Hexane to oil) | 22.61 | 1 | 22.61 | 1.74 | 0.2123 |
| C (MeOH to oil) | 1640.57 | 1 | 1640.57 | 125.94 | < 0.0001 |
| AB | 27.62 | 1 | 27.62 | 2.12 | 0.171 |
| AC | 53.23 | 1 | 53.23 | 4.09 | 0.0661 |
| BC | 9.30 | 1 | 9.30 | 0.71 | 0.4146 |
| ABC | 2.88 | 1 | 2.88 | 0.22 | 0.6466 |
| Residual | 156.31 | 12 | 13.03 | | |
| Total | 3673.21 | 19 | | | |

From Tables 5.4 and 5.5, it is clear that the co-solvents did not affect the ME content. Also, the interaction term between temperature and methanol to oil molar ratio (Factor AC) had no significant effect. The regression model in terms of coded unit for 5.5-mL reactor for the employed THF and hexane process are given in Equations 5.1 and 5.2, respectively.

$$\%ME = 79.79 + 12.32A + 9.08C \quad (5.1)$$

$$\%ME = 78.24 + 10.51A + 10.11C \quad (5.2)$$

where $\%ME$ is ME content in biodiesel product (%wt)

A is temperature in terms of coded unit, derived by Equation (4.3)

C is methanol to oil molar ratio in terms of coded unit, derived by Equation (4.4).

For the 5.5-mL reactor, the regression model indicated that the effect of temperature and methanol to oil molar ratio had a similar magnitude and also had positive effect. In comparison with the regression model for a 250-mL reactor (Eq. 4.1 and 4.2), the overall mean (the first term on the right hand side) was higher. This indicates that the ME content in the biodiesel product, which is obtained from the same temperature and methanol to oil molar ratio in the 5.5-mL reactor, is always higher than that obtained from the 250-mL reactor. Additionally, the interaction term between temperature and methanol to oil molar ratio (AC) has no significant effect in 5.5-mL which was mentioned that the amount of methanol affects the transition temperature.

5.5. Effect of delayed quenching time

5.5.1. Effect of delayed quenching time in a 5.5-mL batch reactor

In this section, we hypothesized that the ME content from scale-up reactor was lower than the lab-scale reactor due to the delayed and deficient quenching of the product as it leaves the reactor outlet. Since the transesterification reaction is reversible, it should be stopped immediately by quenching to ambient temperature as quickly and sufficiently as possible. The outlet tube of scale-up reactor, approximately 2 m. long, was exposed to air before immersing into the cooling bath as the effect of delayed quenching did not come to full attention in our previous study [20]. This hypothesis was tested in 5.5-mL reactor before modification of our cooling system of the scale-up reactor. Preliminary results from 5.5-mL reactor are shown Figure 5.3.

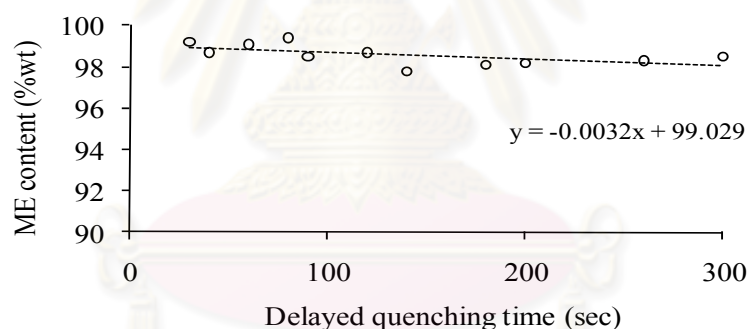


Figure 5.3 The ME content versus the delayed quenching time in 5.5-mL tube reactor.

According to Figure 5.3, the ME content slightly reduced with delayed quenching time. However, the effect of delayed quenching time in batch system was probably different from continuous flow system. Therefore, this hypothesis was tested consequently in a scale-up reactor by replacing of the cooling bath with a heat exchanger.

5.5.2. Effect of delay quenching time in scale-up reactor

Refer to Figure 3.1, the cooling bath was replaced with double-pipe heat exchanger using tap water as cooling medium as shown in Figure 5.4.

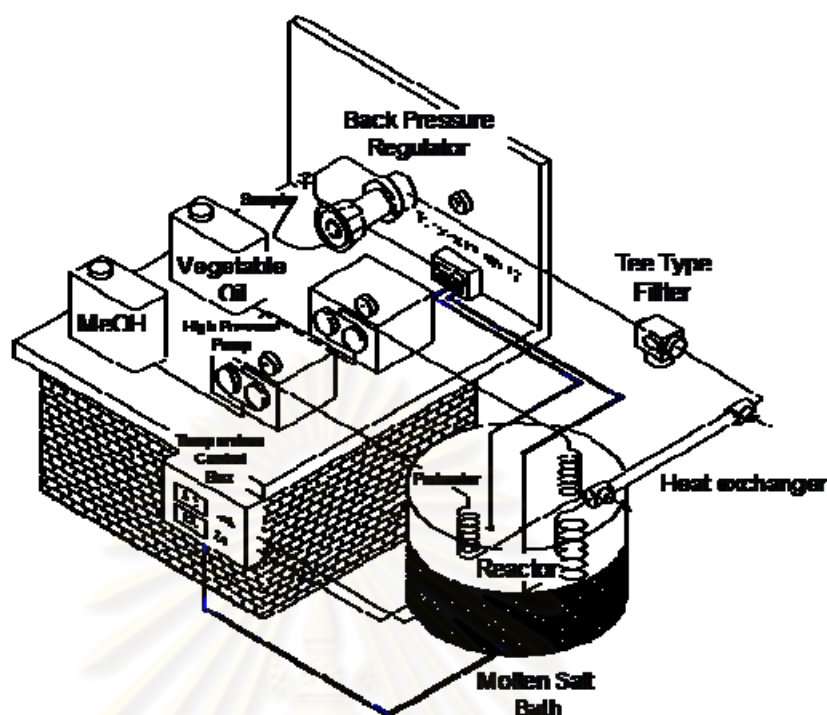


Figure 5.4 The scale-up reactor after replaced cooling bath with heat exchanger.

After the cooling system was modified, the scale-up reactor was tested on the conditions in our previous study [20] to investigate the effect of delay quenching time in continuous flow reactor and the results are illustrated in Table 5.6.

Table 5.6 The ME content in products from scale-up reactor with different cooling systems

| | Pressure (MPa) | Temperature (°C) | MeOH to oil molar ratio | %ME content |
|----------------|----------------|------------------|-------------------------|-------------|
| Cooling bath | 13.1 | 300 | 22.1 | 69.24 |
| | 13.1 | 300 | 22.1 | 71.12 |
| | 11.9 | 350 | 30.3 | 79.36 |
| Heat exchanger | 13.0 | 300 | 21.1 | 70.12 |
| | 13.2 | 300 | 22.2 | 70.59 |
| | 12.1 | 350 | 30.1 | 80.11 |

According to Table 5.1, the ME content only increased slightly after upgrading the cooling system, thus it could be concluded that the delayed and deficient quenching of product had no significant effect on the ME content in the scale-up reactor.

5.6. Effect of pressure and process optimization

The effect of pressure was reinvestigated because the investigation range in our previous study (10.0 to 15.0 MPa) shows that pressure had no significant effect on ME content [20], but some studies reported that pressure has strong effect at pressure over 15.0 MPa [11, 61].

The effect of pressure was studied by Central Composite Design (CCD) within the pressure range of 15.0 to 20.0 MPa, temperature range of 270 to 330 °C and methanol to oil molar ratio range of 35:1 to 20:1. In addition, the effect of co-solvent was neglected by adding 20% v/v of hexane in all experiments. The experimental design and results from CCD are illustrated in Table 5.7 and the ANOVA table in Table 5.8.

Table 5.7 The experimental conditions and results from CCD to reinvestigate the effect of pressure, temperature and methanol to oil molar ratio in scale-up reactor

| Run | Temperature (°C) | Pressure (MPa) | MeOH to Oil molar ratio | %ME content |
|-----|------------------|----------------|-------------------------|-------------|
| 1 | 299.0 | 16.5 | 27.0 | 76.3 |
| 2 | 270.0 | 18.1 | 36.6 | 32.7 |
| 3 | 300.0 | 19.1 | 26.7 | 83.2 |
| 4 | 300.0 | 16.6 | 27.0 | 78.3 |
| 5 | 300.0 | 13.9 | 27.0 | 39.0 |
| 6 | 330.0 | 14.9 | 37.5 | 73.0 |
| 7 | 270.0 | 15.0 | 38.3 | 29.5 |
| 8 | 330.0 | 15.0 | 18.9 | 45.5 |
| 9 | 270.0 | 15.0 | 18.3 | 22.2 |
| 10 | 330.0 | 18.0 | 37.8 | 91.5 |
| 11 | 300.0 | 16.6 | 27.1 | 80.6 |
| 12 | 270.0 | 18.0 | 18.3 | 24.6 |
| 13 | 300.0 | 16.7 | 13.7 | 35.9 |
| 14 | 351.0 | 16.5 | 27.4 | 60.4 |
| 15 | 330.0 | 18.0 | 19.5 | 65.8 |
| 16 | 255.0 | 16.4 | 27.1 | 12.1 |
| 17 | 300.0 | 16.5 | 45.9 | 82.4 |
| 18 | 300.0 | 16.5 | 26.7 | 78.3 |

Table 5.8 Analysis of variance of results in Table 5.7

| Source | Sum of square | Degree of freedom | Mean square | F-Value | p-Value |
|-----------------|---------------|-------------------|-------------|---------|----------|
| A (Temperature) | 4898.2 | 1 | 4898.2 | 90.92 | < 0.0001 |
| B (Pressure) | 941.4 | 1 | 941.4 | 17.47 | 0.0031 |
| C (MeOH:Oil) | 2059.7 | 1 | 2059.7 | 38.23 | 0.0003 |
| A ² | 3312.1 | 1 | 471.0 | 8.74 | 0.0182 |
| B ² | 471.0 | 1 | 3312.1 | 61.48 | < 0.0001 |
| C ² | 724.9 | 1 | 724.9 | 13.46 | 0.0063 |
| AB | 126.1 | 1 | 126.1 | 2.34 | 0.1646 |
| AC | 239.5 | 1 | 239.5 | 4.45 | 0.0680 |
| BC | 1.1 | 1 | 1.1 | 0.02 | 0.8888 |
| Residual | 431.0 | 8 | 53.9 | | |
| Total | 11213.2 | 17 | | | |

From Table 5.8, the second order regression model for scale-up reactor can be written as Equation 5.3. The interaction terms (AB, AC and BC) were not included to the regression model because their p-value were less than 0.05, and indicated they had no significant effect on the ME content. The coefficient of determination of this regression model (R^2) was calculated and found to be 0.9732. Additionally, all statistical analysis of the regression model for scale-up reactor is given in Appendix A. The predicted and observed values were plotted in Figure 5.5.

$$\%ME = 75.90 + 21.02A + 9.60B + 13.78C - 16.89A^2 - 3.72B^2 - 4.57C^2 \quad (5.3)$$

$\%ME$ is ME content in biodiesel product (%wt)

A is temperature in terms of coded unit, derived by the Equation (5.4)

$$A = \frac{\text{Temperature } (^{\circ}\text{C}) - 330}{30} \quad (5.4)$$

C is the methanol to oil molar ratio in terms of coded unit, derived by the Equation (5.5)

$$B = \frac{\text{Pressure (MPa)} - 16.5}{1.5} \quad (5.5)$$

C is the methanol to oil molar ratio in terms of coded unit, derived by the Equation (5.6)

$$C = \frac{\text{Mole of MeOH (mol)} - 27.5}{7.5} \quad (5.6)$$

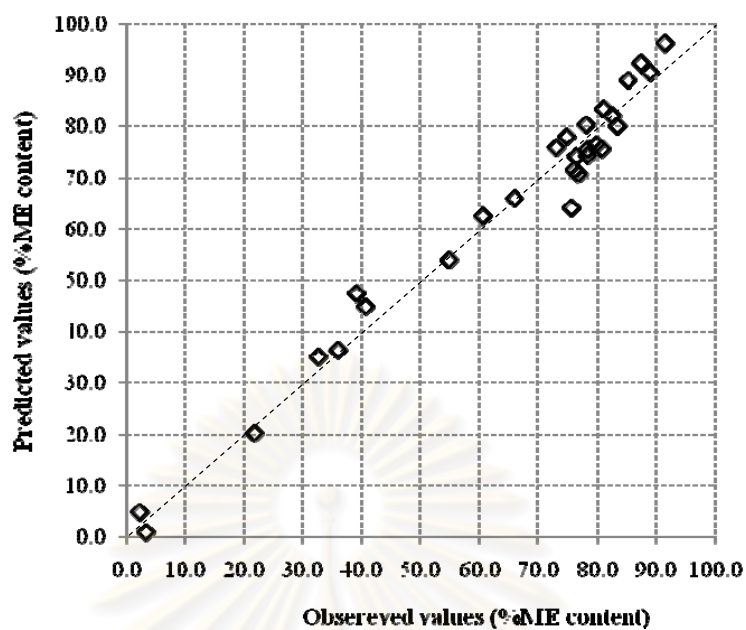


Figure 5.5 The plot of experimented and calculated value by Equation 5.3.

From the coefficient of Equation (5.3), it can be concluded that the effect of pressure was smaller than the effect of temperature and methanol to oil molar ratio. The response surface can be created by regression model as shown in Figure 5.6.

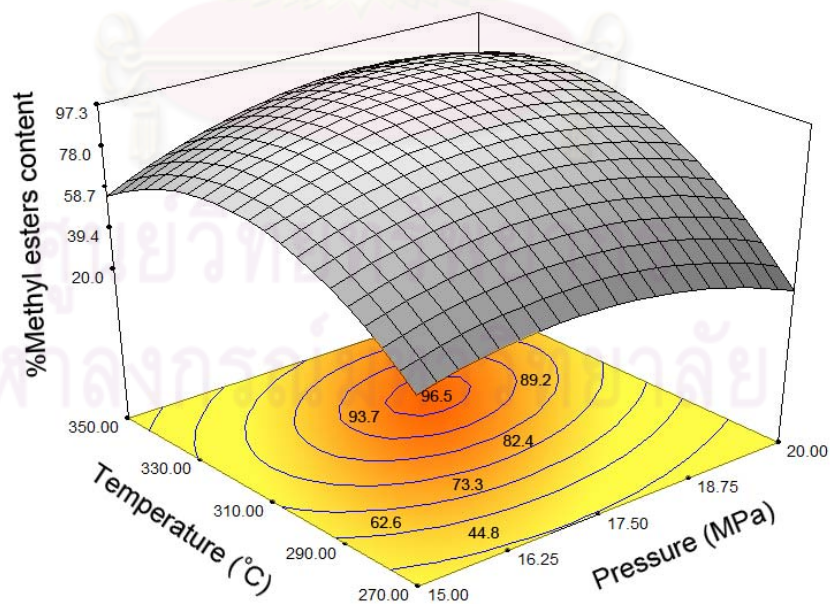


Figure 5.6 The response surface of ME content versus temperature and pressure at the methanol to oil of 35:1.

The optimization process was conducted by Design Expert ® 6.0 software with a maximum ME content as objective function. From the response surface in Figure 5.6, the ME content over 96.5 % could be found at temperature range of 310 to 330 °C, pressure range of 17.5 to 18.5 MPa and methanol to oil molar ratio of 35:1 to 40:1. The maximum ME content in Table 5.7 was 91.5 % at 330 °C, 18.0 MPa and 38:1 methanol to oil molar ratio which was also located within the optimal range.

Even though some repetition experiments were conducted within the optimal range, but the highest ME content to be only approximately 93 % was found from the scale-up reactor. This was lower than the target value of 96.5 %, probably because the optimal range from the regression model was narrower than the controllable range of the operating parameters, especially for pressure and methanol to oil molar ratio. For instance, the observed pressure slightly fluctuated at the vegetable oil pump. In addition, the methanol and vegetable oil flow rate can deviate from the initial value during the run as the real-time flow rate measurement was not available.

CHAPTER VI

RESIDENCE TIME ESTIMATION METHOD

6.1. Description of the compressible flow model as a tool to estimate the residence time

6.1.1. Thermodynamic model

A thermodynamic model was used to evaluate the changes in the compressibility factor of the reaction mixture, and was established as being suitable as long as the reaction proceeds in the tubular reactor [85, 89]. However, experimental fluid properties and / or experimental vapor-liquid equilibrium (VLE) data of binary sub-systems are required to find the most suitable thermodynamic model in order to predict such properties and fluid physical state for the reaction system. In actuality, the real reaction system composed of various types of triglyceride, e.g., tripalmitin, triolein, palmito-diolein and palmito-linoleo-olein etc., five to eight types of fatty acid methyl esters (FAMES), and reaction intermediates, such as mono- and diglycerides. To simplify the calculation, we assumed that the reaction system consists of methanol, triolein, methyl oleate and glycerol, with triolein and methyl oleate representing the palm olein oil and biodiesel (mixture of FAMES), respectively, in accordance with the major fatty acid composition of palm olein oil as mentioned in Section 3.3.2. Therefore, we employed the existing VLE measurements of triolein + methanol, methyl oleate + methanol and glycerol + methanol binary systems from the literature. This simplification was chosen because of the availability of experimental data in the literature for these binary systems, but not more complex ones.

It is important to note here that the high pressure / high temperature VLE or density experimental data for the triolein / methanol mixture are quite difficult to obtain because of the high reactivity of the mixture under these high operating pressures and temperatures. To find the best model to predict the thermodynamic behavior of the quaternary mixture, we intended to test the classical Peng-Robinson equation of state (PR) [90] with the mixing rules developed by Huron and Vidal [91] and modified by Michelsen [92] (MHV2 mixing rules). This approach allows the cubic equation of state PR, suitable for high pressure but poor for mixtures containing polar compounds, to be applied for high-pressure calculations of mixtures involving polar compounds. As the

MHV2 mixing rules are based on the calculation of the excess Gibbs energy at zero pressure, this also requires a suitable activity coefficient model, in addition to the equation of state. Here we decided to use the UNIQUAC [93] activity coefficient model, because the coupling of this model to a cubic EOS via the MHV2 mixing rules has already been shown to be a good model for predicting the high-pressure fluid phase equilibria of mixtures containing polar compounds [94], as it is the case here. Moreover, this model is available in Simulis® Thermodynamics (ProSim, France), commercial software for the calculation of fluid phase equilibria and fluid properties.

6.1.2. Compressible flow model

The general mole balance in a tubular reactor [95] and the transesterification kinetics of refined-bleached-de-odorized (RBD) palm oil in SCM [72] are illustrated in equations (6.1) and (6.2) respectively

$$\frac{dX_A}{dV} = \frac{-r_A}{F_{A0}} \quad (6.1)$$

$$-r_A = kC_A^{0.95}C_B^{1.05} \quad (6.2)$$

where X , V , r_A and F_{A0} are conversion, reactor volume (m^3), rate of transesterification reaction (mol/s.m^3) and molar flow rate at reactor inlet (mol/s), respectively. The subscript A and B referred to triolein and methanol, respectively.

The chemical kinetics of RBD palm oil was investigated in a 4.7-mL batch reactor at 30.0 MPa within the temperature range of 200 to 400 °C, a methanol to oil molar ratio range of 3:1 to 80:1, and a reaction time range of 0.5 to 30 min. The rate constant and reaction order were found by an integral method or numerical fitting of the experimental data to the kinetic model, resulting in a high coefficient of determination (R^2) value, at 0.9578, even though it does not include the thermal degradation reaction [72]. The rate constant was defined as a function of temperature as shown in equation (6.3).

$$k = 4.34 \times 10^5 \times \exp\left(-\frac{1.05 \times 10^5}{RT}\right) \quad (6.3)$$

where k , R and T are the rate constant ($\text{m}^3/\text{mol.s}$), universal gas constant (J/mol.K) and temperature (K), respectively

In a continuous isothermal reactor, concentration and total molar flow rate of mixture corresponding to inlet flow rate can be written as Equation (6.4) and (6.5) respectively.

$$C = \frac{F}{v_m} \quad (6.4)$$

$$v_m = v_{m0} \left(\frac{z_m}{z_{m0}} \right) \frac{P_0}{P} \quad (6.5)$$

where C , F , v , z , and P are concentration (mol/m^3), molar flow rate (mol/s), volumetric flow rate (m^3/s), compressibility factor and pressure (MPa), respectively. The subscripts m and 0 refer to mixture and reactor inlet, respectively.

From the experimental observations, values of pressure were found to be slightly different between the high-pressure pump and the reactor outlet. Therefore, the zero pressure drop assumption was applied and P kept equal to P_0 . Finally, all equations were combined and rearranged to model the conversion change along the tubular reactor, as shown in equation (6.6).

From the experimental observation, values of pressure were found to be slightly different between the high-pressure pump and the reactor outlet; therefore, the zero pressure drop assumption was applied and P kept equal to P_0 . Finally, all Equations were combined and rearranged to model the conversion change along the tubular reactor as shown in Equation (6.6).

$$\frac{dX_A}{dL} = \frac{kAF_{A0}}{v_{m0}^2} (1 - X_A)^{0.95} \left(\frac{F_{B0}}{F_{A0}} - 3X_A \right)^{1.05} \left(\frac{z_{m0}}{z_m} \right)^2 \quad (6.6)$$

This governing Equation was numerically solved for conversion prediction as function of reactor length employing the Runge-Kutta method using the Matlab® software (ODE45) coupled with the Simulis® Thermodynamic toolbox, to evaluate the compressibility factor and the physical state of the mixture as the reaction proceeds inside the tube. Note that the Matlab® software read the compressibility factor as function of conversion through Simulis® Thermodynamic toolbox. The compressibility factor of the quaternary mixture was estimated by the thermodynamic model described in Section 5.1.1 with adjusted binary interaction parameters.

Finally, the calculated mole fraction of methyl oleate which represents ME content in biodiesel product was estimated from final conversion and compared with experimental results. It should be notice that the simple compressible flow model is a tool

to estimate the molar volume of the mixture and then use for calculating the residence time of biodiesel production with SCM

Additionally, assuming a constant compressibility factor leads to equation (6) being reduced to equation (6.7). The computation was done to estimate the magnitude of the effect of compressibility factor development upon ME content and solved by the Runge-Kutta 4th order method using the Matlab® software. The volumetric flow rate of the mixture at the inlet of the reactor (v_{m0}) was determined by the PR-MHV2-UNIQUAC thermodynamic model.

$$\frac{dX_A}{dL} = \frac{kAF_{A0}}{v_{m0}^2} (1 - X_A)^{0.95} \left(\frac{F_{B0}}{F_{A0}} - 3X_A \right)^{1.05} \quad (6.7)$$

6.2. Fitting of the thermodynamic model and binary interaction parameters

The VLE studies of binary systems from the literature [14, 17, 55] were fitted by the PR-MHV2-UNIQUAC thermodynamic model, in order to obtain a set of binary interaction parameters for UNIQUAC as a function of temperature. This fitting was carried out using the least square method with a Simulis® Thermodynamics add-in, inserted in MS-Excel worksheet. The critical properties of triolein, methyl oleate and glycerol were estimated by the Constantinou–Gani group-contribution method [74, 75]. The interaction coefficients are given in Table 6.1.

Table 6.1 Calculated binary interaction coefficients for UNIQUAC model.

| Binary mixture | Ref. | Type of data | A_{12} (K) | A_{21} (K) |
|-----------------------------|------|--------------------------------|---------------------|---------------------|
| Triolein + methanol | [14] | Isothermal VLE 473 to 503K | $11559.00 - 23.43T$ | $-8072.30 + 16.85T$ |
| Methyl oleate + methanol | [55] | Isothermal VLE 523 to 573 K | $1698.00 - 3.60T$ | $-5713.30 + 12.06T$ |
| Glycerol + methanol | [17] | Isothermal VLE 493 to 573 K | $1850.00 - 4.02T$ | $-4801.17 + 10.48T$ |

The VLE experimental data for triolein + methanol, methyl oleate + methanol and glycerol + methanol, and the results from PR-MHV2-UNIQUAC model are shown in Tables 6.2 to 4 and Figures 6.2 to 6.4. The relative error of methanol mole fraction in liquid (x) and vapor (y) phase was calculated from equation (6.8). Thus, the minus and plus sign illustrated the under and overestimated value respectively.

$$\%Relative\ Error = \frac{(Calculated\ value - Experimental\ value)}{Experimental\ value} \times 100 \quad (6.8)$$

The PR-MHV2-UNIQUAC model had maximum relative error of 5% for the triolein + methanol and 3% for methyl oleate + methanol, whereas it had maximum relative error of 10% for the glycerol + methanol system that was higher than the relative error of the specific models in the literature due to the difference polarity of those mixtures, especially for triolein + methanol and glycerol + methanol. The polarity of the compounds can be ranked by their dielectric constants, being 41.14, 32.60, 3.12 and 3.11 for glycerol, methanol, methyl oleate and triolein, respectively [96]. Thus, the attractive and repulsive forces within the glycerol + methanol system were somewhat higher than both the triolein + methanol and methyl oleate + methanol systems, and affected the thermodynamic model for VLE prediction. For example, the Peng–Robinson (PR EOS) and the van der Waals (VdW) mixing rule models were tested on the triolein + methanol system and give an approximately 2% relative error [19], whereas the Peng–Robinson Stryjek–Vera (PR-SV) EOS and ASOG mixing rule (PRASOG model) give an approximately 3% relative error for the glycerol + methanol VLE system [17].

Table 6.2 Methanol mole fraction in liquid (x) and vapor (y) phase of triolein + methanol VLE [14].

| T (K) | P (Bar) | Experimental result | | Calculated result | | %Relative Error of x | %Relative Error of y |
|----------|------------|---------------------|--------|-------------------|--------|---------------------------|---------------------------|
| | | x | y | x | y | | |
| 473 | 39.7 | 0.9744 | 0.9997 | 0.9800 | 1.0000 | 0.575 | 0.030 |
| 473 | 36.7 | 0.9413 | 0.9998 | 0.9543 | 1.0000 | 1.383 | 0.020 |
| 473 | 34.1 | 0.9087 | 0.9996 | 0.9269 | 1.0000 | 2.004 | 0.040 |
| 473 | 29.2 | 0.8540 | 0.9996 | 0.8750 | 1.0000 | 2.461 | 0.040 |
| 483 | 45.3 | 0.9655 | 0.9999 | 0.9800 | 1.0000 | 1.502 | 0.010 |
| 483 | 42.5 | 0.9557 | 0.9999 | 0.9665 | 1.0000 | 1.125 | 0.009 |
| 483 | 39.9 | 0.9292 | 1.0000 | 0.9337 | 1.0000 | 0.487 | 0.000 |
| 483 | 31.1 | 0.8642 | 0.9998 | 0.8166 | 1.0000 | -5.504 | 0.020 |
| 493 | 48.6 | 0.9755 | 0.9997 | 0.9773 | 1.0000 | 0.187 | 0.029 |
| 493 | 48.0 | 0.9729 | 0.9997 | 0.9756 | 1.0000 | 0.276 | 0.028 |
| 493 | 43.5 | 0.9569 | 0.9999 | 0.9566 | 1.0000 | -0.027 | 0.008 |
| 493 | 40.4 | 0.9170 | 0.9999 | 0.9287 | 1.0000 | 1.271 | 0.009 |

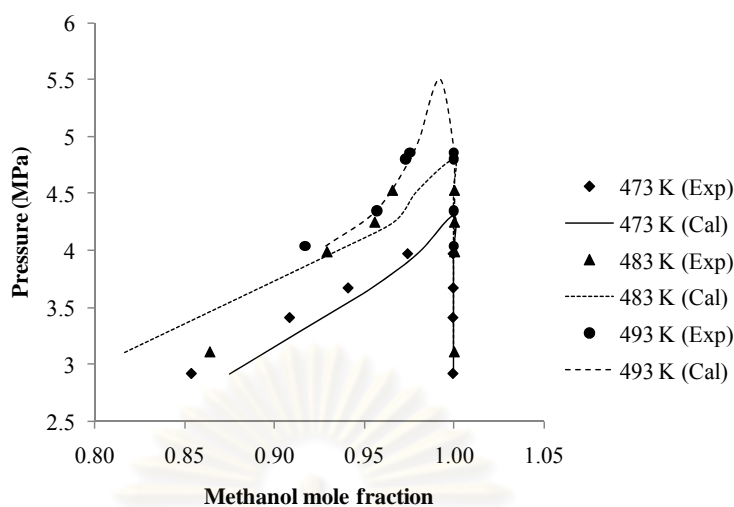


Figure 6.1 Experimental (Exp) and calculated (Cal) P-x-y diagram of triolein + methanol VLE. The experimental data were measured twice at each point and they have the average deviations of 3.09 % and 0.15 % for liquid and vapor phase measurement, respectively [14].

Table 6.3 The methanol mole fraction in liquid (x) and vapor (y) phase of methyl oleate + methanol VLE [55].

| T (K) | P (Bar) | Experimental result | | Calculated result | | %Relative Error of x | %Relative Error of y |
|----------|------------|---------------------|--------|-------------------|--------|-------------------------|-------------------------|
| | | x | y | x | y | | |
| 523 | 24.5 | 0.4650 | 1.0000 | 0.4521 | 0.9951 | -2.780 | -0.489 |
| 523 | 53.5 | 0.7310 | 0.9999 | 0.7326 | 0.9958 | 0.219 | -0.316 |
| 523 | 64.6 | 0.8140 | 1.0000 | 0.8106 | 0.9954 | -0.415 | -0.463 |
| 523 | 70.2 | 0.8630 | 1.0000 | 0.8465 | 0.9949 | -1.906 | -0.510 |
| 523 | 78.0 | 0.9160 | 1.0000 | 0.8949 | 0.9937 | -2.300 | -0.633 |
| 548 | 45.9 | 0.5750 | 1.0000 | 0.5716 | 0.9930 | -0.597 | -0.697 |
| 548 | 61.0 | 0.6930 | 1.0000 | 0.6750 | 0.9936 | -2.593 | -0.643 |
| 548 | 79.0 | 0.7900 | 1.0000 | 0.7724 | 0.9935 | -2.233 | -0.647 |
| 548 | 88.0 | 0.8380 | 0.9930 | 0.8125 | 0.9933 | -3.043 | 0.029 |
| 548 | 94.8 | 0.8610 | 0.9910 | 0.8394 | 0.9930 | -2.508 | 0.205 |
| 573 | 60.3 | 0.6070 | 1.0000 | 0.6204 | 0.9889 | 2.209 | -1.106 |
| 573 | 70.1 | 0.6990 | 1.0000 | 0.6764 | 0.9901 | -3.238 | -0.993 |
| 573 | 83.9 | 0.7510 | 0.9960 | 0.7440 | 0.9916 | -0.936 | -0.440 |
| 573 | 102.5 | 0.8330 | 0.9880 | 0.8172 | 0.9942 | -1.896 | 0.623 |
| 573 | 114.5 | 0.8600 | 0.9860 | 0.8532 | 0.9959 | -0.795 | 1.001 |

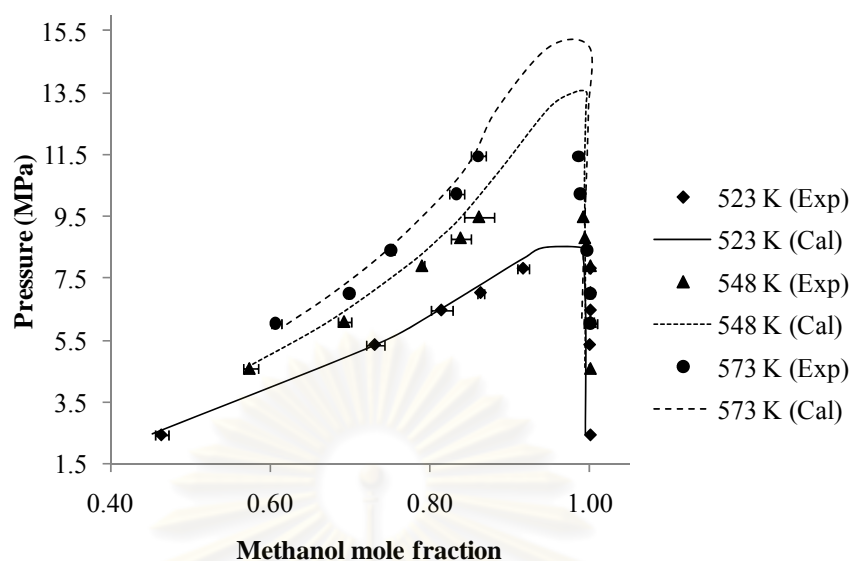


Figure 6.2 Experimental (Exp) and calculated (Cal) P-x-y diagram of methyl oleate + methanol VLE. The experimental data were measured four times at each point and the average deviations were shown in figure as error bars [55].

Table 6.4 The methanol mole fraction in liquid (x) and vapor (y) phase of glycerol + methanol VLE [17].

| T (K) | P (Bar) | Experimental result | | Calculated result | | %Relative Error of x | %Relative Error of y |
|----------|------------|---------------------|--------|-------------------|--------|---------------------------|---------------------------|
| | | x | y | x | y | | |
| 493 | 30.3 | 0.4780 | 1.0000 | 0.4898 | 0.9924 | 2.464 | -0.757 |
| 493 | 34.1 | 0.5500 | 1.0000 | 0.5577 | 0.9927 | 1.392 | -0.729 |
| 493 | 38.6 | 0.6450 | 1.0000 | 0.6503 | 0.9930 | 0.825 | -0.703 |
| 493 | 42.3 | 0.7010 | 1.0000 | 0.7418 | 0.9932 | 5.821 | -0.676 |
| 493 | 46.7 | 0.8500 | 1.0000 | 0.8523 | 0.9939 | 0.276 | -0.607 |
| 493 | 51.2 | 0.9650 | 1.0000 | 0.9299 | 0.9955 | -3.642 | -0.452 |
| 523 | 46.4 | 0.4840 | 1.0000 | 0.4681 | 0.9816 | -3.287 | -1.836 |
| 523 | 52.1 | 0.5650 | 1.0000 | 0.5248 | 0.9812 | -7.119 | -1.882 |
| 523 | 60.8 | 0.6890 | 1.0000 | 0.6217 | 0.9795 | -9.766 | -2.051 |
| 523 | 67.9 | 0.8070 | 1.0000 | 0.7269 | 0.9769 | -9.925 | -2.312 |
| 523 | 71.6 | 0.8680 | 1.0000 | 0.8055 | 0.9749 | -7.197 | -2.510 |
| 543 | 54.1 | 0.4310 | 1.0000 | 0.4506 | 0.9708 | 4.546 | -2.921 |
| 543 | 61.8 | 0.5090 | 1.0000 | 0.5084 | 0.9698 | -0.117 | -3.024 |
| 543 | 69.9 | 0.5920 | 1.0000 | 0.5709 | 0.9674 | -3.562 | -3.259 |
| 543 | 79.1 | 0.6970 | 1.0000 | 0.6479 | 0.9623 | -7.043 | -3.770 |
| 543 | 86.1 | 0.7800 | 0.9900 | 0.7175 | 0.9546 | -8.008 | -3.576 |

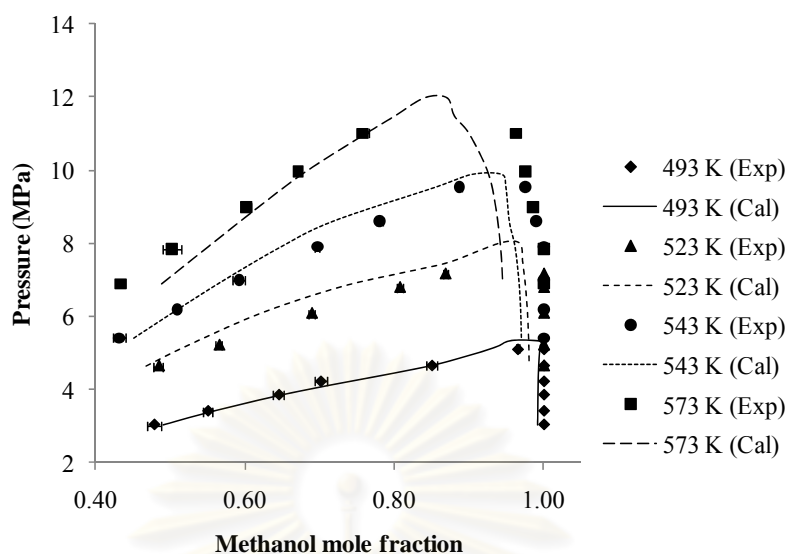


Figure 6.3 Experimental (Exp) and calculated (Cal) P-x-y diagram of glycerol + methanol VLE. The experimental data were measured four to six times at each point and the average deviations were shown in figure as error bars [17].

6.3. ME content prediction by the compressible flow model

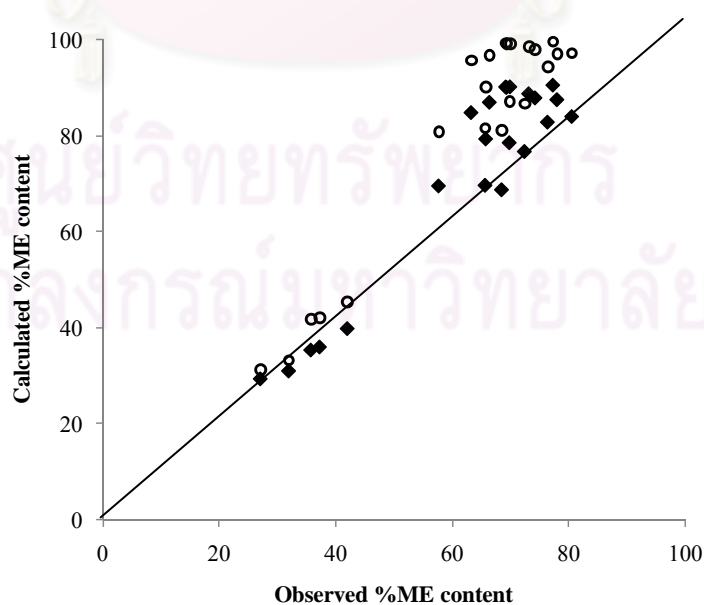
The compressible flow model was tested in various reacting conditions as shown in Table 6.5, and then in Figure 6.5, observed values were plotted against calculated values. Furthermore, the %relative error and residence time for each condition in Table 6.5 can be calculated by Equation (6.8) and (6.9), respectively. The residence time estimation procedure is described in Section 6.4.

$$\tau = \int_V \frac{dV}{u} \quad (6.9)$$

Table 6.5 The observed and calculated ME content from various reacting conditions.

| No. | T (°C) | P (MPa) | MeOH:Oil molar ratio | τ (min) | Exp. value | ME content (%) | | %Relative error | |
|-----|-----------|------------|----------------------------|-----------------|---------------|----------------|---------------|-----------------|---------------|
| | | | | | | Cal. value* | Cal. value ** | Cal. value* | Cal. value ** |
| 1 | 278 | 35 | 12.0 | 42.21 | 35.75 | 35.18 | 41.70 | -1.6 | 16.6 |
| 2 | 280 | 20 | 14.4 | 42.36 | 37.25 | 35.81 | 41.95 | -3.9 | 12.6 |
| 3 | 280 | 35 | 41.4 | 46.52 | 27.09 | 29.17 | 31.13 | 7.7 | 14.9 |
| 4 | 282 | 20 | 38.9 | 45.25 | 31.95 | 30.82 | 33.16 | -3.5 | 3.8 |
| 5 | 285 | 35 | 21.0 | 44.65 | 42.01 | 39.65 | 45.32 | -5.6 | 7.9 |
| 6 | 300 | 20 | 27.8 | 39.71 | 68.50 | 68.60 | 81.03 | 0.2 | 18.3 |
| 7 | 300 | 35 | 36.7 | 40.55 | 65.67 | 69.53 | 81.56 | 5.9 | 24.2 |
| 8 | 300 | 35 | 39.6 | 40.57 | 69.82 | 78.42 | 87.05 | 12.3 | 24.7 |
| 9 | 320 | 20 | 23.7 | 34.04 | 80.55 | 83.88 | 97.19 | 4.1 | 20.7 |
| 10 | 320 | 20 | 23.7 | 34.05 | 76.38 | 82.71 | 94.20 | 8.3 | 23.3 |
| 11 | 320 | 35 | 37.3 | 41.96 | 57.68 | 69.40 | 80.86 | 20.3 | 40.2 |
| 12 | 320 | 35 | 22.8 | 40.08 | 65.78 | 79.20 | 90.10 | 20.4 | 36.9 |
| 13 | 320 | 35 | 38.7 | 41.00 | 72.42 | 76.59 | 86.60 | 5.8 | 19.6 |
| 14 | 350 | 20 | 24.8 | 35.84 | 73.15 | 88.63 | 98.41 | 21.2 | 34.5 |
| 15 | 350 | 20 | 16.9 | 36.17 | 74.24 | 87.76 | 97.87 | 18.2 | 31.8 |
| 16 | 350 | 20 | 27.8 | 37.48 | 63.26 | 84.70 | 95.69 | 33.9 | 51.3 |
| 17 | 350 | 35 | 17.1 | 35.67 | 69.35 | 89.95 | 99.14 | 29.7 | 42.9 |
| 18 | 350 | 35 | 35.2 | 35.62 | 69.94 | 90.07 | 99.18 | 28.8 | 41.8 |
| 19 | 350 | 35 | 27.8 | 38.53 | 66.41 | 86.86 | 96.72 | 30.8 | 45.6 |
| 20 | 350 | 35 | 35.9 | 35.41 | 69.19 | 90.05 | 99.22 | 30.2 | 43.4 |
| 21 | 352 | 20 | 17.1 | 34.05 | 77.30 | 90.42 | 99.54 | 17.0 | 28.8 |
| 22 | 352 | 35 | 43.4 | 38.39 | 78.00 | 87.39 | 97.01 | 12.0 | 24.4 |

As calculated by * equation (6.6) or ** equation (6.7) (see the text)

**Figure 6.5** The plot of experimented and calculated ME content by Eq. 6.6 (◆) or Eq.6.7 (○).

According to Figure 6.5, the model was good for estimating %ME content at temperature range of 280 – 320 °C, while calculated %methyl esters at 320 – 350 °C were overestimated. It was noticed that %relative error of calculated values from Equation (6.6) was increasing with reaction temperature as illustrated in Figure 6.6, whereas the pattern of %relative error with methanol to oil molar ratio and pressure were scattered as shown in Figure 6.7 and 6.8 respectively.

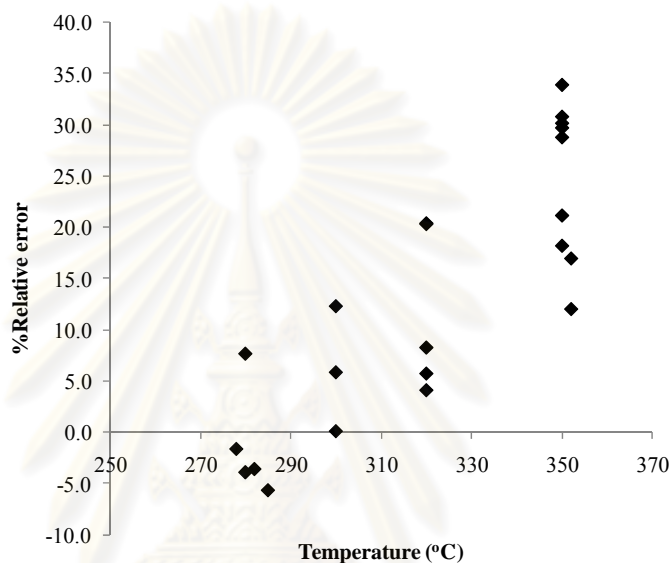


Figure 6.6 The relationship between percentage of relative error of calculated value from Eq. 6.6 and reaction temperature.

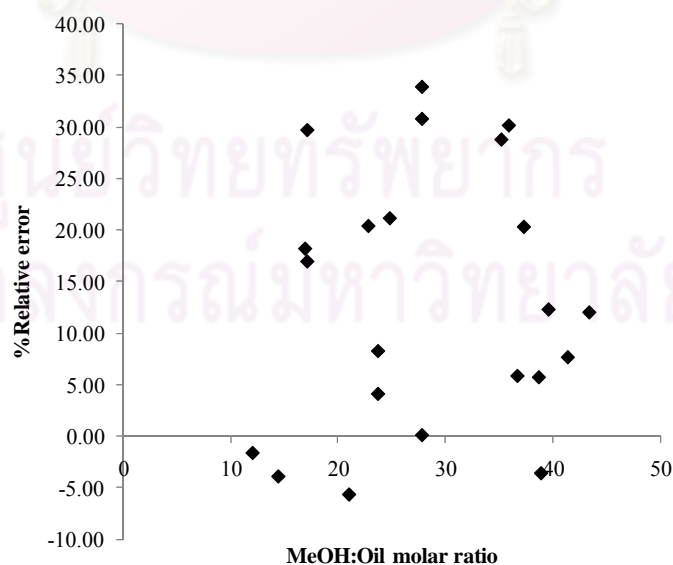


Figure 6.7 The relationship between percentage of relative error of calculated value from Eq. 6.6 and methanol to oil molar ratio.

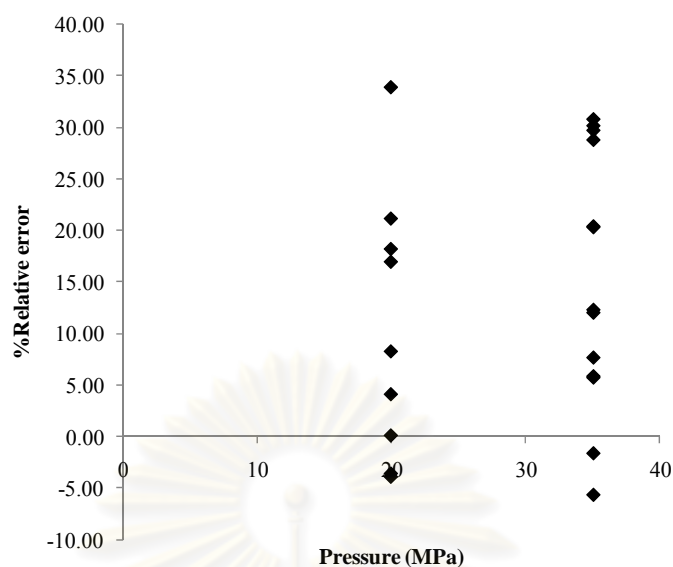


Figure 6.8 The relationship between percentage of relative error of calculated value from Eq. 6.6 and pressure.

Within the temperature range of 320 – 350 °C, the calculated %ME values were higher than experimented values because the observed %ME was presumed to be reduced by the thermal degradation reaction. Indeed, RBD palm olein oil consists of approximately 46% oleic acid and 11% linoleic acid, respectively [97]. It has been reported that thermal degradation of unsaturated fatty acids occurs at the same temperature range and residence time of 320 – 350 °C over 30 min. For example, methyl oleate and methyl linoleate decompose by approximately 10% and 20% by weight, respectively, in SCM at 350 °C after 30 min contact time [58]. Therefore, by extrapolation to this system, 4.6% and 2.2% of methyl oleate and linoleate, respectively, were degradable and so the observed ME content was reduced by 6.8% at 350 °C for over 30 min residence time.

Variation in the compressibility factor slows down the rate of transesterification slightly, as shown by comparison with calculated values from equation (6.6), which accounts only for chemical kinetics, and which were approximately 2 – 13% higher than the values derived from equation (6.7). At a temperature of 280 °C, the difference between the calculated values derived from equations (6.6) and (6.7) decreased with increasing methanol to oil molar ratios due to the irreversible assumption of kinetic model was more valid at high methanol to oil molar ratio [72]. This can be observed, for instance, by comparison of the difference between the calculated values in either runs 1 and 3 or runs 2 and 4. However, the effect of the changes in the compressibility factor upon the rate of transesterification had the same magnitude, being approximately 10%, at temperatures above 300 °C.

An example of the change in the compressibility factor and the molar volume of the mixture are shown in Figures 6.9 and 6.10, respectively. Values from run nos. 1 – 5 were selected to demonstrate the effect of pressure on the changes in the compressibility factor, which, as expected, were higher at 35.0 MPa than at 20.0 MPa. In addition, the values from run nos. 17 and 22 illustrate the effect of temperature on the changes in the compressibility factor and the molar volume of mixture. It was clear that the compressibility factor and molar volume at $\sim 350^\circ\text{C}$ rose faster than the values at $\sim 280^\circ\text{C}$. At a constant temperature and pressure, the changes in the compressibility factor and the molar volume at a low methanol to oil molar ratio was faster than that seen at a high methanol to oil molar ratio. Therefore, the compressibility factor and the molar volume of the mixture were both enhanced with increasing reactor length and they had a steeper slope at high temperatures and lower methanol to oil molar ratios.

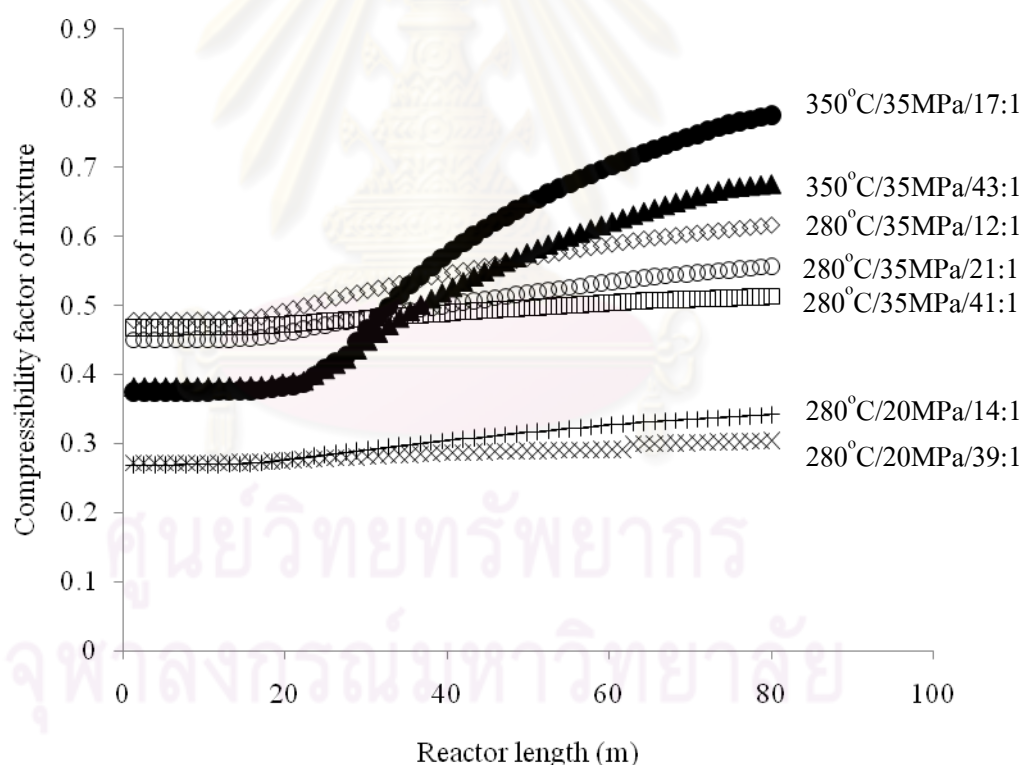


Figure 6.9 The changes in the compressibility of the reaction mixture along the length of the tubular reactor in run no. 1 (◇), 2 (+), 3 (□), 4 (×), 5 (○), 17 (●) and 22 (▲). The abbreviations on the figure are the experimental conditions as the operational temperature ($^\circ\text{C}$)/pressure (MPa)/methanol to oil (molar ratio).

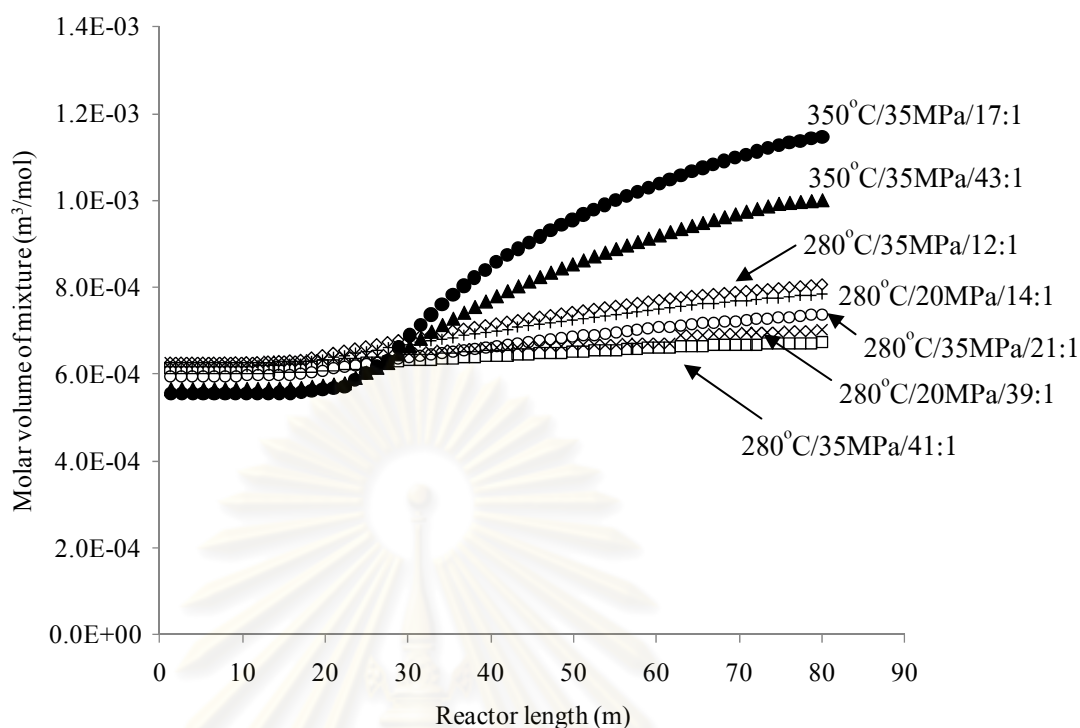


Figure 6.10 The changes in the molar volume of the reaction mixture along the length of the tubular reactor in run no. 1 (◇), 2 (+), 3 (□), 4 (×), 5 (○), 17 (●) and 22 (▲). The abbreviations on the figure are the experimental conditions as the operational temperature (°C)/pressure (MPa)/methanol to oil (molar ratio).

The deviation of the predicted %ME values at high temperatures may be due to a number of reasons. Firstly, the real mixture is slightly different from the simulated mixture, as mentioned in Section 3.1. Since the exact chemical formula of vegetable oils does not exist, the deviation from this cause could not be avoided but could probably be minimized by some approaches, such as using a group contribution method to estimate a single pseudo-triglyceride molecule [56, 57, 86]. Secondly, thermodynamic model predictions at high temperatures have, in general, a higher relative error than at low temperatures. For example, the PR-MHV2-UNIQUAC prediction of glycerol + methanol system had maximum relative error of 10% at 523 K compared to 5% at 493 K. Thirdly, the coefficient of determination of kinetics model at 0.9578 [72], ~4% of random error was taken into account in our compressible flow model.

6.4. Residence time estimation procedure

Refer to Equation 6.9, this is the general residence time estimation in tubular reactor [98].

$$\tau = \int_V \frac{dV}{u} \quad (6.9)$$

where V and u are reactor volume (m^3) and linear velocity of fluid (m/sec), respectively. Since, the differential reactor volume can be decomposed to the product of cross-sectional area and reactor length, while the linear velocity is the product of total molar flow rate and molar volume of the mixture, then Equation 6.9 can be rewritten as Equation 6.10.

$$\tau = \frac{A}{F_0} \int_{L_1}^{L_2} \frac{dL}{v_m(L)} \quad (6.10)$$

The development of molar volume of mixture can be separated into constant and increasing interval as illustrate in Figure 6.10, Equation 6.10 is rewritten as Equation 6.11 then simplify to Equation 6.12.

$$\tau = \frac{A^2}{F_0} \left[\int_0^{L_1} \frac{dL}{v_m(L)} + \int_{L_1}^{80} \frac{dL}{v_m(L)} \right] \quad (6.11)$$

$$\tau = \frac{A^2}{F_0} \left[\frac{L_1}{v_1} + \int_{L_1}^{80} \frac{dL}{v_m(L)} \right] \quad (6.12)$$

where A , F , v , and L are reactor cross-sectional area (m^2), total molar flow rate (mol/s), molar volume (m^3/mol) and reactor length (m), respectively. The subscript 0, 1 and m refer to reactor inlet, constant molar volume interval and mixture, respectively. The development of molar volume within increasing interval as a function of reactor length, $v_m(L)$, can be evaluated by fitting of cubic polynomial to PR-MHV2-UNIQUAC model prediction and integrated numerically by adaptive Gauss-Kronrod method in Matlab® software.

CHAPTER VII

CONCLUSIONS AND RECOMMENDATION

7.1. Conclusions

7.1.1. Effects of co-solvents on the production of biodiesel from PKO in SCM

The reaction of co-solvent with other reactants (vegetable oil and methanol) did not occur at supercritical conditions. However, the addition of liquid co-solvents did not allow the reaction to be completed at milder conditions due to the critical properties of the co-solvents, which are close to those of methanol. The addition of co-solvents (THF and hexane) in this process did not show either negative or positive effects on methyl esters content, thus THF and hexane are appropriate co-solvents for reduced viscosity of PKO in the scale-up reactor.

7.1.2. Effects of additional parameters and scale-up reactor optimization

The transesterification of PKO in SCM achieves equilibrium after 30 min reaction time in a 250-mL reactor and less than 10 min in a 5.5-mL reactor. The methyl esters content from crude vegetable oil was slightly lower than that of refined vegetable oil, plausibly because of the lower triglyceride content. The delayed and deficient quenching time had no significant effect on ME content for biodiesel production with SCM in both 5.5-mL batch and continuous reactor.

For scale-up reactor optimization, the optimal conditions (ME content over 96.5 %) located with temperature range of 310 to 330 °C, pressure range of 17.5 to 18.5 MPa and methanol to oil molar ratio of 35:1 to 40:1. However, the actual highest ME content of approximately 93 % was observed from the scale-up reactor probably due to the optimal range in the regression model was narrower than the controllable range of the operating parameters.

7.1.3. Residence time estimation method

The simple compressible flow model as a tool for residence time estimation was successfully derived and checked within 280 to 350 °C, 20 to 35 MPa and 12:1 to 42:1 methanol to oil molar ratio. The PR-MHV2-UNIQUAC thermodynamic model with adjusted binary interaction coefficients was employed to evaluate the development of the compressibility factor during reaction progress along the reactor. Although the thermodynamic model fitting of VLE from literatures had maximum relative error of approximately 10 % for glycerol + methanol VLE, the simple compressible flow model was proven to be adequate at temperature below 320 °C.

Nevertheless, its prediction was over-estimated values due to the interfering of thermal degradation reaction at temperature over 320 °C, that were not taken into account in this model.

In addition, the simple compressible flow model demonstrated that the chemical kinetics of biodiesel production with SCM was retarded by the development of the compressibility factor along the reactor, especially at low methanol to oil molar ratio. In conclusion, the residence time can be estimated by integration of molar volume of reaction mixture which calculated by the PR-MHV2-UNIQUAC thermodynamic model.

7.2. Recommendation

In this work the continuous production of biodiesel with SCM in a tubular reactor was explored. Some issues have arisen from this exploration and warrant further researches as following aspects:

7.1.1. Thermal degradation of unsaturated fatty acids (UFA) in SCM

Since thermal degradation reaction of UFA plays an important role on biodiesel production in SCM, but the details of this reaction especially in SCM are limited. Furthermore, thermal degradation of UFA in SCM under high pressure is somewhat different from the degradation at atmospheric pressure or pyrolysis. Even though thermal degradation reaction can avoid by keep operating temperature in range of 270 – 300 °C or use the gradual heating technique to maintain the maximum ME content, but these approaches reduce the rate of transesterification and the simplicity of process which are strong points of biodiesel production with SCM. On the other hand, thermal degradation of UFA has been reported to improve the fuel properties of biodiesel, except the ME content, that is produced from SCM process at temperature over 400 °C. Therefore, the additional studies on thermal degradation of UFA in SCM are interesting to improve the biodiesel production with SCM process.

7.1.2. Mixing intensity of a tubular reactor for biodiesel production with SCM

Effect of mixing intensity for biodiesel production with SCM has not been fully addressed in either batch or continuous studies, whereas it affects ME content as mentioned in Section 2.4.2.5. For instance, the better mixing intensity allows the reaction to complete shortly in a batch reactor at constant temperature. Consequently, a tubular reactor performance for biodiesel production with SCM might be enhanced by assisting of some mixing equipment such as pre-mixing tank or static mixers.

7.1.3. Residence time distribution in a tubular reactor for biodiesel production with SCM

The effect of compressibility changes on ME content in biodiesel production with SCM has been successfully discovered in this work, while dispersion effect which generally influences the efficiency of a tubular reactor did not take into account. The dispersion effect can be determined experimentally by residence time distribution measurement. However, the residence time distribution measurement requires more precise equipments such as real-time temperature, pressure, flow rate and tracer monitoring system. Thus, further researches on residence time distribution in a tubular reactor could perform the better understanding on the biodiesel production with SCM.



REFERENCES

- [1] Bender, M. Economic feasibility review for community-scale farmer cooperatives for biodiesel. Bioresource Technology 70(1999): 81-87.
- [2] Kulkarni, M.G. and A.K. Dalai. Waste Cooking Oils An Economical Source for Biodiesel: A Review. Industrial & Engineering Chemistry Research 45(2006): 2901-2913.
- [3] Coronado, C.R., J.A. de Carvalho Jr, and J.L. Silveira. Biodiesel CO₂ emissions: A comparison with the main fuels in the Brazilian market. Fuel Processing Technology 90(2009): 204-211.
- [4] Hu, Z., P. Tan, X. Yan, and D. Lou. Life cycle energy, environment and economic assessment of soybean-based biodiesel as an alternative automotive fuel in China. Energy 33(2008): 1654-1658.
- [5] Wu, Y.-p.G., Y.-f. Lin, and C.-T. Chang. Combustion characteristics of fatty acid methyl esters derived from recycled cooking oil. Fuel 86(2007): 2810-2816.
- [6] Saka, S. and D. Kusdiana. Biodiesel fuel from rapeseed oil as prepared in supercritical methanol. Fuel 80(2001): 225 - 231.
- [7] Demirbas, A. Biodiesel from vegetable oils via transesterification in supercritical methanol. Energy Conversion and Management 43(2002): 2349 - 2356.
- [8] Han, H., W. Cao, and J. Zhang. Preparation of biodiesel from soybean oil using supercritical methanol and CO₂ as co-solvent. Process Biochemistry 40(2005): 3148-3151.
- [9] Bunyakiat, K., S. Makmee, R. Sawangkeaw, and S. Ngamprasertsith. Continuous Production of Biodiesel via Transesterification from Vegetable Oils in Supercritical Methanol. Energy and Fuels 20(2006): 812-817.
- [10] Minami, E. and S. Saka. Kinetics of hydrolysis and methyl esterification for biodiesel production in two-step supercritical methanol process. Fuel 85(2006): 2479-2483.
- [11] He, H., T. Wang, and S. Zhu. Continuous production of biodiesel fuel from vegetable oil using supercritical methanol process. Fuel 86(2007): 442-447.
- [12] Busto, M., S.A. D'Ippolito, J.C. Yori, M.E. Iturria, C.L. Pieck, J.M. Grau, and C.R. Vera. Influence of the Axial Dispersion on the Performance of Tubular Reactors during the Noncatalytic Supercritical Transesterification of Triglycerides. Energy and Fuels 20(2006): 2642-2647.

- [13] D'Ippolito, S.A., J.C. Yori, M.E. Iturria, C.L. Pieck, and C.R. Vera. Analysis of a Two-Step, Noncatalytic, Supercritical Biodiesel Production Process with Heat Recovery. Energy and Fuels 21(2007): 339-346.
- [14] Glišić, S., O. Montoya, A. Orlovic, and D. Skala. Vapor-liquid equilibria of triglycerides-methanol mixtures and their influence on the biodiesel synthesis under supercritical conditions of methanol. Journal of the Serbian Chemical Society 72(2007): 13-27.
- [15] Glišić, S.B. and D.U. Skala. Phase transition at subcritical and supercritical conditions of triglycerides methanolysis. The Journal of Supercritical Fluids 54(2010): 71-80.
- [16] Shimoyama, Y., T. Abeta, and Y. Iwai. Prediction of vapor-liquid equilibria for supercritical alcohol + fatty acid ester systems by SRK equation of state with Wong-Sandler mixing rule based on COSMO theory. The Journal of Supercritical Fluids 46(2008): 4-9.
- [17] Shimoyama, Y., T. Abeta, L. Zhao, and Y. Iwai. Measurement and calculation of vapor-liquid equilibria for methanol + glycerol and ethanol + glycerol systems at 493-573 K. Fluid Phase Equilibria 284(2009): 64-69.
- [18] Shimoyama, Y., Y. Iwai, B.S. Jin, T. Hirayama, and Y. Arai. Measurement and correlation of vapor-liquid equilibria for methanol + methyl laurate and methanol + methyl myristate systems near critical temperature of methanol. Fluid Phase Equilibria 257(2007): 217-222.
- [19] Tang, Z., Z. Du, E. Min, L. Gao, T. Jiang, and B. Han. Phase equilibria of methanol-triolein system at elevated temperature and pressure. Fluid Phase Equilibria 239(2006): 8-11.
- [20] Sawangkeaw, R. Continuous production of biodiesel from vegetable oils via transesterification in supercritical methanol in a pilot scale reactor. Master thesis Department of Chemical Technology, Faculty of Science Chulalongkorn University, 2005
- [21] Ma, F. and M.A. Hanna. Biodiesel production: a review. Bioresource Technology 70(1999): 1-15.
- [22] Meher, L.C., D.V. Sagar, and S.N. Naik. Technical aspects of biodiesel production by transesterification-a review. Renewable and Sustainable Energy Reviews 10(2006): 248-268.

- [23] Basha, S.A., K.R. Gopal, and S. Jebaraj. A review on biodiesel production, combustion, emissions and performance. Renewable and Sustainable Energy Reviews 13(2009): 1628-1634.
- [24] Lee, S.Y., M.A. Hubbe, and S. Saka. Prospects for biodiesel as a byproduct of wood pulping - A review. BioResource 1(2006): 150-171.
- [25] Sharma, Y.C., B. Singh, and S.N. Upadhyay. Advancements in development and characterization of biodiesel: A review. Fuel 87(2008): 2355-2373.
- [26] Zullaikah, S., C.-C. Lai, S.R. Vali, and Y.-H. Ju. A two-step acid-catalyzed process for the production of biodiesel from rice bran oil. Bioresource Technology 96(2005): 1889-1896.
- [27] Berchmans, H.J. and S. Hirata. Biodiesel production from crude *Jatropha curcas* seed oil with a high content of free fatty acids. Bioresource Technology 99(2008): 1716-1721.
- [28] Marchetti, J.M., V.U. Miguel, and A.F. Errazu. Heterogeneous esterification of oil with high amount of free fatty acids. Fuel 86(2007): 906-910.
- [29] Di Serio, M., M. Cozzolino, M. Giordano, R. Tesser, P. Patrono, and E. Santacesaria. From homogeneous to heterogeneous catalysts in biodiesel production. Industrial and Engineering Chemistry Research 46(2007): 6379-6384.
- [30] Di Serio, M., R. Tesser, L. Pengmei, and E. Santacesaria. Heterogeneous catalysts for biodiesel production. Energy and Fuels 22(2008): 207-217.
- [31] Ngamcharussrivichai, C., W. Wiwatnimit, and S. Wangnoi. Modified dolomites as catalysts for palm kernel oil transesterification. Journal of Molecular Catalysis A: Chemical 276(2007): 24-33.
- [32] Li, L., W. Du, D. Liu, L. Wang, and Z. Li. Lipase-catalyzed transesterification of rapeseed oils for biodiesel production with a novel organic solvent as the reaction medium. Journal of Molecular Catalysis B: Enzymatic 43(2006): 58-62.
- [33] Du, W., Y. Xu, D. Liu, and J. Zeng. Comparative study on lipase-catalyzed transformation of soybean oil for biodiesel production with different acyl acceptors. Journal of Molecular Catalysis B: Enzymatic 30(2004): 125-129.
- [34] Fukuda, H., A. Kondo, and H. Noda. Biodiesel fuel production by transesterification of oils. Journal of Bioscience and Bioengineering 92(2001): 405-416.

- [35] Ranganathan, S.V., S.L. Narasimhan, and K. Muthukumar. An overview of enzymatic production of biodiesel. Bioresource Technology 99(2008): 3975-3981.
- [36] Li, N.-W., M.-H. Zong, and H. Wu. Highly efficient transformation of waste oil to biodiesel by immobilized lipase from *Penicillium expansum*. Process Biochemistry 44(2009): 685-688.
- [37] Robles-Medina, A., P.A. González-Moreno, L. Esteban-Cerdán, and E. Molina-Grima. Biocatalysis: Towards ever greener biodiesel production. Biotechnology Advances 27(2009): 398-408.
- [38] Wang, Y., H. Wu, and M.H. Zong. Improvement of biodiesel production by lipozyme TL IM-catalyzed methanolysis using response surface methodology and acyl migration enhancer. Bioresource Technology 99(2008): 7232-7237.
- [39] Kusdiana, D. and S. Saka. Kinetics of transesterification in rapeseed oil to biodiesel fuel as treated in supercritical methanol. Fuel 80(2001): 693 - 698.
- [40] Pinnarat, T. and P.E. Savage. Assessment of noncatalytic biodiesel synthesis using supercritical reaction conditions. Industrial and Engineering Chemistry Research 47(2008): 6801-6808.
- [41] Kusdiana, D. and S. Saka. Effects of water on biodiesel fuel production by supercritical methanol treatment. Bioresource Technology 91(2004): 289-295.
- [42] Demirbas, A. Biodiesel from waste cooking oil via base-catalytic and supercritical methanol transesterification. Energy Conversion and Management 50(2009): 923-927.
- [43] Diasakou, M., A. Louloudi, and N. Papayannakos. Kinetic of the non-catalytic transesterification of soybean oil. Fuel 77(1998): 1297 - 1320.
- [44] Magmae, S., K. Bunyakiat, and S. Ngamprasertsith. Experimental production of biodiesel from vegetable oil as prepared in supercritical methanol by continuous process. Master Chemical Technology Chulalongkorn University, 2002
- [45] Kusdiana, D. and S. Saka. Catalytic effect of metal reactor in transesterification of vegetable oil. Journal of the American Oil Chemists' Society 81(2004): 103-104.
- [46] Warabi, Y., D. Kusdiana, and S. Saka. Reactivity of triglycerides and fatty acids of rapeseed oil in supercritical alcohols. Bioresource Technology 91(2004): 283-287.

- [47] Cao, W., H. Han, and J. Zhang. Preparation of biodiesel from soybean oil using supercritical methanol and co-solvent. Fuel 84(2005): 347-351.
- [48] Wang, L., H. He, Z. Xie, J. Yang, and S. Zhu. Transesterification of the crude oil of rapeseed with NaOH in supercritical and subcritical methanol. Fuel Processing Technology 88(2007): 477-481.
- [49] Demirbas, A. Biodiesel from sunflower oil in supercritical methanol with calcium oxide. Energy Conversion and Management 48(2007): 937-941.
- [50] Wang, C.-W., J.-F. Zhou, W. Chen, W.-G. Wang, Y.-X. Wu, J.-F. Zhang, R.-A. Chi, and W.-Y. Ying. Effect of weak acids as a catalyst on the transesterification of soybean oil in supercritical methanol. Energy and Fuels 22(2008): 3479-3483.
- [51] Yin, J.-Z., M. Xiao, A.-Q. Wang, and Z.-L. Xiu. Synthesis of biodiesel from soybean oil by coupling catalysis with subcritical methanol. Energy Conversion and Management 49(2008): 3512-3516.
- [52] Wang, L. and J. Yang. Transesterification of soybean oil with nano-MgO or not in supercritical and subcritical methanol. Fuel 86(2007): 328-333.
- [53] Sawangkeaw, R., K. Bunyakiat, and S. Ngamprasertsith. Effect of co-solvents on production of biodiesel via transesterification in supercritical methanol. Green Chemistry 9(2007): 679-685.
- [54] Anitescu, G., A. Deshpande, and L.L. Tavlarides. Integrated technology for supercritical biodiesel production and power cogeneration. Energy and Fuels 22(2008): 1391-1399.
- [55] Fang, T., Y. Shimoyama, T. Abeta, Y. Iwai, M. Sasaki, and M. Goto. Phase equilibria for the mixtures of supercritical methanol + C18 methyl esters and supercritical methanol + α -tocopherol. The Journal of Supercritical Fluids 47(2008): 140-146.
- [56] Hegel, P., G. Mabe, S. Pereda, and E.A. Brignole. Phase Transitions in a Biodiesel Reactor Using Supercritical Methanol. Ind. Eng. Chem. Res. 46(2007): 6360-6365.
- [57] Hegel, P., A. Andreatta, S. Pereda, S. Bottini, and E.A. Brignole. High pressure phase equilibria of supercritical alcohols with triglycerides, fatty esters and cosolvents. Fluid Phase Equilibria 266(2008): 31-37.
- [58] Imahara, H., E. Minami, S. Hari, and S. Saka. Thermal stability of biodiesel in supercritical methanol. Fuel 87(2008): 1-6.

- [59] Diaz, M.S., S. Espinosa, and E.A. Brignole. Model-Based Cost Minimization in Nuncatalytic Biodiesel Production Plants. Energy & Fuels 23(2009): 5587-5595.
- [60] van Kasteren, J.M.N. and A.P. Nisworo. A process model to estimate the cost of industrial scale biodiesel production from waste cooking oil by supercritical transesterification. Resources, Conservation and Recycling 50(2007): 442-458.
- [61] He, H., S. Sun, T. Wang, and S. Zhu. Transesterification Kinetics of Soybean Oil for Production of Biodiesel in Supercritical Methanol. Journal of the American Oil Chemists' Society 84(2007): 399-404.
- [62] Demirbas, A. Thermal Degradation of Fatty Acids in Biodiesel Production by Supercritical Methanol. Energy, Exploration & Exploitation 25(2007): 63-70.
- [63] Marulanda, V.F., G. Anitescu, and L.L. Tavlarides. Biodiesel Fuels through a Continuous Flow Process of Chicken Fat Supercritical Transesterification. Energy & Fuels (2009).
- [64] Marulanda, V.F., G. Anitescu, and L.L. Tavlarides. Biodiesel Fuels through a Continuous Flow Process of Chicken Fat Supercritical Transesterification. Energy & Fuels 24(2009): 253-260.
- [65] Marulanda, V.F., G. Anitescu, and L.L. Tavlarides. Investigations on supercritical transesterification of chicken fat for biodiesel production from low-cost lipid feedstocks. The Journal of Supercritical Fluids 54(2010): 53-60.
- [66] Madras, G., C. Kolluru, and R. Kumar. Synthesis of biodiesel in supercritical fluids. Fuel 83(2004): 2029-2033.
- [67] Rathore, V. and G. Madras. Synthesis of biodiesel from edible and non-edible oils in supercritical alcohols and enzymatic synthesis in supercritical carbon dioxide. Fuel 86(2007): 2650-2659.
- [68] Yin, J.-Z., M. Xiao, and J.-B. Song. Biodiesel from soybean oil in supercritical methanol with co-solvent. Energy Conversion and Management 49(2008): 908-912.
- [69] Kiwjaroun, C., C. Tubtimdee, and P. Piumsomboon. LCA studies comparing biodiesel synthesized by conventional and supercritical methanol methods. Journal of Cleaner Production 17(2009): 143-153.

- [70] Bazaev, A.R., I.M. Abdulagatov, E.A. Bazaev, A.A. Abdurashidova, and A.E. Ramazanova. PVT measurements for pure methanol in the near-critical and supercritical regions. The Journal of Supercritical Fluids 41(2007): 217-226.
- [71] Varma, M.N. and G. Madras. Synthesis of Biodiesel from Castor Oil and Linseed Oil in Supercritical Fluids. Industrial & Engineering Chemistry Research 46(2007): 1-6.
- [72] Song, E.-S., J.-w. Lim, H.-S. Lee, and Y.-W. Lee. Transesterification of RBD palm oil using supercritical methanol. The Journal of Supercritical Fluids 44(2008): 356-363.
- [73] Pereda, S., E.A. Brignole, and S.B. Bottini. Advances in phase equilibrium engineering of supercritical reactors. The Journal of Supercritical Fluids 47(2009): 336-343.
- [74] Constantinou, L., R. Gani, and J.P. O'Connell. Estimation of the acentric factor and the liquid molar volume at 298 K using a new group contribution method. Fluid Phase Equilibria 103(1995): 11-22.
- [75] Constantinou, L. and R. Gani. New group contribution method for estimating properties of pure compounds. AIChE Journal 40(1994): 1697-1710.
- [76] Imahara, H., J. Xin, and S. Saka. Effect of CO₂/N₂ addition to supercritical methanol on reactivities and fuel qualities in biodiesel production. Fuel 88(2009): 1329-1332.
- [77] Boocock, D., S. Konar, V. Mao, C. Lee, and S. Buligan. Fast formation of high-purity methyl esters from vegetable oils. Journal of the American Oil Chemists' Society 75(1998): 1167-1172.
- [78] Boocock, D., S. Konar, and H. Sidi. Phase diagrams for oil/methanol/ether mixtures. Journal of the American Oil Chemists' Society 73(1996): 1247-1251.
- [79] Çaylı, G. and S. Küsefoğlu. Increased yields in biodiesel production from used cooking oils by a two step process: Comparison with one step process by using TGA. Fuel Processing Technology 89(2008): 118-122.
- [80] Bournay, L., D. Casanave, B. Delfort, G. Hillion, and J.A. Chodorge. New heterogeneous process for biodiesel production: A way to improve the quality and the value of the crude glycerin produced by biodiesel plants. Catalysis Today 106(2005): 190-192.
- [81] Lene, F., V.C. Knud, and N. Birgir. A review of the current state of biodiesel production using enzymatic transesterification. Biotechnology and Bioengineering 102(2009): 1298-1315.

- [82] Aimaretti, N., D.L. Manuale, V.M. Mazziari, C.R. Vera, and J.C. Yori. Batch Study of Glycerol Decomposition in One-Stage Supercritical Production of Biodiesel. Energy & Fuels 23(2009): 1076-1080.
- [83] Yazdani, S.S. and R. Gonzalez. Anaerobic fermentation of glycerol: a path to economic viability for the biofuels industry. Current Opinion in Biotechnology 18(2007): 213-219.
- [84] Wong, D.S.H. and S.I. Sandler. A theoretically correct mixing rule for cubic equations of state. AIChE Journal 38(1992): 671-680.
- [85] Glišić, S. and D. Skala. The problems in design and detailed analyses of energy consumption for biodiesel synthesis at supercritical conditions. The Journal of Supercritical Fluids 49(2009): 293-301.
- [86] Espinosa, S., T. Fornari, S.B. Bottini, and E.A. Brignole. Phase equilibria in mixtures of fatty oils and derivatives with near critical fluids using the GC-EOS model. Journal of Supercritical Fluids 23(2002): 91-102.
- [87] Montgomery, D. Design and Analysis of Experiments. 5 ed New York: John Wiley and son, 2001.
- [88] Cert, A., W. Moreda, and M.C. Prez-Camino. Chromatographic analysis of minor constituents in vegetable oils. Journal of Chromatography A 881(2000): 131-148.
- [89] Glišić, S., I. Lukic, and D. Skala. Biodiesel synthesis at high pressure and temperature: Analysis of energy consumption on industrial scale. Bioresource Technology 100(2009): 6347-6354.
- [90] Peng, D.-Y. and D.B. Robinson. A New Two-Constant Equation of State. Industrial & Engineering Chemistry Fundamentals 15(1976): 59-64.
- [91] Huron, M.-J. and J. Vidal. New mixing rules in simple equations of state for representing vapour-liquid equilibria of strongly non-ideal mixtures. Fluid Phase Equilibria 3(1979): 255-271.
- [92] Søren, D. and L.M. Michael. High-pressure vapor-liquid equilibrium with a UNIFAC-based equation of state. AIChE Journal 36(1990): 1829-1836.

- [93] Anderson, T.F. and J.M. Prausnitz. Application of the UNIQUAC Equation to Calculation of Multicomponent Phase Equilibria. 1. Vapor-Liquid Equilibria. Industrial & Engineering Chemistry Process Design and Development 17(1978): 552-561.
- [94] Camy, S., J.S. Pic, E. Badens, and J.S. Condoret. Fluid phase equilibria of the reacting mixture in the dimethyl carbonate synthesis from supercritical CO₂. The Journal of Supercritical Fluids 25(2003): 19-32.
- [95] Foglor, H.S. Elements of chemical reaction engineering. 3 ed New Jersey: Prentice Hall, 1999.
- [96] Perry, R.H. and D.W. Green. Perry's Chemical Engineers Handbook. 7 ed New York: McGraw-Hill, 1999.
- [97] Anderson, D. Bailey's Industrial Oil and Fat Products. 6 ed. A Primer on Oils Processing Technology ed. F. Shahidi. Vol. 2: John Wiley & Sons, 2005.
- [98] Mann, U. Principles of chemical reactor analysis and design: new tools for industrial chemical reactor operation. 2 ed: John Wiley & Sons, 2008.

ศูนย์วิทยทรัพยากร
จุฬาลงกรณ์มหาวิทยาลัย



APPENDICES

ศูนย์วิทยทรัพยากร
จุฬาลงกรณ์มหาวิทยาลัย

APPENDIX A THE STATISTICAL ANALYSIS OF THE REGRESSION MODEL FOR SCALE-UP REACTOR

Table A1. The statistical values of the regression model for scale-up reactor from Design Expert ® 6.0 software

| Statistical term | value |
|----------------------------|--------|
| Overall mean | 64.36 |
| Overall standard deviation | 4.75 |
| C.V. | 7.38 |
| R ² | 0.9732 |
| Adjusted R ² | 0.9655 |
| PRESS | 938.67 |
| Predicted R ² | 0.9468 |
| Adequate Precision | 40.11 |

Overall mean (Mean) and standard deviation (SD) are calculated from the ME content of all experimental conditions. The coefficient of variation (C.V.) is a measure of unexplained or residual variation of the data relative to the size of mean. The variation expressed as a percentage of the overall mean and standard deviation, as shown in Equation A1.

$$C.V. = \frac{SD}{Mean} \times 100 \quad (A1)$$

Coefficient of determination (R²) is a measure of the amount of variation around the mean explained by the model, while adjusted R² is the ordinary R² value which is adjusted by the number of terms in the regression model. The adjusted R² was slightly lower than the R² that indicated the excluding of interaction terms has no significant impact on prediction of the model.

Predicted Residual Sum of Squares (PRESS) is a measure of how well the model predicts the responses in a new experiment and employ to calculate the predicted R². Small values of PRESS are desirable. The predicted R² of 0.9468 is in reasonable agreement, which differ less than 0.2, with the Adjusted R-Squared of 0.9655.

Adequate precision measures the signal to noise ratio and the value greater than 4 is desirable. The regression model has adequate precision of 40.11 which indicates that it will give reasonable performance in prediction within the design space.

The estimated coefficients and its standard error for the regression model for scale-up reactor are shown in Table A2.

Table A2. The estimated coefficients and its standard error in the regression model for scale-up reactor at $\pm 95\%$ confident interval from Design Expert $\text{\textcircled{R}}$ 6.0 software

| Factor | Estimated coefficient | Degree of freedom | Standard Error of estimated coefficient | Estimated coefficient at 95% confident interval | |
|----------------|-----------------------|-------------------|---|---|--------|
| | | | | Low | High |
| Constant | 75.90 | 1 | 1.86 | 72.03 | 79.78 |
| A-T | 21.02 | 1 | 1.21 | 18.50 | 23.54 |
| B-P | 9.60 | 1 | 1.00 | 7.52 | 11.68 |
| C-MeOH:Oil | 13.78 | 1 | 0.97 | 11.76 | 15.79 |
| A ² | -16.89 | 1 | 1.01 | -18.98 | -14.80 |
| B ² | -3.72 | 1 | 0.75 | -5.27 | -2.16 |
| C ² | -4.57 | 1 | 0.78 | -6.19 | -2.95 |

From Table A2, it was clear that the standard errors are approximately less than 10% of their estimated coefficients. Therefore, this regression model was adequate to predict the methyl ester content for scale-up reactor.

Observed and predicted values, residual, standardized residual and Cook's distance are illustrated in Table A3. The residual, which represents the random or unexplained error in experiments, is a different between observed and predicted values. The standardized residual is the residual divided by the estimated standard deviation of the residual.

Table A3. The residual analysis of actual and predicted value for the regression model for scale-up reactor

| Run Order | Actual Value | Predicted Value | Residual | Standardized Residual | Cook's Distance |
|-----------|--------------|-----------------|----------|-----------------------|-----------------|
| 1 | 76.34 | 74.10 | 2.24 | 0.51 | 0.01 |
| 2 | 54.72 | 53.95 | 0.76 | 0.18 | 0.00 |
| 3 | 83.23 | 80.05 | 3.19 | 0.78 | 0.03 |
| 4 | 78.25 | 75.42 | 2.83 | 0.65 | 0.01 |
| 5 | 38.96 | 47.46 | -8.50 | -2.37 | 0.60 |
| 6 | 72.97 | 75.90 | -2.93 | -0.67 | 0.01 |
| 7 | 32.54 | 35.10 | -2.56 | -0.62 | 0.02 |
| 8 | 40.49 | 44.89 | -4.40 | -1.07 | 0.05 |
| 9 | 3.16 | 0.92 | 2.24 | 0.56 | 0.02 |
| 10 | 91.46 | 96.17 | -4.71 | -1.05 | 0.02 |
| 11 | 80.63 | 75.60 | 5.02 | 1.15 | 0.03 |
| 12 | 21.60 | 20.21 | 1.39 | 0.34 | 0.01 |
| 13 | 35.86 | 36.39 | -0.52 | -0.16 | 0.00 |
| 14 | 60.41 | 62.56 | -2.15 | -0.53 | 0.01 |
| 15 | 65.77 | 65.97 | -0.20 | -0.05 | 0.00 |
| 16 | 2.10 | 4.85 | -2.75 | -0.80 | 0.08 |
| 17 | 82.37 | 82.09 | 0.27 | 0.08 | 0.00 |
| 18 | 78.25 | 74.28 | 3.97 | 0.91 | 0.02 |
| 19 | 75.50 | 64.10 | 11.40 | 2.85 | 0.47 |
| 20 | 80.91 | 83.35 | -2.44 | -0.55 | 0.01 |
| 21 | 85.10 | 88.96 | -3.86 | -0.88 | 0.02 |
| 22 | 87.40 | 92.28 | -4.88 | -1.11 | 0.03 |
| 23 | 88.90 | 90.51 | -1.61 | -0.41 | 0.01 |
| 24 | 76.70 | 70.68 | 6.02 | 1.41 | 0.07 |
| 25 | 76.00 | 71.47 | 4.53 | 1.06 | 0.04 |
| 26 | 74.70 | 77.97 | -3.27 | -0.76 | 0.02 |
| 27 | 78.00 | 80.31 | -2.31 | -0.53 | 0.01 |
| 28 | 79.70 | 76.46 | 3.24 | 1.02 | 0.19 |

From Table A3, it was clear that the residual and standardized residual were represented as the random error with a normal distribution. The normality and randomness of the residuals can be checked as show in Figure A1 - A3. Furthermore, all the cook's distance are less than unity shows that there are no recording errors and the experimented points is not far from the remaining cases.

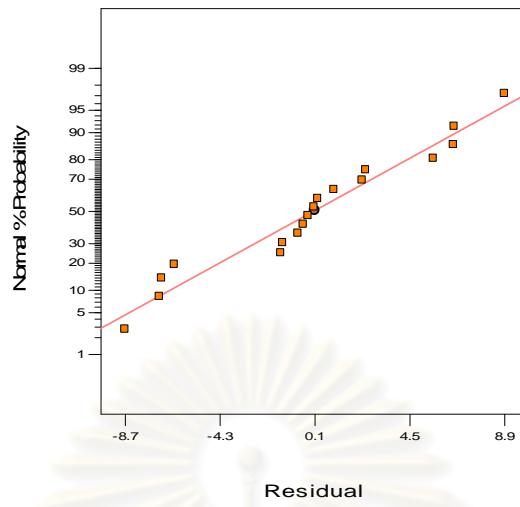


Figure A1. The normal plot of the residuals.

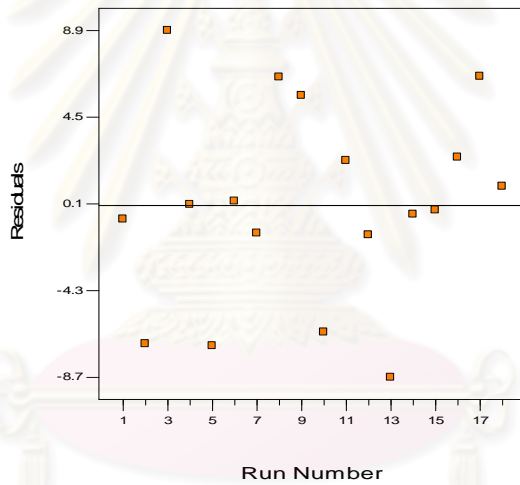


Figure A2. The relationship between residuals and run number.

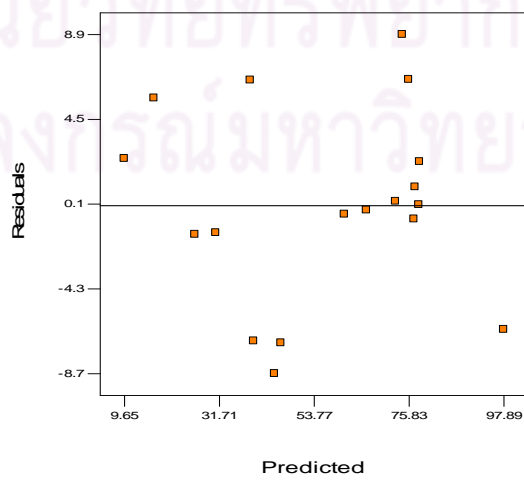


Figure A3. The relationship between residuals and predicted values.

APPENDIX B THE EXAMPLES OF PROGRAMING CODE FOR MATLAB® SOFTWARE WITH SIMULIS TOOLBOX

Function B1. Code for creates Simulis calculator in Matlab® software

```
function [] = CreateSimulisCal
% Create a Simulis Calculator
BDF = stCALCreate;
fprintf('\n');
% Edit the parameters of the Simulis Calculator
modified = stCALEdit(BDF);
if modified
    fprintf('The Simulis Calculator Object has been modified.\n');
else
    fprintf('The Simulis Calculator Object has NOT been modified.\n');
end
fprintf('\n');
% Edition of the INPUT unit system of the Simulis Calculator Object
modifiedInput = stCALSystemEdit(BDF,1);
if modifiedInput
    fprintf('The INPUT unit system of the Simulis Calculator Object has been
modified.\n');
else
    fprintf('The INPUT unit system of the Simulis Calculator Object has NOT
been modified.\n');
end
fprintf('\n');
% Edition of the OUTPUT unit system of the Simulis Calculator Object
modifiedOutput = stCALSystemEdit(BDF,2);
if modifiedOutput
    fprintf('The OUTPUT unit system of the Simulis Calculator Object has
been modified.\n');
else
    fprintf('The OUTPUT unit system of the Simulis Calculator Object has NOT
been modified.\n');
end
fprintf('\n');
% Save the Simulis Calculator Object in a text file
fprintf('The Simulis Calculator Object is saved in "BDFCal.txt".\n');
fprintf('Have A Nice Day!!! \n');
txt = stCALSaveToText(BDF);
fid = fopen('BDFCal.txt','w+');
fprintf(fid,'%s',txt);
fclose(fid);
fprintf('\n');
% Free the Simulis Calculator
stCALFree(BDF);
end
```

Function B1. Code for loads, edit and save Simulis calculator in Matlab® software

```
function [] = LoadSimulisCal
% Create a blank Simulis Calculator
BDFCalEd = stCALCreate;
fprintf('\n');
% Load the Simulis Calculator from a text file
fid = fopen('BDFCalEd.txt','r');
txt = '';
continueRead = 0;
while (continueRead==0)
    line = fgets(fid);
```

```

    if (line == -1)
        continueRead = 1;
    else
        txt=[txt line];
    end
end
fclose(fid);
stCALLoadFromText(BDFCalEd,txt);
fprintf('The Simulis Compounds Object has been loaded from the file called
"compounds.txt".\n');
fprintf('\n');
% Edition of the parameters of the Simulis Calculator Object
modified = stCALEdit(BDFCalEd);
if modified
    fprintf('The Simulis Calculator Object has been modified.\n');
else
    fprintf('The Simulis Calculator Object has NOT been modified.\n');
end
fprintf('\n');
% Edition of the INPUT unit system of the Simulis Calculator Object
modifiedInput = stCALSystemEdit(BDFCalEd,1);
if modifiedInput
    fprintf('The INPUT unit system of the Simulis Calculator Object has been
modified.\n');
else
    fprintf('The INPUT unit system of the Simulis Calculator Object has NOT
been modified.\n');
end
fprintf('\n');
% Edition of the OUTPUT unit system of the Simulis Calculator Object
modifiedOutput = stCALSystemEdit(BDFCalEd,2);
if modifiedOutput
    fprintf('The OUTPUT unit system of the Simulis Calculator Object has
been modified.\n');
else
    fprintf('The OUTPUT unit system of the Simulis Calculator Object has NOT
been modified.\n');
end
fprintf('\n');
% Save the Simulis Calculator Object in a text file
fprintf('The Simulis Calculator Object is saved in "BDFCalEd.txt".\n');
txt = stCALSaveToText(BDFCalEd);
fid = fopen('BDFCalEd.txt','w+');
fprintf(fid,'%s',txt);
fclose(fid);
fprintf('\n');
% Free the Simulis Calculator
stCALFree(BDFCalEd);
end

```

Function B3. Code for show the compound names Simulis calculator in Matlab ® software

```

function ShowCompName
%Create the blank Simulis Calculator
BDFCalEd = stCALCreate;
fprintf('\n');
% Load the Simulis Calculator from a text file
fid = fopen('BDFCalEd.txt','r');
txt = '';
continueRead = 0;
while (continueRead==0)
    line = fgets(fid);
    if (line == -1)
        continueRead = 1;
    end
end

```

```

        else
            txt=[txt line];
        end
    end
end
fclose(fid);
stCALLoadFromText(BDFCalEd,txt);
%Show Component Name
cmpdCount = stCALCompoundCount(BDFCalEd);
if (cmpdCount==0)
    fprintf('Error: Where are your compounds? \n');
else
    fprintf('- Number of compounds = %d\n',cmpdCount);
    fprintf('\n');
    displayName = '';
    for i=1:cmpdCount
        displayName = strcat(displayName,
stCALCompoundDisplayName(BDFCalEd,i));
        fprintf('%d - %s\n',i,strtrim(displayName(i,:)));
    end
end
end

```

Function B4. Code for calculates the initial compressibility factor and molar volume of mixture by Simulis calculator in Matlab ® software

```

function [zm0 vm0] = z0v0Cal(T,P,x)
%Create the blank Simulis Calculator
BDFCalEd = stCALCreate;
% Load the Simulis Calculator from a text file
fid = fopen('BDFCalEd.txt','r');
txt = '';
continueRead = 0;
while (continueRead==0);
    line = fgets(fid);
    if (line == -1);
        continueRead = 1;
    else
        txt=[txt line];
    end
end
fclose(fid);
stCALLoadFromText(BDFCalEd,txt);
% Calculate z0 and v0 from Simulis Calculator
[zmL zmV] = stCALZm(BDFCalEd,T,P,x,0,0,0);
[vmL vmV] = stCALVm(BDFCalEd,T,P,x,0,0,0);
end

```

Function B5. Code for calculates the compressibility factor of mixture in Matlab ® software

```

function [zmL zmV CalT VapRat] = zCal(T,P,X,F0)
%Create the blank Simulis Calculator
BDFCalEd = stCALCreate;
% Load the Simulis Calculator from a text file
fid = fopen('BDFCalEd.txt','r');
txt = '';
continueRead = 0;
while (continueRead==0);
    line = fgets(fid);
    if (line == -1);
        continueRead = 1;
    else
        txt=[txt line];
    end
end

```

```

end
end
fclose(fid);
stCALLoadFromText(BDFCalEd,txt);
% Generate mole fraction vector
FA0 = F0(1);
FB0 = F0(2);
FA = FA0*(1 - X);
FB = FA0*((FB0/FA0) - 3*X);
FC = FA0*((0/FA0) + 3*X);
FD = FA0*((0/FA0) + X);
F = [FA FB FC FD];
x = F/sum(F0);
% Calculate z from Simulis Calculator
[zml zmV CalT VapRat] = stCALZm(BDFCalEd,T,P,x,0,0,0);
end

```

Function B6. Code for writes Equation 6.6 in Matlab ® software

```

% dx/dL = -k(T)*X(L)*z(T,P,L)*P(L)
function dXdL = KEPode(X,kA,FA0,FB0,z0,T,P,F0)
dXdL = kA*(1-X)^0.9565.*((FB0/FA0)-3*X)^1.0493*(z0/(zCal(T,P,X,F0)))^2.0058;

```

Function B7. Code for solves Equation 6.6 in Matlab ® software

```

function [MECont] = ModelAutoRun(T,P,WA0,WB0)
% Reactor design
OD = 1/8; % [=] in
thk = 0.029; % [=] in
D = (OD - 2*thk)*2.54; % [=] cm
A = D*D*pi()/4; % [=] cm2
RL = 8000; % Reactor lenght [=] cm
% Operating condition
T = T + 273; % [=] K
R = 8.314; % [=] j/mol.K
% A = Oil, B = MeOH % W0 = mass flow rate
WA0 = WA0/60; % [=] g/s
WB0 = WB0/60; % [=] g/s
% F0 = Mol flow rate
FA0 = WA0/850; % [=] mol/s
FB0 = WB0/32; % [=] mol/s
F0 = [FA0 FB0 0 0]; % [=] mol/s
% v0 = total vol flow rate at REACTING CONDITION
% V = molar volume of mixture and v0 = V*F0
x0 = F0./sum(F0);
[z0 Vm] = z0v0Cal(T,P,x0);
v0 = Vm*sum(F0); % [=] cm3/s
% Song (2008) The Journal of Supercritical Fluids, 44(3),pp. 356-363
k = 4.3376e8*exp(-1.0527e5/(R*T)); % [=] mL/mol.s
% Solve ODE
kA = (k*A*FA0^1.0058)/(v0^2.0058); % [=] 1/cm
Lspan = [0 RL];
IC = 0; % X(t=0) = 0
[L X] = ode45(@(L,X) KEPode(X,kA,FA0,FB0,z0,T,P,F0),Lspan,IC);
% Calculate Methyl ester content
theta = F0./F0(1);
F = [FA0*(1-X) FA0*(theta(2)-3*X) FA0*(theta(3)+3*X) FA0*(theta(4)+X)];
x = F/sum(F);
% Set xMeOH = xGlyOH = 0 (after MeOH and glycerol were separated)
x(2) = 0;
x(4) = 0;
MECont = 100*x(3)/sum(x);

```

BIOGRAPHY

The author who is responsible for this dissertation is Mr. Ruengwit Sawangkeaw. He was born on 24th January, 1981 at Lopburi Province, Thailand. He graduated with Bachelor of Applied Science in Industrial Chemistry (1998 – 2002) from the Faculty of Applied Science, King Mongkut's Institute of Technology North Bangkok, Thailand. He completed Master of Science in Chemical Technology (2002 – 2005) from the Department of Chemical Technology, Faculty of Science, Chulalongkorn University, Thailand.

Ruengwit started his doctorate program in second semester of the 2005 academic year in Department of Chemical Technology, Faculty of Science, Chulalongkorn University. He received financial support from Clean and Green Fuel Research Unit, and Graduate School, Chulalongkorn University in the first and second year. He was a co-author in the article names “Continuous production of biodiesel via transesterification from vegetable oils in supercritical methanol” which was accepted to publish in “Energy and Fuels”. His first paper entitles “Effect of co-solvents on production of biodiesel via transesterification in supercritical methanol” accepted for publication in “Green chemistry”.

Ruengwit was also received complementary financial grant from Chulalongkorn University Dutsadi Phiphat Scholarship do research at Institut National Polytechnique de Toulouse, Laboratoire de Génie Chimique in France for eight months. His second article on “A review of laboratory-scale research on lipid conversion to biodiesel with supercritical methanol (2001-2009)” accepted for publication in “The Journal of Supercritical Fluids”. He also presented his work at 1 conference in Malaysia and 3 conferences in Thailand.